UNIVERSIDADE DE SÃO PAULO
ESCOLA POLITÉCNICA
DEPARTAMENTO DE ENGENHARIA DE MINAS E DE PETRÓLEO

PEDRO ESTEVES ARANHA

Desenvolvimento de metodologias baseadas em dados para predição de anomalias e garantia da integridade de poços na produção offshore de petróleo utilizando abordagens de aprendizado de máquina

SÃO PAULO
2025

PEDRO ESTEVES ARANHA

Desenvolvimento de metodologias baseadas em dados para predição de anomalias e garantia da integridade de poços na produção offshore de petróleo utilizando abordagens de aprendizado de máquina

Versão Corrigida

(Versão original encontra-se na unidade que aloja
o Programa de Pós-graduação)

Tese apresentada à Escola Politécnica da Universidade de São Paulo para obtenção do título de Doutor em Ciências.

Área de Concentração: Engenharia de Minas

Orientador: Prof. Dr. Marcio Augusto Sampaio Pinto
Coorientadora: Profa. Dra. Nara Angélica Policarpo

SÃO PAULO
2025

Este exemplar foi revisado e corrigido em relação à versão original, sob responsabilidade única do autor e com a anuência de seu orientador.

São Paulo, _____ de _____ de _____

Assinatura do autor: _____

Assinatura do orientador: _____

Catalogação-na-publicação

Aranha, Pedro Esteves
Desenvolvimento de Metodologias Baseadas em Dados para Predição de Anomalias e Garantia da Integridade de Poços na Produção Offshore de Petróleo Utilizando Abordagens de Aprendizado de Máquina / P. E. Aranha -- versão corr. -- São Paulo, 2025.
122 p.

Tese (Doutorado) - Escola Politécnica da Universidade de São Paulo. Departamento de Engenharia de Minas e de Petróleo.

1.Integridade de Poço 2.Fechamento Espúrio 3.Aprendizado de Máquina 4.Anomalias I.Universidade de São Paulo. Escola Politécnica. Departamento de Engenharia de Minas e de Petróleo II.t.

ARANHA, P. E. **Desenvolvimento de metodologias baseadas em dados para predição de anomalias e garantia da integridade de poços na produção offshore de petróleo utilizando abordagens de aprendizado de máquina**. 2025. Tese (Doutorado em Engenharia de Minas) – Escola Politécnica, Universidade de São Paulo, São Paulo, 2025.

Aprovado em:

Banca Examinadora

Prof. Dr. _____

Instituição: _____

Julgamento: _____

Prof. Dr. _____

Instituição: _____

Julgamento: _____

Prof. Dr. _____

Instituição: _____

Julgamento: _____

Prof. Dr. _____

Instituição: _____

Julgamento: _____

Prof. Dr. _____

Instituição: _____

Julgamento: _____

ACKNOWLEDGMENTS

Foremost, I would like to thank my family and friends for their support.

I would like to express my sincere gratitude to my advisor Prof. Marcio Sampaio and my co-advisor Prof. Nara Angélica Policarpo for the support of my study and research, and for sharing all their knowledge.

Thanks to PETROBRAS that has provided support during the research.

Finally, I would like to thank Escola Politécnica of the University of São Paulo (USP) and Laboratory of Petroleum Reservoir Simulation and Management (LASG).

RESUMO

ARANHA, Pedro Esteves. **Desenvolvimento de Metodologias Baseadas em Dados para Predição de Anomalias e Garantia da Integridade de Poços na Produção Offshore de Petróleo Utilizando Abordagens de Aprendizado de Máquina.** 2025. Tese (Doutorado) – Escola Politécnica, Universidade de São Paulo, 2025.

Prever de forma confiável o comportamento dos poços offshore em relação à integridade de seus componentes durante a produção e antecipar mudanças de comportamento e anomalias ainda são pouco abordados na literatura. O autor visa tratar essa questão por meio de uma abordagem orientada a dados e métodos de Aprendizado de Máquina. O objetivo é desenvolver metodologias para prever o comportamento com base em dados de sensores de poços, com um mínimo de dependência de informações geológicas detalhadas, propriedades dos fluidos ou detalhes específicos do poço. Os eventos de anomalia em poços offshore registrados nas bases de dados foram mapeados. Em seguida, os dados foram extraídos de séries temporais e processados. A relevância dos atributos foi analisada, e métodos de tratamento apropriados foram explorados. Modelos preditivos foram desenvolvidos. Inicialmente, o modelo *Novelty and Outlier Detection* foi desenvolvido para prever fechamentos espúrios das Down Hole Safety Valve (DHSV). Em seguida, um modelo híbrido combinando um *autoencoder* LSTM e uma abordagem analítica foi desenvolvido para detectar anomalias, capaz de discernir vários tipos de anomalias além dos eventos de fechamentos espúrios de DHSV, mas ainda deficiente em eventos de anomalias de poços com Completação Inteligente (IWC). Como parte final do trabalho foi realizado o desenvolvimento e aplicação de um modelo utilizando *Transformers* para prever anomalias nas Interval Control Valves (ICV) utilizadas em poços de Completação Inteligente, de forma a complementar os modelos desenvolvidos anteriormente e cobrir os eventos de anomalias relacionadas à integridade do poço ocorrendo em poços offshore.

Palavras-Chave: Integridade de Poço, Fechamento Espúrio, Aprendizado de Máquina, Anomalias.

ABSTRACT

ARANHA, Pedro Esteves. **Development of Data-Driven Methodologies for Predicting Anomalies and Ensuring Well Integrity in Offshore Oil Production Using Machine Learning Approaches**. 2025. Thesis (Doctorate) – Escola Politécnica, University of São Paulo, 2025.

To reliably predict the behavior of offshore wells concerning the integrity of their components during production and to anticipate changes in behavior and anomalies are topics that are rarely addressed in literature. The author aims to address this issue through a data-driven approach and Machine Learning methods. The objective is to develop methodologies to predict behavior based on well sensor data, with minimal reliance on detailed geological information, fluid properties, or specific well details. Anomaly events in offshore wells recorded in databases were mapped. Subsequently, data was extracted from time series and processed. The relevance of attributes was analyzed, and appropriate treatment methods were explored. Predictive models were developed. Initially, the Novelty and Outlier Detection model was developed to predict spurious closures of Down Hole Safety Valves (DHSV). Following this, a hybrid model combining an LSTM autoencoder and an analytical approach was developed to detect anomalies, capable of discerning various types of anomalies beyond the spurious closure events of DHSV, but still deficient in detecting anomaly events in wells with Intelligent Well Completion (IWC). As the final part of the work, a model utilizing Transformers was developed and applied to predict anomalies in Interval Control Valves (ICV) used in wells with Intelligent Well Completion, complementing the previously developed models and covering anomaly events related to well integrity occurring in offshore wells.

Keywords: Well Integrity, Spurious Closure, Machine Learning, Anomalies.

LIST OF FIGURES

LIST OF TABLES

LIST OF ABBREVIATIONS

ACC	Accuracy
ACCb	Balanced accuracy
AdaBoost	Adaptive boosting
ANP	Brazilian national agency for petroleum, natural gas and biofuels
AUC-ROC	Area under the receiver operating characteristic curve
cp	Calculated parameter
CBM	Condition-based monitoring
CHOKE	Choke position in the well production/injection line
CNN	Convolutional Neural Network
DD	Decision Diagram
DHSV	Down hole safety valve
DP	Differential Pressure
DT	Decision tree
F1	F1-SCORE
FP	Number of false positives
FN	Number of false negatives
FPR	False positive rate
GAN	Generative Adversarial Networks
ICV	Interval Control Valves
IWC	Intelligent Well Completion
K-NN	K-nearest neighbors
LOF	Local outlier factor
LSTM	Long short-term memory
M1	Master valve 1 in wet Christmas tree
M2	Master valve 2 in wet Christmas tree
ntotal	Total number of samples
NPT	Non-productive time
P-I-PDG	Pressure in front Intermediate Zone - Pressure Downhole Gauge
P-L-PDG	Pressure in front Lower Zone - Pressure Downhole Gauge
P-TPT	Pressure on temperature/pressure transducer
P-PDG	Pressure on pressure downhole gauge
P-SURFACE	Surface Pressure in the well production/injection line

P-U-PDG	Pressure in front Upper Zone - Pressure Downhole Gauge
P-MON-CKP	Pressure in the production choke on the surface
PDG	Pressure downhole gauge
PXO	Pig cross-over valve in wet Christmas tree
REC	Recall
RF	Random forest
RNN	Recurrent Neural Network
SD	Standard deviation
SGIP	Well Integrity Management System
SP	Specificity
SVM	Support vector machines
TadGAN	Time series Anomaly Detection using Generative Adversarial Networks
TD	Detection time
TN	Number of true negatives
TP	Number of true positives
TPR	True positive rate
T-I-PDG	Temperature in front Intermediate Zone - Pressure Downhole Gauge
T-L-PDG	Temperature in front Lower Zone - Pressure Downhole Gauge
T-PDG	Temperature on Pressure Downhole Gauge
T-U-PDG	Temperature in front Upper Zone - Pressure Downhole Gauge
T-TPT	Temperature on temperature/pressure transducer
TPT	Temperature and pressure transmitter
TRANS	Transformer Model
W1	Wing valve 1 in wet Christmas tree
W2	Wing valve 2 in wet Christmas tree
XO	Cross-over valve in wet Christmas tree
WIMS	Well integrity management system
WCT	Wet Christmas Tree

SUMMARY

CHAPTER 1 – INTRODUCTION

The design of an oil well is a complex task that involves the analysis of various engineering aspects, such as the reliability of the casing, the behavior of formations (whether saline or not) during drilling, among others. Each of these aspects is analyzed by professionals with distinct specialties, making the design of a well a multidisciplinary task composed of several subprojects that must be integrated (BOURGOYNE Jr. et al. 1986; MITCHELL and MISKA 2016).

After the design phase, there are stages including drilling, equipment installation in the well (completion), installation of a Christmas tree, connection to the platform/production plant, and finally, production operations. At the end of the productive life, the well is permanently abandoned (BOURGOYNE Jr. et al. 1986; MITCHELL and MISKA 2016).

An oil well is drilled in phases, resulting in a telescopic geometric structure, meaning that concentric casing columns with smaller diameters and greater depths are installed at the end of each phase. At the end of drilling, a production tubing column is installed, through which produced or injected fluids are conducted in the well. The casings strings and production tubing are the main components of the well structure. Due to its telescopic structure, various annular spaces in the well are isolated, especially in subsea wells, where only access to annulus A is available, corresponding to the space between the production/injection tubing and the production casing. CAHILL (2011) emphasizes the importance of monitoring other well annuli, mentioning the existence of a tool that could monitor annulus B but has not yet found practical application in the industry. Figure 1 illustrates the generic geometry of annular spaces in an offshore oil well.

Figure 1 - Schematic structure of offshore oil wells.

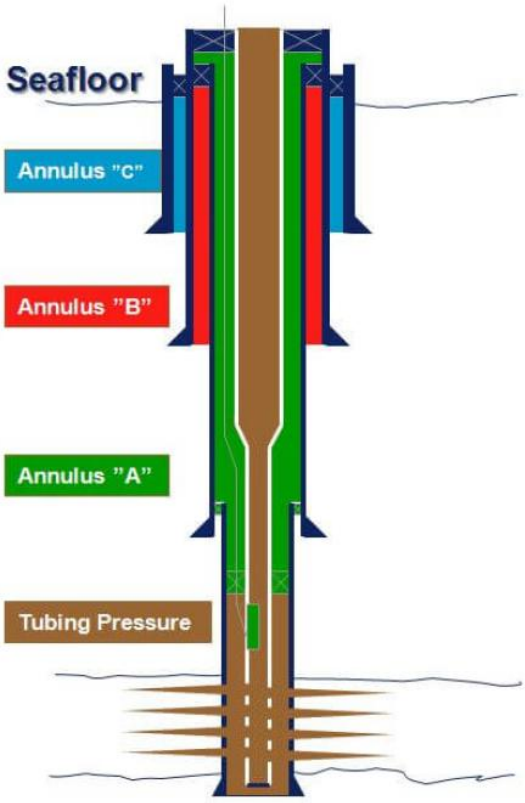

Source: CAHILL (2011).

In this context, monitoring the well during production is essential to analyze whether the constructed well is operating within the safety limits established in the design.

Despite all the care taken in sizing the well structure, considering the worst-case scenario with maximum load and minimum resistance, unforeseen events can occasionally occur during its operation. For example, a valve maneuver can excessively pressurize a casing, compromising the entire well structure. This situation can lead to significant financial losses – the construction of a well can cost hundreds of millions of dollars, and the cost of recovery, depending on the damage, is difficult to predict. It can also result in immeasurable environmental damage, particularly oil spills into the sea, which are difficult to contain.

CAMPOS et al. (2019) presents a case of a well with integrity loss and oil leakage into the sea, and the entire operation involved in permanent abandonment using a new interception well. Such cases harm various ecosystems and damage the

reputation of the oil company. There are recorded cases where over 60% of wells in a field experienced casing failures during their production (YUAN et al., 2013).

In 2016, the need for methodologies and models for predicting behavior and managing well integrity became crucial with the publication of ANP Resolution Nº. 46/2016, which established the Operational Safety Regime for the Integrity of Oil and Natural Gas Wells and approved Sistema de Gerenciamento de Integridade de Poços(SGIP). The SGIP defines essential requirements and minimum standards for operational safety and environmental preservation to be met by companies holding exploration and production rights with contracts with ANP in oil and natural gas wells in Brazil (National Agency of Petroleum, Natural Gas, and Biofuels, 2016). In this context, the use of machine learning and deep learning models has the potential to contribute to the analysis of whether the constructed well is operating within established safety limits and to anticipate operational problems.

To ensure well integrity and promote operational safety, constant monitoring is necessary. The monitoring of variables such as pressure and temperature is limited to verifying whether the well is operating within the parameters specified in the design (known as the operational envelope). One examples at the operational level, only a comparison is made between pressure and temperature measurements at the wellhead (Christmas tree) and sensors (PDG – Pressure Downhole Gauge) near the reservoir to check if they are within the design values. Measurements outside the expected range can indicate various situations, such as equipment failure, incorrect reservoir behavior predictions, human errors in well operation, or design flaws. Another common use of the monitored variables – primarily pressure and temperature near the reservoir and at the wellhead – is in diagnosing problems after they occur, such as abrupt interruptions in the production/injection of a specific well, unexpected pressure communication between the tubing and annulus, oil leakage to the seafloor, among others.

The information from these well sensors can be used not only to diagnose a problem that has already occurred but also to prevent its occurrence. However, due to the complex nature of the system involving many variables and various cause-and-effect relationships, identifying the cause of a problem based on, for example, an abnormal pressure sensor reading is not a simple task and often requires several days of data analysis.

To address the need for well integrity monitoring, data-driven models were devised using an unsupervised approach, were implemented a Novelty and Outlier Detection model, a hybrid model combining an LSTM autoencoder and a rule-based analytic approach and the development of Transformer model.

1.1 Literature Review

Predicting the behavior of oil wells and reservoirs using machine learning methods has been the subject of recent publications. Some works related to parameter optimization during well construction and the prediction of behavior in completed offshore wells during production, injection, and in production lines using machine learning methods are summarized below.

According to GIDH et al. (2012), a model using neural networks was developed to optimize operational drilling parameters such as torque, flow rate, pumping pressure, and weight on bit, aiming to maximize the Rate of Penetration (ROP). The study aimed to reduce human factors in parameter application, removing subjectivity from the system.

TOGNI (2018) proposed a predictive model using machine learning to evaluate the expected drilling time, allowing for a failure analysis (decision during well construction) if the actual drilling time exceeds the planned time. This work uses surface parameters (torque, weight on bit, flow rate, pressure) and assesses the overall context of drilling failures, such as pipe sticking, pipe differential sticking, and bit wear.

ZHAO et al. (2017) developed a drilling event detection model through data analysis, including parameters such as torque, weight on bit, flow rate, pumping pressure, drilling rate, wellbore geometry, lithology, and sensors installed in the Bottom Hole Assembly (BHA) of the drilling column. The proposed method is based on the Symbolic Aggregate Approximation (SAX) technique for anomaly detection (e.g., pipe sticking, pipe differential sticking, and bit wear) during drilling.

NOSHI and SCHUBERT (2018) presented a series of machine learning models (Random Forest, Principal Component Analysis (PCA), Support Vector Machine (SVM), Artificial Neural Network (ANN), and K-Means Clustering) for applications aimed at maximizing drilling rates. This work provides an analysis of the

advantages and disadvantages of those machine learning models applied to drilling. One of their approaches is the use of probabilistic techniques such as Bayesian networks, which are graphically similar to decision trees.

AGOSTINI and SAMPAIO (2020) introduced a probabilistic machine learning model applied to drilling to determine bit wear and the appropriate moment for pulling the drilling assembly, conducting an extensive comparative analysis of models from the literature (Random Forest, PCA, SVM, ANN, and K-Means Clustering). AGOSTINI and SAMPAIO (2020) also developed a new probabilistic neural network (PNN) model for the case of drilling with an 8.5-inch PDC bit in carbonate reservoirs, using surface sensor data (torque, weight on bit, flow rate, etc.) and downhole data obtained from MWD sensors in the drilling column.

MARINS et al. (2021) proposed a random forest model and an optimized non-convex Bayesian model for the detection and classification of operational issues that may occur during well production. They used a publicly available database (VARGAS et al., 2019) containing problem classifications that occur in offshore wells and production lines. From this database, they developed a Condition-Based Monitoring (CBM) strategy for the detection and classification of eight different operational issues that may occur during offshore well production, such as sudden increases in Basic Sediments and Water (BSW), spurious closure of Down Hole Safety Valves (DHSV), gas lift production instability, production choke restriction, scaling formation, and hydrate formation in the production line.

LIU et al. (2011) developed a semi-supervised system for predicting problems, primarily tubing leaks, during onshore well production. They applied a Random Peek classifier inspired by semi-supervised learning, assuming some prior knowledge about the data distribution, which helped increase accuracy.

VARGAS et al. (2017) proposed the use of k-nearest neighbors (kNN) and Sliding Window in the detection and classification of four types of operational problems, such as spurious closure of Down Hole Safety Valves (DHSV), natural production loss, production line blockage, and closure of the choke valve. The models were trained and tested using both real data (Christmas Tree and PDG sensors) and data generated from commercial simulators (OLGA).

MACHADO et al. (2022) proposed an anomaly detection model with an LSTM autoencoder and SVM (Support Vector Machines) classifier, improving performance for faults with slow dynamics, particularly by enhancing detection times.

Recent evaluations of techniques such as Isolation Forest, One-class Support Vector Machine (OCSVM), Local Outlier Factor (LOF), Elliptical Envelope, and Autoencoder (both feedforward and LSTM architectures) showcased the Local Outlier Factor as the top performer in various scenarios (FERNANDES, et al. (2024)) other study explores a density-based unsupervised machine learning model, the Local Outlier Factor (LOF), to detect anomalies in subsea production/injection wells through sensor (SILVA, et al. (2024)).

OLIVEIRA et al. (2025) explores the application of TranAD, a deep transformer network model, for detecting anomalies in offshore oil and gas well operations using the 3W dataset, a public repository of multivariate time-series data. The study emphasizes the importance of ensuring well integrity to enhance safety, environmental protection, and production efficiency. TranAD's attention-based architecture addresses challenges like data imbalances, anomaly rarity, and operational complexities, enabling robust detection through adversarial training and predictive-reconstructive learning. The research investigates two training approaches well-specific and generalized models and highlights the potential of advanced real-time anomaly detection systems to optimize offshore well monitoring and reduce risks.

1.2 Objective

The objective is to develop data-driven approaches utilizing machine learning methods to identify anomalies in valves and well components and provide insights, ensuring the integrity of offshore wells, with minimal dependence on detailed geological information, fluid properties, or specific well details, while addressing practical constraints.

1.3 Motivation and Methodology

The motivation for this research lies in the importance of predictability in the well integrity, particularly with the publication of the SGIP (Well Integrity Management System) by the ANP (National Agency of Petroleum, Natural Gas, and Biofuels) in 2016.

The project's distinctive feature lies in its utilization of actual sensor data from active wells in the Brazilian Pre-Salt region, both in production and injection.

The specific methodology is as follows:

- Data processing to select the most relevant variables for the integrity problem of barrier elements, annular column communication, leaks in control lines, and valve malfunction, defining the ideal format for their use. For this, it will be used process production data, such as time series of: (i) pressure and temperature from sensors located in the Christmas tree, in the production bore and annulus; (ii) pressure and temperature from PDG sensors positioned near the reservoir; (iii) pressure from Christmas tree and DHSV valves; (iv) pressure from high and low-pressure hydraulic control systems (HP/LP), and (v) return flow for Christmas tree and DHSV valve control.
- Evaluate machine learning techniques and choose the most suitable one(s) for the prediction task, considering their complexity and performance in reproducing well behavior.
- Adapt the proposed prediction methodology to address practical limitations such as sensor limitations in wells, platform processing capabilities, well constraints, and production system characteristics.
- Employ the predictor in actions supporting well integrity management, including the anticipation of events such as spurious valve closures, loss of integrity in barrier elements, annular column communication, control line leaks and valve anomalies.

All the algorithms were implemented using Python 3.9 programming language, in a CPU Precision 3571, 12th Gen Intel(R) Core(TM) i7-12800H 2.40 GHz, 32GB RAM, GPU Nvidia T600 4GB.

1.4 Thesis overview

The thesis comprises five interconnected chapters that revolve around the utilization of data-driven models for predicting anomalies related to well integrity and real-time monitoring of well behavior. These models are developed using sensor data obtained from public databases and industry data from production and injection wells located in the Brazilian Pre-Salt region.

Concerning this, this thesis is comprised of published papers where in Chapter 2 is presented the development of predictive models for real-time monitoring of well behavior using sensor data from production wells. An Unsupervised Novelty and Outlier Detection model has been introduced with a specific focus on predicting instances of unexpected subsurface safety valve closures in subsea wells. This model effectively classifies anomalies observed in these systems by leveraging real-world pressure and temperature data sourced from published literature. The methodology involves the implementation of a sliding window for assembling training and test sets. Additionally, a comprehensive investigation is conducted into the impact of hyperparameters and the model's threshold value (cp threshold). The results highlight the effectiveness of the developed model, observed through the accuracy achieved around 99.9% in predicting spurious closure events of the Down Hole Safety Valve (DHSV). On the same dataset, comparing with previous works the developed model performs better. Furthermore, the model's applicability is validated through testing in ultradeep water subsea wells within the pre-salt area of the Santos Basin. The significance lies in the potential for this research to enhance anomaly prediction in offshore wells, consequently reducing the costly interventions due to equipment malfunctions. Timely detection and corrective actions, facilitated by the model, can mitigate production loss and safeguard well integrity, addressing critical concerns in the oil and gas industry. The full text from Chapter 2 was published as a full manuscript by *Journal of Petroleum Exploration and Production Technology*.

The Chapter 3 describes a system for real-time monitoring of unwanted events using the production sensor data from oil wells. It uses a combination of LSTM autoencoder and a rule-based analytic approach to perform the detection of anomalies from sensor data. Initial studies are conducted to determine the behavior and correlations of pressure and temperature values for the most common combinations of well valve states. The proposed methodology uses pressure and temperature sensor

data, from which a decision diagram classifies the well status, and this response is applied to the training of recurrent neural networks devoted to anomaly detection. Datasets related to several operations in wells located at different oil fields are used to train and validate the dual approach presented. The combination of the two techniques enables the deep neural network to evolve constantly through the normal data collected by the analytical method. The developed system exhibits high accuracy, with true positive detection rates exceeding 90% in the early stages of anomalies identified in both simulated and actual well production scenarios. It was implemented in more than 20 Floating Production Storage and Offloading (FPSO), monitoring more than 250 production/injection subsea wells, and can be applied both in real-time operation and in testing scenarios. The full text from Chapter 3 was published as a full manuscript by the *SPE Journal.*

In Chapter 4 is described the development and application of a transformer model to predict anomalies in inflow control valves (ICV) used in Intelligent Well Completion (IWC), aiming to complement the application of the two models developed in the previous Chapters 2 and 3. Testing results indicate that TRANS-D outperformed previous models, achieving a balanced accuracy (ACCb) of 0.9694 and an F1-score of 0.9574 for predicting ICV closure or partial closure events, representing a 38.5% accuracy increase over existing models. These outcomes highlight the model's precision and reliability, showing significant advancements over earlier approaches like DD+LSTM and LOF. Additionally, the transformer model exhibited accuracy in detecting spurious DHSV closure events, reaching approximately 98.6% accuracy using a publicly available database, comparable to or exceeding other documented models.

The model's capacity to handle diverse and complex data patterns establishes it as a tool for anomaly detection in critical offshore well operations. A notable advantage of the TRANS-D algorithm is its resilience to concept and data drift, common in dynamic offshore settings. By maintaining high detection rates as reservoir conditions evolve, TRANS-D ensures consistent and reliable anomaly detection, crucial for minimizing production interruptions and ensuring well integrity over time. This distinction highlights the model's adaptability to different operational environments, demonstrating its reliability and effectiveness. Rapid anomaly detection enables operators to quickly address issues related to production or injection, mitigating the impacts associated with ICV closure. Without the transformer model,

human detection of anomalies could take time, resulting in significant economic consequences. The full text from Chapter 4 was published as a full manuscript by the *Petroleum Exploration and Development*.

In Chapter 5, the conclusions of this thesis will be pointed out and presenting future research proposals.

CHAPTER 2 - UNSUPERVISED MACHINE LEARNING MODEL FOR PREDICTING ANOMALIES IN SUBSURFACE SAFETY VALVES AND APPLICATION IN OFFSHORE WELLS DURING OIL PRODUCTION

2.1 Introduction

An oil well is drilled in phases (BOURGOYNE Jr. et al. 1986; MITCHELL and MISKA 2016), resulting in a telescopic geometric structure, whereby concentric casing columns with smaller diameters are successively installed at greater depths at the end of each phase. At the end of drilling, a production column, through which the fluids produced or injected into the well are conducted, is installed, such that the casings and the production column constitute the main components of the well structure. Due to its telescopic structure, several annuli in the well are isolated, especially in subsea wells (CAHILL, 2011), making it difficult to obtain information for decision-making during the well productive life.

Despite the careful dimensioning of well structures, unforeseen conditions can occur during operation (BRECHAN et al. 2019), such as valve maneuvers that over-pressurize casings or corrosions issues (LUIBIMOVA and KUZINA (2021); SHAKER and JAAFAR (2022)). Such situations can compromise the entire well structure, resulting in high financial losses - construction of subsea oil wells can cost hundreds of millions of dollars, and the cost of recovery, depending on the damage, is unpredictable. Furthermore, such events can have immeasurable environmental impacts (SHAKER and SADEQB (2022)), especially if oil spills into the sea, which would be difficult to contain. CAMPOS et al. (2019) reported a case where a well with integrity loss and leakage into the sea required permanent abandonment using a new interception well, causing harm to several ecosystems and eroding the image of the oil company. Unfortunately, cases like this are not uncommon, as YUAN et al. (2013) documented casing failure in over 60% of wells in a given field during production.

Nowadays, oil and gas fields are maturing and creating new threats. This urged the operating companies and industry researchers to have an intensive focus on well integrity. Building Well Integrity Management System (WIMS) establishes standardized criteria to guarantee that the integrity of all wells is preserved during their lifespan, functions properly in healthy condition, and can operate consistently to fulfill the expected YAKOOT et al. (2021). In 2016, the importance of methodologies and

models for predicting well behavior and managing well integrity became increasingly apparent with the publication of the AGÊNCIA NACIONAL DO PETRÓLEO, GÁS NATURAL E BIOCOMBUSTÍVEIS (2016). This resolution instituted the Operational Safety Regime for Well Integrity of Oil and Natural Gas and approved the Technical Regulation of the Brazilian Well Integrity Management System. The Brazilian Well Integrity Management System established essential requirements and minimum standards of operational safety and environmental preservation to be met by companies holding exploration and production rights under contracts with the ANP in oil and natural gas wells in Brazil. Many applications in machine learning and deep learning models were studied in different petroleum engineering and geosciences segments such as petroleum exploration, reservoir characterization, oil well drilling, production, and well stimulation (TARIQ et al. (2021)) and still have the potential to contribute to the analysis of whether the constructed well is operating within established safety limits and to the anticipation of operational problems.

Advancements in data management have empowered oil companies to build extensive databases, consolidating diverse data types from various sources, including machine sensors, economic metrics, human resources, production metrics, fluid data, and well mechanical conditions. These databases serve as a foundation for robust algorithms aimed at averting failures in the oil industry, such as pipeline leak detection (LIU et al. (2019)), production hydrate detection (MARINS and NETTO (2018)), inflow detection during drilling (TANG et al. (2019)), and artificial lift failure (LIU et al. (2011)).

While some researchers (ANJOS et al. (2020); ARANHA et al. (2022)) have applied digital twin technology to monitor well integrity in real-time, capturing thermo-mechanical behavior and loads on tubular and well components, this approach does not encompass all potential subsurface or control system-related phenomena. For instance, it may not address wear, column holes, equipment malfunctions, or spurious valve closures – areas where machine learning could proactively anticipate issues and prevent operational losses. Improved anomaly prediction in offshore wells is crucial due to the high costs of rig interventions, preventable through early model-driven detection, minimizing production loss, and safeguarding well integrity. Some studies have explored machine learning's potential in this domain:

VARGAS et al. (2017) investigated K-Nearest Neighbors (K-NN) and Floating Window algorithms to detect issues like DHSV closure, production loss, line

obstructions, and control valve closure. Real and simulated data demonstrated these methods' feasibility in real plant applications.

MARINS et al. (2021) introduced Condition-Based Monitoring (CBM) using Random Forest and Bayesian models to classify eight operational problems. Achieving over 94% accuracy, their models offered minimal detection delays, allowing operators ample time for damage mitigation.

TURAN and JASCHKE (2021) evaluated various machine learning algorithms, with Decision Trees standing out, effectively classifying failures except for spurious DHSV closure.

MACHADO et al. (2022) proposed an anomaly detection model with an LSTM autoencoder and Support Vector Machines (SVM) classifier, improving performance for faults with slow dynamics, particularly by enhancing detection times.

Unsupervised machine learning offers promise in scenarios with scarce labeled data, like oil well production (ELAVARASAN et al. 2018), by uncovering hidden patterns from unlabeled data. This study focused on using unsupervised machine learning algorithms for anomaly detection in multivariate oil production time series data, particularly targeting spurious DHSV closures. The model leveraged the Scikit-learn package's Novelty and Outlier Detection algorithm, exploring local outlier factor (LOF) estimator. The developed model was tested in subsea wells (internal database) located in the Santos Basin, showcasing its potential for enhancing operational safety and efficiency.

2.2 Methodology

The work consisted of carrying out an evaluation of the Novelty and Outlier Detection algorithm of the Scikit-learn framework, investigating the impact of:

(i) the hyperparameters of the Local Outlier Factor (LOF) estimator (BREUNIG et al. (2000));

(ii) the temporal windows for training, that is, how many time steps to enter the predictor and how many steps to be estimated/tested in the data from the public database (VARGAS et al. (2019)), which has classified datasets for the spurious DHSV closure problem and after applying in anomalies detection in offshore wells.

Based on this, the temporal window formation routine, training, and testing process implemented for the unsupervised algorithm at each time step used can be seen in the schematic view of Figure 2.

Figure 2 - Schematic view of the temporal window routine.

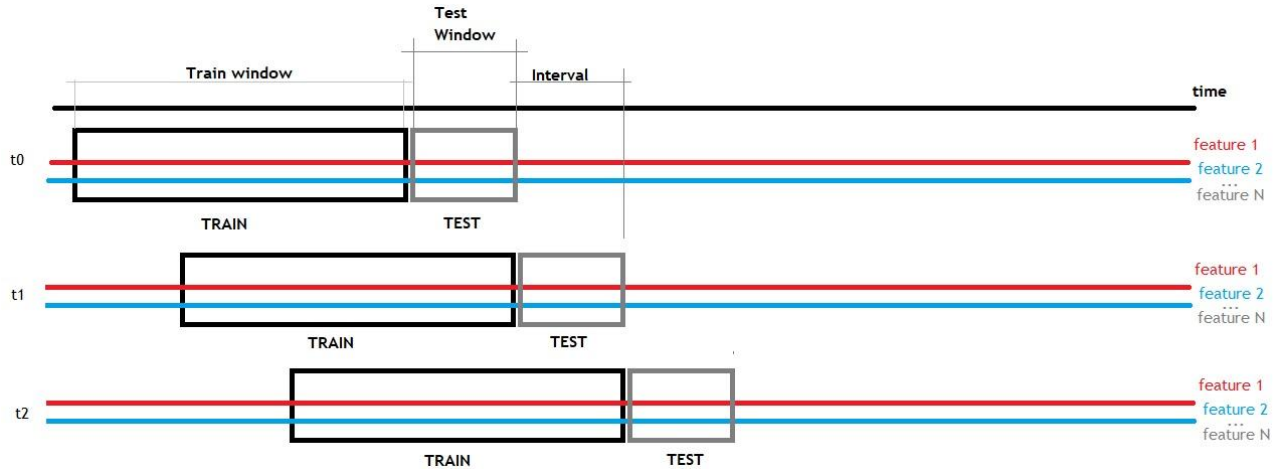

The implemented methodology followed the eight steps depicted in Figure 3 and described below:

1) For the public database (VARGAS et al. (2019)), the data in .csv files were read to define the size of the dataset. For the case studies (internal database), the sensor data were read from a database for a defined period (size) after they were acquired by the real-time monitoring system;

2) Applied for the public base, the pre-processing was performed for the classifier (class), with transient and steady-state failure states unified as a single anomalous state, to give as much time as possible for the operator to intervene and minimize the losses. For this reason, in all experiments, it was opted to use only the normal and fault instead of having a transient state. The proposed method was a one-class classifier: This scheme consists of a single classifier to discriminate only between normal and faulty status. Therefore, in this case, all fault, transient status, and not-a-number (NaN) values in the class are combined into a unique class which is classified against the normal-operation class. There was no not-a-number (NaN) value in the variable monitoring data;

3) Normalization was applied using StandardScaler (SCIKIT-LEARN 2022);

4) The training and test sets were defined for the time step, based on acquisition timestamp;

5) The training set defined at each window was applied to the Novelty and Outlier Detection algorithm with previously defined hyperparameters, generating a model;

6) The test window was then evaluated with this model, whereby the response (cp index) was calculated, which varied from 1 to -1 for each test set of data, with an average cp being calculated from an analysis window with the results provided by the model;

7) The average cp of this test window was then compared with a threshold value for assigning the normal or faulty state, in this case, the threshold used (cp threshold) was 0 (zero), with average cp positive or equal to zero the model classified as normal state, if average cp was negative value the model classified as faulty state;

8) With the test set evaluated as normal, a time step defined by the parameterized interval value was given, and the process was repeated until the end of the data set. If the evaluation fails, a time step was given but the model was not retrained, only a new set of tests was evaluated.

Figure 3 - Flowchart containing the steps of the proposed methodology.

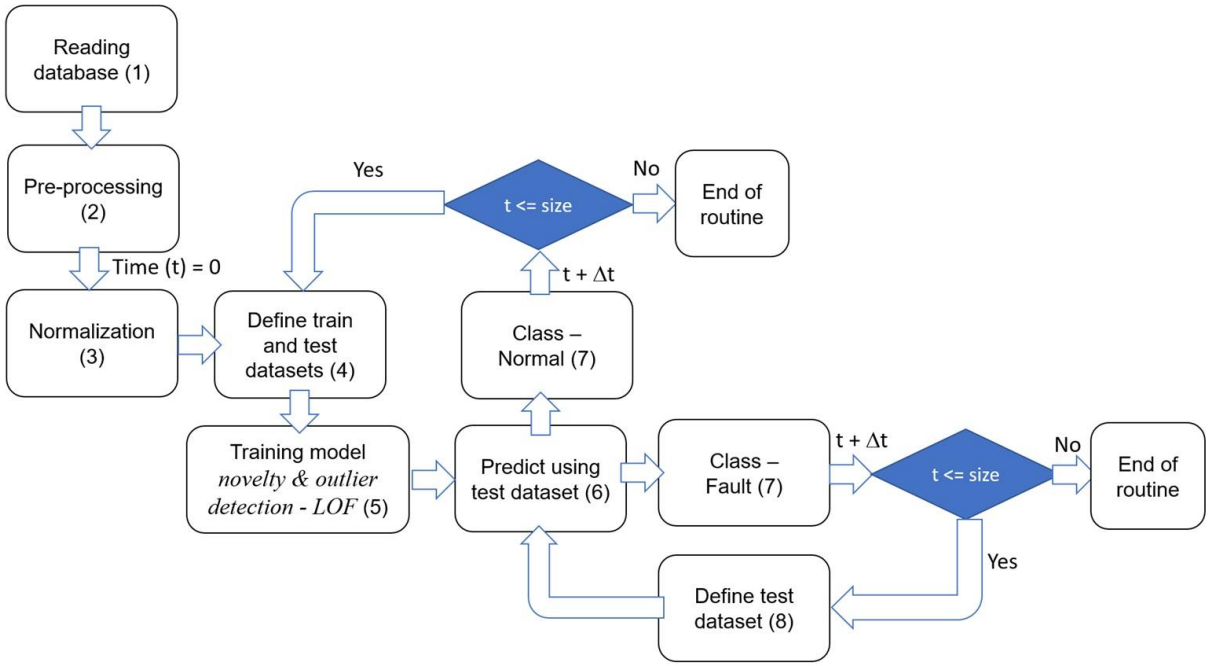

2.2.1 Novelty and Outlier Detection Algorithm

The Local Outlier Factor (LOF) algorithm (BREUNIG et al. (2000)) is an unsupervised anomaly detection method that calculates the local density deviation of a given data point in relation to its neighbors. It considers the samples that have a substantially lower density than their neighbors as outliers. The number of neighbors considered (parameter n_neighbors) is normally set to 1) greater than the minimum number of samples that a cluster must contain so that other samples can be local outliers concerning this cluster, and 2) less than the maximum number of samples close to samples that could potentially be local outliers. In practice, this information is usually not available and, for practical purposes, n_neighbors should be set. The key difference between the LOF algorithm and existing notions of outliers is that being outlying is not a binary property.

For any positive integer k, the k-distance of object p, denoted as k-distance (p), is defined as the distance d(p,o) between p and an object o ∈ D such that:

(i) for at least k objects o'∈ D \ {p} it holds that d(p,o') ≤ d(p,o), and

(ii) for at most k-1 objects o'∈ D \ {p} it holds that d(p,o') < d(p,o).

Given the k-distance of p, the k-distance neighborhood of p contains every object whose distance from p is not greater than the k-distance, i.e., Nk-distance(p)(p) = { q ∈ D\{p} | d(p, q) ≤ k- distance(p) }. These objects q are called the k-nearest neighbors of p. Let k be a natural number. The reachability distance of object p concerning object o is defined as reach-distk(p, o) = max { k-distance(o), d(p, o) }.

Figure 4 illustrates the idea of reachability distance with k = 4. Intuitively, if object p is far away from o (e.g. p2 in the figure), then the reachability distance between the two is simply their actual distance. However, if they are "sufficiently" close (e.g., p1 in the figure), the actual distance is replaced by the k-distance of o. The reason is that in so doing, the statistical fluctuations of d(p,o) for all the p's close to o can be significantly reduced. The strength of this smoothing effect can be controlled by the parameter k. The higher the value of k, the more similar the reachability distances for objects within the same neighborhood.

Figure 4 - Reach-dist(p 1,o) and reach-dist(p2,o), for k=4.

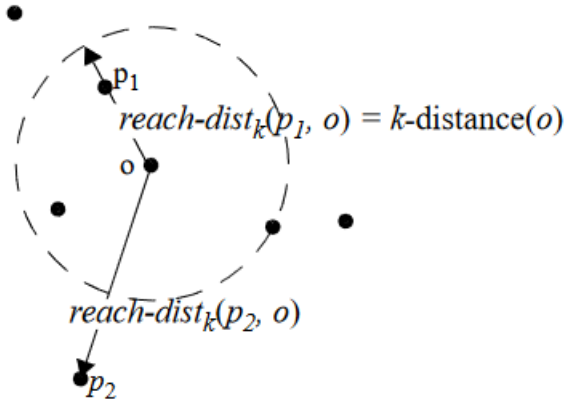

Source: (Breunig et. al 2000).

In a typical density-based clustering algorithm, two parameters define the notion of density: (i) a parameter MinPts specifying a minimum number of objects, and (ii) a parameter specifying a volume. These two parameters determine a density threshold for the clustering algorithms to operate. That is, objects or regions are connected if their neighborhood densities exceed the given density threshold. To detect density-based outliers, however, it is necessary to compare the densities of different sets of objects, which means that it has to determine the density of sets of objects dynamically. Therefore, the MinPts was kept as the only parameter, and the values $\mathrm{reach}-\mathrm{dist}_{\mathrm{MinPts}}(\mathrm{p},\mathrm{o})$ was used, for $\mathrm{o} \in \mathrm{N}_{\mathrm{MinPts}}(\mathrm{p})$, as a measure of the volume to determine the density in the neighborhood of an object p.

The local reachability density (lrd) of p is defined as:

$$\mathrm{lrd}_{\mathrm{MinPts}}(\mathrm{p}) = \frac{1}{\left(\frac{\mathrm{o} \in \sum \mathrm{N}_{\mathrm{MinPts}}(\mathrm{p})\mathrm{reach}-\mathrm{dist}_{\mathrm{MinPts}}(\mathrm{p},\mathrm{o})}{|\mathrm{N}_{\mathrm{MinPts}}(\mathrm{p})|}\right)} \quad (1)$$

Intuitively, the local reachability density of an object p is the inverse of the average reachability distance based on the MinPts-nearest neighbors of p. Note that the local density can be ∞ if all the reachability distances in the summation are 0 (zero). This may occur for an object p if there are at least MinPts objects, different from p, but sharing the same spatial coordinates, i.e., if there are at least MinPts duplicates of p in the dataset.

The local outlier factor (LOF) of p is defined as:

$$\mathrm{LOF}_{\mathrm{MinPts}} = \frac{\mathrm{o} \in \sum \mathrm{N}_{\mathrm{MinPts}}(\mathrm{p}) \frac{\mathrm{lrd}_{\mathrm{MinPts}}(\mathrm{o})}{\mathrm{lrd}_{\mathrm{MinPts}}(\mathrm{p})}}{|\mathrm{N}_{\mathrm{MinPts}}(\mathrm{p})|} \quad (2)$$

The outlier factor of object p captures the degree to which p was called an outlier. It is the average of the ratio of the local reachability density of p and those of p's MinPts-nearest neighbors. It is easy to see that the lower p's local reachability density is, and the higher the local reachability densities of p's MinPts-nearest neighbors are, the higher the LOF value of p.

2.2.2 Metrics for performance evaluation

Classification metrics are highlighted and used as a benchmark to evaluate the performance of classification algorithms. Therefore, a set of metrics was used to compare and evaluate the adjusted unsupervised machine learning algorithm.

Accuracy (ACC) considers all normal and fault samples. ACC can be calculated as:

$$\mathrm{ACC} = \frac{\mathrm{TP} + \mathrm{TN}}{\mathrm{n}_{\mathrm{total}}} \quad (3)$$

where TP is the number of true positives, TN is the number of true negatives and n_{total} is the total number of samples. Precision (PR) means the true positive value compared to the false negative. PR can be calculated as:

$$\mathrm{PR} = \frac{\mathrm{TP}}{\mathrm{TP} + \mathrm{FP}} \quad (4)$$

where FP is the number of false positives.

Recall (REC) indicates the proportion of anomalous data that are correctly detected from all anomalies. Typically, in industrial applications, REC is a prominent

metric as false negatives lead to much more harmful results than false alarms or false positives. The REC can be calculated as:

$$\mathrm{REC} = \frac{\mathrm{TP}}{\mathrm{TP} + \mathrm{FN}} \tag{5}$$

where FN is the number of false negatives.

Specificity (SP) estimates the ability of the algorithm to predict true negatives over false positives and can be calculated as:

$$\mathrm{SP} = \frac{\mathrm{TN}}{\mathrm{TN} + \mathrm{FP}} \tag{6}$$

The F1 Score is a harmonic mean between REC and PR, and can be estimated as:

$$\mathrm{F1} = \frac{2(\mathrm{PR} \cdot \mathrm{REC})}{\mathrm{PR} + \mathrm{REC}} \tag{7}$$

For cases with unbalanced data, Accuracy (ACC) is not an appropriate measure; in such cases, it is essential to use balanced accuracy (ACCb), which can be estimated as:

$$\mathrm{ACCb} = \frac{\mathrm{REC} + \mathrm{SP}}{2} \tag{8}$$

The use of F1 as a metric also enables mitigation of the effect of the unbalanced database, since the amount of positive data is much smaller than the negative data in the used database. Accuracy has little sensitivity in cases of temporal classification.

AUC-ROC presents a relationship between the False Positive Rate (FPR) and the True Positive Rate (TPR), where FPR is equivalent to 1 – SP; values close to 1 indicate classifiers with excellent performance. In addition to classification metrics, in time series analysis, the correct identification of a failure is as important as its rapid detection. Detection time (TD) is measured in seconds and defined as the difference

between the time when the calculated parameter (cp) was below the defined threshold (cp threshold), indicating the failure, and the time of the existing failure classification in the database.

2.3 Case studies

2.3.1 Public database and data processing

The developed model was first evaluated on data from well and platform sensors in operation from a public database (VARGAS et al. (2019)), which contains a classification of problems that occurred in wells and production lines and includes real data for spurious DHSV closure. Spurious closure often occurs without any indication on the surface, such as a pressure drop in the hydraulic actuator. The automatic identification of spurious closure of this valve promptly can allow it to be reopened through corrective operating procedures, avoiding production losses and additional costs.

Figure 5 shows a schematic view of an offshore well connected to the production platform and the position of the TPT sensors (pressure and temperature sensor on the Christmas tree), the PDG (Pressure Downhole Gauge), and the subsurface safety valve (DHSV) in an offshore well.

Figure 5 - Schematic view of the offshore well connected to the production platform.

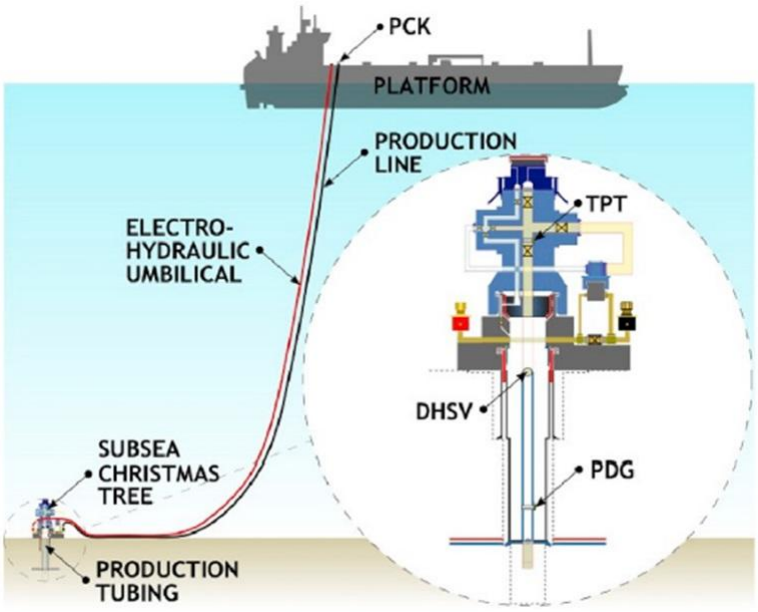

Source: VARGAS et al. (2019)

The main sensors/attributes to be used were: i) pressure and temperature sensors in the TPT of the Wet Christmas Tree; ii) pressure and temperature sensors in the PDG; and iii) surface pressure in the well production/injection line. Table 1 presents the attributes available in the database, descriptions, and units. The available data are in the frequency of one second.

Table 1 - Available attributes in the database with descriptions and units.

Name	Description	Unit
P-TPT	Pressure on temperature/pressure transducer (TPT)	Pa
T-TPT	Temperature on temperature/pressure transducer (TPT)	ºC
P-PDG	Pressure on Pressure Downhole Gauge (PDG)	Pa
P-MON-CKP	Pressure in the production choke on the surface	Pa

When building the database, VARGAS et al. (2019) classified each event instance in addition to failure periods. The transient and steady states of failure were unified as a single anomalous state, that is, a binary classification (normal and failure) was performed. There is no not-a-number (NaN) value in the variable monitoring data. However, there are few data points without labels (NaN values in the class column). For these samples, the data located between the transient and steady-state periods of failure were considered a failure, and the rest as normal. Table 2 presents a summary

of the datasets used. Some datasets of public database related to class 2 were not used due to not have examples of normal data at the beginning of timestamps.

Table 2 - Summary of data statistics.

Id Dataset	Name of Dataset	Data Balance (%)a	Number of Timestamps (#)	Number of Points (#)
1	WELL-00003_20141122214325.csv	74.20	9485	28455
2	WELL-00003_20170728150240.csv	64.74	7047	21123
3	WELL-00003_20180206182917.csv	87.26	5084	15252
4	WELL-00009_20170313160804.csv	47.28	6738	20214
5	WELL-00010_20171218200131.csv	55.89	5310	15930
6	WELL-00011_20140515110134.csv	96.82	20868	62604
7	WELL-00011_20140530100015.csv	74.87	1980	5940
8	WELL-00011_20140606230115.csv	85.47	13232	39696
9	WELL-00011_20140726180015.csv	73.27	3450	10350
10	WELL-00011_20140824000118.csv	83.77	17923	53769
11	WELL-00011_20140916060300.csv	34.51	5614	16842
12	WELL-00011_20140929170028.csv	63.48	2702	8106
13	WELL-00011_20140929220121.csv	25.84	4632	13896
14	WELL-00012_20170320033022.csv	53.81	1703	5109
15	WELL-00013_20170329020229.csv	62.99	9989	29967

[a] Percentage of failure classifications in relation to the total data of each dataset.

2.3.2 Model parameterization

Different combinations of parameters were implemented and tested during the execution of the algorithms. The intention of this study was not to exhaustively test all possible parameterizations, as it would be necessary to test all possibilities of existing parameters, which would be laborious and with a high level of computational cost. However, some hyperparameter adjustments were performed to obtain the best possible results given the mentioned restrictions. The hyperparameters N_neighbors and leaf_size were optimized through hyperparameter tuning, for example, in a grid search procedure. In the current study, the value 32 for N_neighbors and the value 30 for leaf_size were defined in accordance with the database used. All algorithms were implemented using Python 3.9 programming language. Table 3 presents the hyperparameters used in the Local Outlier Factor estimator in the public datasets and for the cases studied, after the grid search procedure.

Table 3 - Hyperparameters used for Local Outlier Factor estimator.

N_neighbors	algorithm	leaf_size	metric	p	contamination	novelty	N job
32	Ball_tree	30	Minkowski	2	Auto	True	None

For the first time step of the public database, an interval of 240 seconds (4 minutes) was defined for the training window, which was composed of 240 samples of each attribute, and the next 60 seconds was defined as the test set size. At each iteration, the model response is calculated (cp index) for each point of the test set, which varies from 1 to -1, a window is then created to analyze the last results provided by the model, and a threshold is defined; in this case, the threshold used (cp threshold) was 0 (zero). Sensitivity studies were also carried out, varying this threshold by 5% (cp threshold +0.05), 10% (cp threshold +0.10), and 20% (cp threshold +0.20). If the failure threshold has not been reached in the test set, a time step of 60 seconds is given (size of the test set), and the training set is again reassigned, now using the last 3 minutes as shown in Figure 3. If the failure threshold has been reached, the model is not retrained, being only tested again for the next time step and test set.

For the real use cases coming from the monitoring system, the number of samples of each attribute was kept the same, containing 240 samples for the training set. However, the data arrives with a much lower frequency than the public base, the data are obtained every 30 seconds, so the training period represents 2 hours (120 minutes) and the test period with 60 samples represents the next 30 minutes.

2.3.3 Real Dataset – Brazil's pre-salt offshore wells

After the evaluation of the developed model using the public database with the hyperparameters and the other model’s parameterization described previously, the developed model was implemented in production/injection subsea wells in the Santos basin, eastern Brazil, all equipped with multiplexed Wet Christmas Trees. A web-based prototype was developed to provide a user-friendly experience for monitoring multiple wells simultaneously. The proposed methodology was integrated into an in-house real-time monitoring system of offshore wells, gathering data from sensors of subsea production/injection wells. An advantage of this system lies in its comprehensiveness in identifying anomalies related to downhole safety valves for hundreds of subsea wells where the anomalies would be difficult for human operators to track. In subsea wells

scenarios, certain challenges have been observed. These include sporadic gaps in sensor data during real-time monitoring and a reduced acquisition frequency in comparison to publicly available data. Consequently, these factors extend the analysis period when compared to the previously utilized public database. Some use cases, compared with human post-classification are presented in the following sequence.

The model was applied in several wells and four case studies are highlighted to illustrate the efficacy of the model developed in monitoring situations and anomalous events detected:

Well #1 is an oil production well in the pre-salt area in Santos Basin, water depth of 1955 m, drilled in five phases with directional trajectory and final depth of 5821 m, equipped with Intelligent Completion Valves and producing in two different zones at 5376 m to 5738 m.

Well #2 is an oil production well in the pre-salt area in Santos Basin, ultradeep water scenario (2029 m), drilled in four phases, directional trajectory, and final depth of 5928 m, equipped with Intelligent Completion Valves and producing in three different zones at 5489 m to 5928 m.

Well #3 is an oil production well in the pre-salt area in Santos Basin, ultradeep water scenario (2041 m), drilled in five phases, directional trajectory, and final depth of 5870 m, equipped with Intelligent Completion Valves and producing in three different zones at 5432 m to 5774 m.

Well #4 is an injector of water well in the pre-salt area in Santos Basin, in water depth of 2022 m, drilled in four phases, vertical trajectory and final depth of 5923 m, equipped with Intelligent Completion Valves, and injecting in two different zones at 5407 m to 5854 m.

2.4 Results and discussion

2.4.1 Evaluation of the proposed model using a public database

The first results presented are the evaluation of the proposed model using the public database (VARGAS et al. (2019)). The analysis and calculation of the metrics for each of the fifteen id datasets varying the thresholds (cp threshold) from 0 to 0.05, 0.1, and 0.2 are shown in Tables 4-7, respectively. The tables show the metrics obtained by applying the unsupervised Novelty and Outlier Detection model of the Scikit-learn 2022 with the hyperparameters shown in Table 3.

Table 4 - Results obtained by the unsupervised model (cp threshold = 0).

Id dataset	ACC	PR	REC	SP	F1	ACCb	AUC-ROC	TD(s)
1	0.9977	0.9977	1	0.9927	0.9988	0.9963	0.9952	16
2	0.9903	0.9902	1	0.9798	0.9950	0.9899	0.9850	45
3	0.9876	0.9897	1	0.8867	0.9948	0.9433	0.9382	46
4	0.9967	0.9990	1	0.9990	0.9995	0.9990	0.9990	4
5	0.9844	0.9935	0.9898	0.9909	0.9917	0.9903	0.9922	20
6	0.9978	1	0.9987	1	0.9993	0.9993	1	-26
7	0.9770	0.9932	1	0.9600	0.9966	0.9800	0.9766	10
8	0.9997	0.9998	1	0.9988	0.9999	0.9994	0.9993	2
9	0.9863	0.9944	1	0.9792	0.9972	0.9896	0.9868	14
10	0.9978	0.9982	1	0.9902	0.9991	0.9951	0.9876	26
11	0.9962	1	0.9917	1	0.9958	0.9958	1	-16
12	0.9976	1	0.9977	1	0.9988	0.9988	1	-4
13	0.9918	1	0.9799	1	0.9898	0.9899	1	-24
14	0.9815	1	0.9955	1	0.9978	0.9977	1	-4
15	0.9966	1	0.9993	1	0.9996	0.9996	1	-4
mean	0.9919	0.9970	0.9968	0.9852	0.9969	0.9910	-	-
SD	0.0071	0.0038	0.0057	0.0295	0.003	0.0143	-	-

Table 5 - Results obtained by the unsupervised model (cp threshold = 0.05).

Id dataset	ACC	PR	REC	SP	F1	ACCb	AUC-ROC	TD(s)
1	0.9977	0.9977	1	0.9927	0.9977	0.9963	0.9952	16
2	0.9903	0.9902	1	0.9798	0.9950	0.9899	0.9850	45
3	0.9876	0.9897	1	0.8867	0.9948	0.9433	0.9382	46
4	0.9967	0.999	1	0.999	0.9995	0.9995	0.9990	4
5	0.9903	0.9936	1	0.9909	0.9967	0.9954	0.9922	19
6	0.9978	1	0.9987	1	0.9993	0.9993	1	-26
7	0.9770	0.9932	1	0.96	0.9966	0.9800	0.9766	10
8	0.9997	0.9998	1	0.9988	0.9999	0.9994	0.9993	2
9	0.9863	0.9944	1	0.9792	0.9972	0.9896	0.9868	14
10	0.9961	0.9962	1	0.979	0.9981	0.9895	0.9876	56
11	0.8343	0.6881	0.9917	0.7466	0.8125	0.8691	0.7174	1125
12	0.9976	1	0.9977	1	0.9988	0.9988	1	-4
13	0.9918	1	0.9799	1	0.9898	0.9899	1	-24
14	0.9815	1	0.9955	1	0.9978	0.9977	1	-4
15	0.9966	1	0.9993	1	0.9996	0.9996	1	-4
mean	0.9814	0.9761	0.9975	0.9675	0.9849	0.9825	-	-
SD	0.0412	0.0798	0.0054	0.0677	0.0478	0.0344	-	-

Table 6 - Results obtained by the unsupervised model (cp threshold = 0.10).

Id dataset	ACC	PR	REC	SP	F1	ACCb	AUC-ROC	TD(s)
1	0.9068	0.8915	1	0.6119	0.9426	0.8059	0.7517	903
2	0.9903	0.9902	1	0.9798	0.9950	0.9899	0.9850	45
3	0.9876	0.9897	1	0.8867	0.9948	0.9433	0.9382	46
4	0.9967	0.9990	1	0.999	0.9995	0.9995	0.9990	4
5	0.9903	0.9936	1	0.9909	0.9967	0.9954	0.9922	19
6	0.9978	1	0.9987	1	0.9993	0.9993	1	-26
7	0.9770	0.9932	1	0.9600	0.9966	0.9800	0.9766	10
8	0.9997	0.9998	1	0.9988	0.9999	0.9994	0.9993	2
9	0.9863	0.9944	1	0.9792	0.9972	0.9896	0.9868	14
10	0.9961	0.9962	1	0.9790	0.9981	0.9895	0.9876	56
11	0.6058	0.4780	1	0.3843	0.6468	0.6921	0.4312	2111
12	0.9976	1	0.9977	1	0.9988	0.9988	1	-4
13	0.9918	1	0.9799	1	0.9898	0.9899	1	-24
14	0.9815	1	0.9955	1	0.9978	0.9977	1	-4
15	0.9966	1	0.9993	1	0.9996	0.9996	1	-4
mean	0.9601	0.9550	0.9981	0.9180	0.9702	0.9580	-	-
SD	0.1006	0.1348	0.0052	0.1782	0.0906	0.0887	-	-

Table 7 - Results obtained by the unsupervised model (cp threshold = 0.20).

Id dataset	ACC	PR	REC	SP	F1	ACCb	AUC-ROC	TD(s)
1	0.8387	0.8255	1	0.3263	0.9044	0.6631	0.5759	1486
2	0.7212	0.7079	1	0.1610	0.8290	0.5805	0.4345	1875
3	0.9876	0.9897	1	0.8867	0.9948	0.9433	0.9382	46
4	0.6366	0.5755	1	0.2906	0.7305	0.6453	0.4331	2343
5	0.9903	0.9936	1	0.9909	0.9967	0.9954	0.9922	19
6	0.9989	0.9998	1	0.9905	0.9999	0.9952	0.9951	4
7	0.9770	0.9932	1	0.9600	0.9966	0.9800	0.9766	10
8	0.9997	0.9998	1	0.9988	0.9999	0.9994	0.9993	2
9	0.9863	0.9944	1	0.9792	0.9972	0.9896	0.9868	14
10	0.9944	0.9943	1	0.9677	0.9971	0.9838	0.981	86
11	0.6058	0.4780	1	0.3843	0.6468	0.6921	0.4312	2111
12	0.9976	1	0.9977	1	0.9988	0.9988	1	-4
13	0.9918	1	0.9799	1	0.9898	0.9899	1	-24
14	0.9815	1	0.9955	1	0.9978	0.9977	1	-4
15	0.9750	0.9676	0.9993	0.9390	0.9832	0.9691	0.9533	326
mean	0.9122	0.9013	0.9982	0.7917	0.9375	0.8949	-	-
SD	0.1408	0.1739	0.0052	0.3172	0.1126	0.1580	-	-

Figure 6 presents an example of a result for id dataset 1, for a threshold (cp threshold) equal to 0, showing a classification (classification) generated by the model that is very close to the classification contained in the database (class), considering the transient and steady-state intervals of failure as failure state. In Figure 6, the x-axis presents the time, and the y-axis presents the variables P-PDG, P-TPT, T-TPT, and P-MON-CKP normalized using StandardScaler (SCIKIT-LEARN 2022) the model classification (classification) and fault classification (class).

Figure 6 - Example of data analysis between model classification (classification) and fault classification (class) in the database for Id dataset 1.

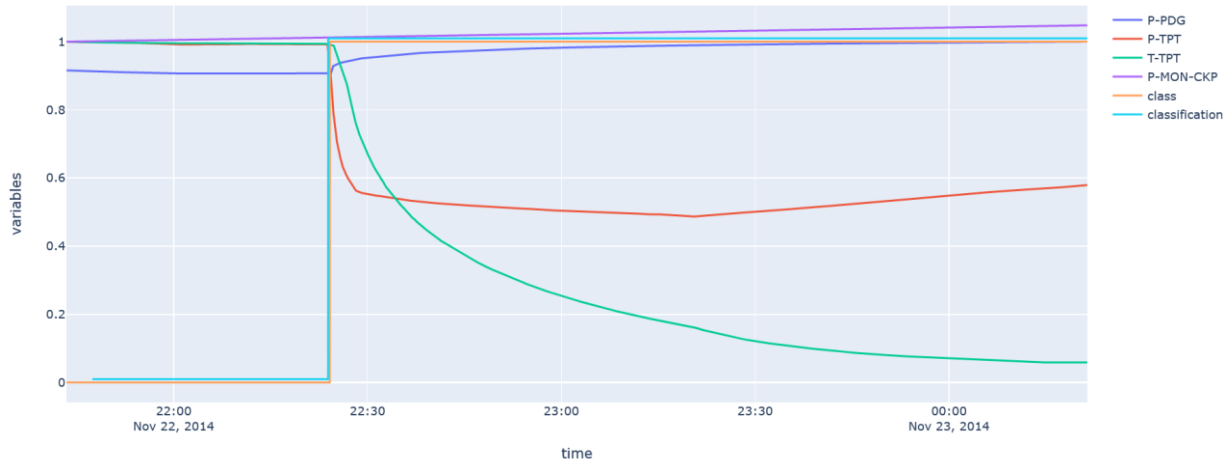

The best result was obtained for a threshold (cp threshold) equal to 0, as can be seen by the balanced accuracy (ACCb), F1-SCORE, and other metrics. The average balanced accuracy for the 15 datasets tested was 0.991 with a standard deviation of 0.014. A worsening in the performance of the model was observed with a positive variation of the threshold (cp threshold). Figure 7 shows the variation of the means calculated for each of the metrics as a function of the value defined as the failure threshold (cp threshold).

Figure 7 - Results obtained for metrics ACC, PR, REC, SP, F1-SCORE, and ACCb (mean values) as a function of threshold variation (cp-threshold).

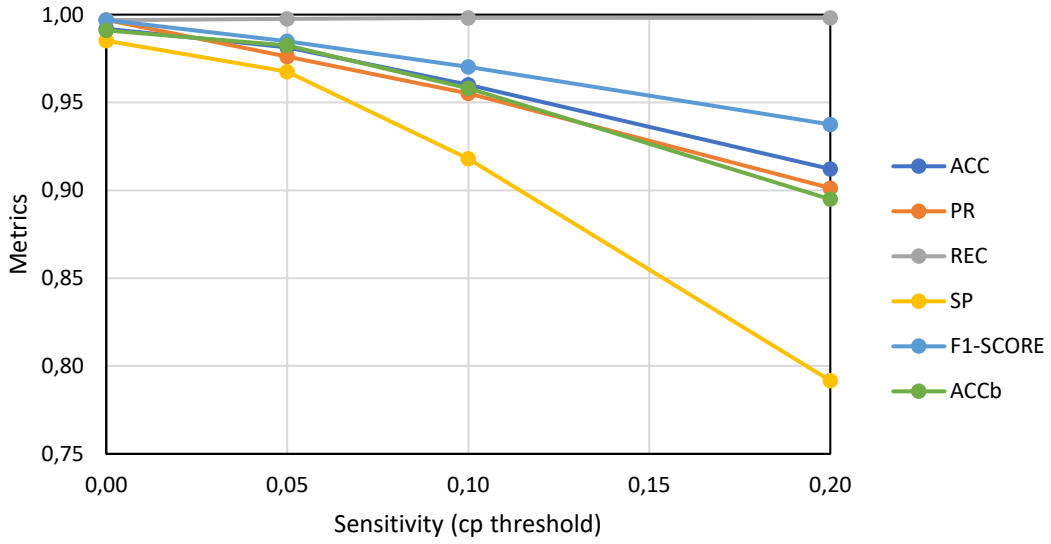

2.4.2 Comparison with other methods

The results of the present study were compared with those of previous studies in the literature using Random Forest (MARINS et al. (2021)), Decision Tree (TURAN and JASCHKE (2021)), and LTSM (MACHADO et al. (2022)). This comparison using the same public database (VARGAS et al. (2019)) is important to analyze the advances achieved between the different methods applied to the detection of the same type of event in subsea wells.

Table 8 presents the summarized results for the four classifiers applied to spurious DHSV closures. RF was used for the Random Forest results of MARINS et al. (2021), DT for the Decision Tree work of TURAN and JASCHKE (2021), and LTSM for the work of MACHADO et al. (2022). Finally, LOF was used for the present study, and comparisons are shown in the ACC, F1-SCORE, and ACCb metrics.

Table 8 - Comparison of metrics between literature and the proposed methods for identifying spurious closure events of DHSV.

Classifiers	Accuracy (ACC)	F1-SCORE	Balanced Accuracy (ACCb)
RF	0.8708	-	-
DT	0.6000	0.4900	-
LSTM (g =0.6)	0.9992	0.9360	-
LOF (cp threshold =0)	0.9991	0.9969	0.9910

The proposed model using a Novelty and Outlier Detection algorithm from the Scikit-learn package (2022) with a Local Outlier Factor (LOF) estimator obtained similar results to the LSTM model when comparing the accuracy metric (ACC) and F1-SCORE. The results for identifying spurious closure events using DT (TURAN and JASCHKE (2021)) were justified by the lower number of instances.

2.4.3 Application in Brazil's pre-salt offshore wells

The five cases to four offshore wells studied, compared with human post-classification (class) are presented in the following sequence. The analyzed data from well #1 is presented in Figure 8 and shows data from the PDG Pressure (P-PDG), TPT Pressure (P-TPT), TPT Temperature (T-TPT) sensors, and Production Choke Position at Topside (CHK, %) along the results of analyses and classifications for a specific

time window at 02/25/2021. The model (blue curve) identified the event properly at 2:32 PM, the anomalous events were corrected by the operator in the sequence with valve cycling performed from 2:54 PM to 5:24 PM, and the human post classification (class) identified the event at 2:54 PM.

Figure 8 - Results for well #1 for the anomalous event detected – PDG, TPT sensors, and Production Choke Position at Topside, comparison between model (classification) and fault classification (class).

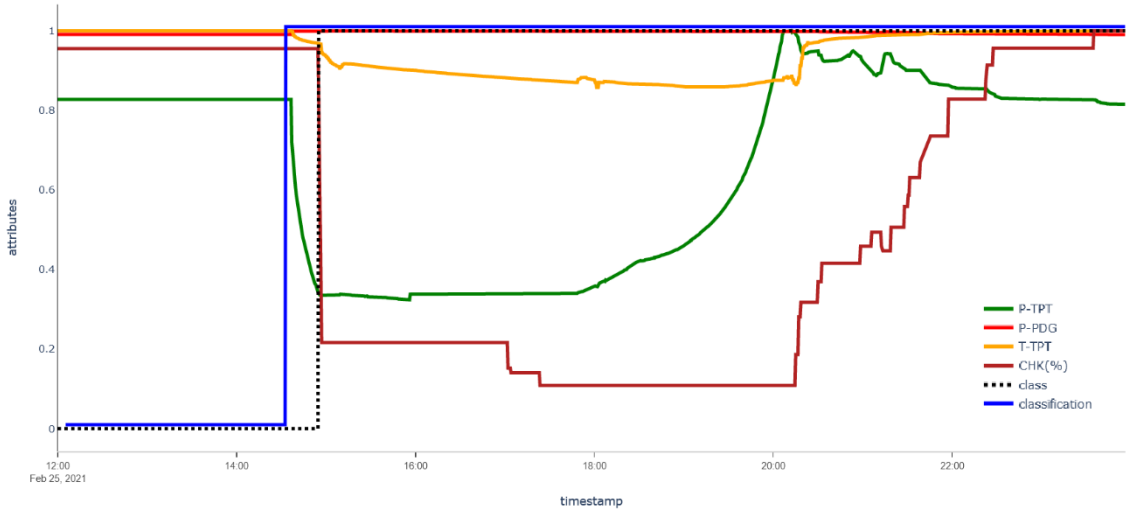

The following example refers to well #2. In this well, the developed system was applied, and identified an anomaly event at 5:57 PM on 04/21/22. In the field, the problem was only detected sometime later and corrected by the operator in the sequence with valve cycling. Figure 9 presents the data from the PDG Pressure (P-PDG), TPT Pressure (P-TPT), TPT Temperature (T-TPT) sensors, and Production Choke Position at Topside (CHK, %) and classifications along the period of 04/21/22 to 04/23/22.

Figure 9 - Results for well #2 for the anomalous event detected – PDG, TPT sensors, and Production Choke Position at Topside, comparison between model (classification) and fault classification (class).

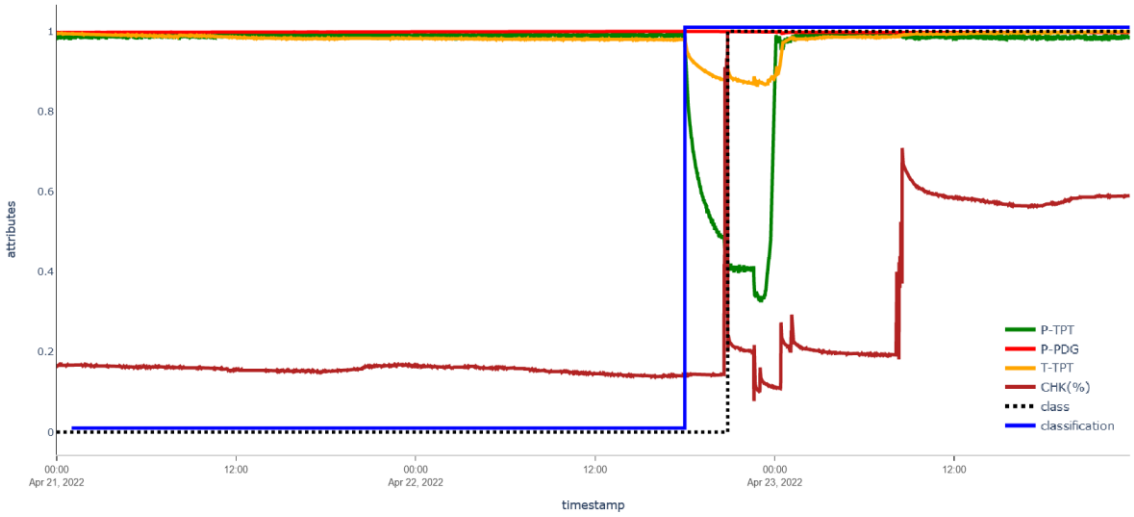

Figure 10 presented data and results for the first anomalous event at well #3, on 06/04/2022. The model identified the anomaly at 4:14 PM (curve classification) and correctly classified it as spurious closure of DHSV. It is important to note that the operator then proceeded with the valve cycling and reopening procedure, resuming production in a safe condition. After the reopening well at 11:50 PM, the system restarts to analyze.

Figure 10 - Results for well #3 for the first anomalous event detected – PDG, TPT sensors, and Production Choke Position at Topside, comparison between model (classification) and fault classification (class).

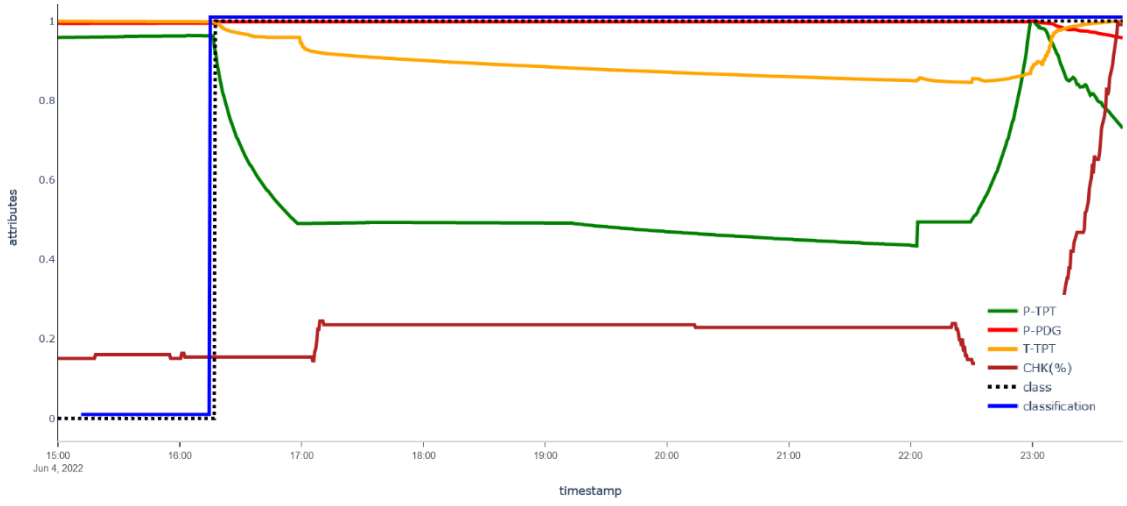

After some time, a second anomalous event for well #3, on 06/06/2022, was identified and presented in Figure 11. The model identified the anomaly at 6:29 PM (curve classification) and correctly classified the spurious closure of DHSV. It is important to note that the operator again proceeded with the valve cycling and reopening procedure, resuming production in a safe condition. After the reopening well on 06/07/23 at 6:50 AM, the system restarts to analyze.

Figure 11 - Results for well #3 for the second anomalous event detected – PDG, TPT sensors, and Production Choke Position at Topside, comparison between model (classification) and fault classification (class).

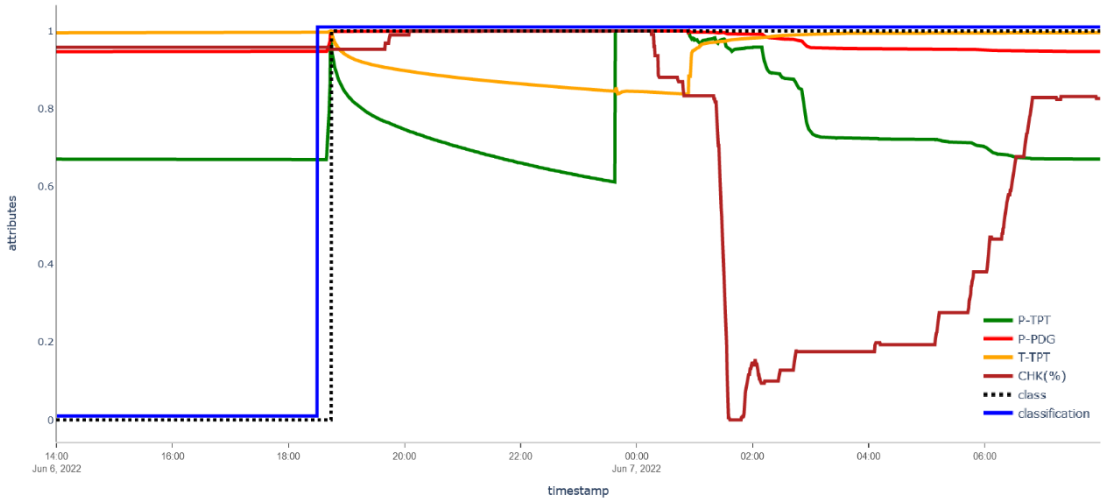

Figure 12 presents data and results for well #4, on 04/25/2022. The model identified the anomaly at 10:44 AM (curve classification) and correctly classified it as spurious closure of DHSV. In the field, the problem was only detected sometime later.

Figure 12 - Results for well #4 for anomalous event detected – PDG, TPT sensors, and Production Choke Position at Topside, comparison between model (classification) and fault classification (class).

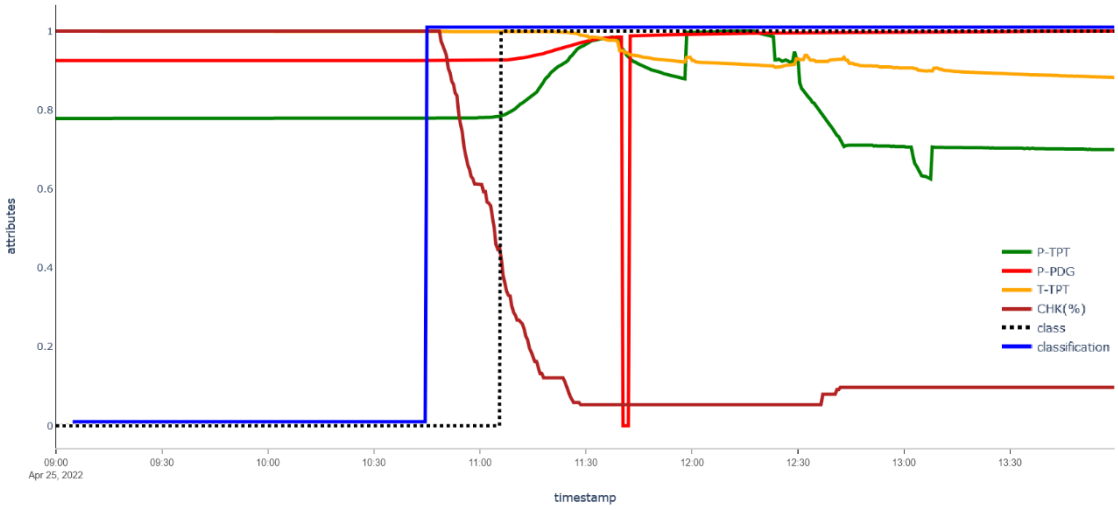

Table 9 presents the Accuracy, F1-SCORE, and the balanced accuracy values (ACCb) calculated for the cases studied when compared with the human post-classification (class).

Table 9 - Comparison of metrics for cases studied in this dataset.

Well	Accuracy (ACC)	F1-SCORE	Balanced Accuracy (ACCb)
#1	0.9606	0.9797	0.8819
#2	0.9561	0.9438	0.9191
#3 – 1st event	0.9635	0.9972	0.9257
#3 – 2nd event	0.9848	0.9909	0.9587
#4	0.9106	0.9430	0.7870

The proposed system performs well on the task of anomaly detection, presenting detection rates exceeding 90% in the real field production scenarios studied. Changes in well and reservoir conditions over time impose concept and data drift in time series, which are challenging factors for machine learning models.

2.5 Conclusions

This study focused on using an unsupervised machine learning algorithm for anomaly detection in multivariate oil production time series data, particularly targeting spurious subsurface safety valve closures. The main findings can be found as follows:

Highly Accurate Anomaly Detection: The proposed model demonstrates good performance with a balanced accuracy (ACCb) of 0.9910 and an F1-SCORE of 0.9969 when predicting spurious DHSV closure events, addressing the challenge of unbalanced databases.

Threshold Optimization: The model achieved optimal results with a threshold (cp threshold) set at 0, as evidenced by superior ACCb and F1-SCORE metrics.

Innovation in Anomaly Detection: It was introduced a Novelty and Outlier Detection algorithm using Local Outlier Factor (LOF) from the Scikit-learn package, showcasing competitive accuracy with LSTM models and superior F1-SCORE.

Real-World Application: The proposed LOF-based method exhibits excellent accuracy, with over 90% detection rates in offshore well production scenarios. This early anomaly identification minimizes non-productive time (NPT) and significantly boosts oil production.

Robustness to Concept and Data Drift: The model's ability to maintain high detection rates in the face of changing well and reservoir conditions highlights its resilience to concept and data drift in time series data, a critical factor in real-world applications.

Field Testing: The model's applicability was validated in ultradeep water subsea wells in the pre-salt area of the Santos Basin, demonstrating its potential to enhance anomaly prediction in offshore wells, ultimately reducing costly equipment malfunctions and safeguarding well integrity.

Industry Impact: This research addresses pressing concerns in the oil and gas industry by enabling timely anomaly detection and corrective actions, leading to improved operational safety and substantial cost reduction.

In summary, the research introduces an innovative approach to anomaly detection in offshore well production scenarios, offering high accuracy, robustness, and real-world applicability.

CHAPTER 3 - A SYSTEM TO DETECT OIL WELL ANOMALIES USING DEEP LEARNING AND DECISION DIAGRAM DUAL APPROACH

3.1 Introduction

For decades, the oil and gas industry has been a key player in the global economy by meeting the world's energy demand. According to ZHONG et al. (2020), fossil sources currently satisfy almost 75% of the world's total demand and are expected to remain the primary energy source for several more years. To improve efficiency and safety, the industry is evolving and embracing digital transformation by incorporating advanced technologies like artificial intelligence, cloud computing, automation, big data, and the Internet of Things.

The oil and gas industry processes are highly complex, requiring careful execution throughout the entire chain, from exploration to distribution. In this context, the adoption of artificial intelligence methodologies stands out as a game-changing initiative to ensure safety, robustness and predictability. GURINA et al. (2020) developed an anomaly detection approach for directional drilling operations, while ANIFOWOSE et al. (2019) compared traditional and sophisticated machine learning techniques for predicting petroleum reservoir permeability. ZHAO et al. (2022) combine machine learning and numerical simulation to model fracture propagation in shale formation. WANG and Chen (2019) utilized Long Short-Term Memory networks (LSTMs) to learn the pressure transient behavior in naturally fractured tight reservoirs. In TANG et al. (2021), Generative Adversarial Networks (GANs) are employed along with gradient boosting algorithms to predict shale reservoir quality in searching for sweet spots.

The smooth and safe production of oil wells requires continuous attention to ensure that the fluid from the reservoir reaches the surface efficiently. However, due to varying temperature and pressure conditions throughout the well's lifecycle, issues such as equipment failure, poorly performed operations, or unforeseen circumstances during the design stage may arise. As a result, monitoring equipment is installed to observe the behavior of the well. According to HÜFFNER et al. (2019), pressure and temperature sensors are typically located at the bottom of the production column, specifically the Permanent Downhole Gauge (PDG), and at the Wet Christmas-Tree,

in the case of the Temperature/Pressure Transducer (TPT). The data transmitted from these sensors can be used to assess the condition of the well.

In many industries, including the oil industry, monitoring various data of interest through sensors is a common practice to detect possible undesired conditions in structures and prevent accidents. VARGAS et al. (2019) emphasize that detecting and classifying rare undesirable events is a crucial task in various activities monitored by humans. VENKATASUBRAMANIAN (2003) adds that the mission of responding to unexpected events involves promptly detecting anomalous behaviors, diagnosing their root causes, and taking appropriate control actions to bring operations back to a healthy, safe, and operational state.

To achieve autonomous monitoring, various intelligent techniques are applied, including machine learning methodologies and, more specifically, deep learning. These latter can be particularly useful in identifying possible anomalies in the data collected by sensors. MARCHI et al. (2015) and MALHOTRA et al. (2015) propose methodologies that use deep learning to detect abnormal behavior in time series data. CHENG et al. (2022) apply deep learning techniques for the prediction and detection of scale buildup in production wells. A systematic review on the use of artificial intelligence in oil well drilling and production is provided by D'ALMEIDA et al. (2022).

Machine learning techniques have been applied to well production monitoring for the detection of specific events. ALHARBI et al. (2022) address anomaly detection in production data, comparing the performance of models that he refers to as white-box and black-box, with respect to their explainability. Among the models tested, DT stands out for its interpretability and performance. TURAN and JASCHKE (2021) applied different classifiers such as Adaptive Boosting (AdaBoost), Linear and Quadratic Discriminant Analysis, DT and Random Forest (RF) to the analysis of well production problems presented in VARGAS et al. (2019). The authors state that DT achieved a balanced accuracy of 88%, performing better than more robust techniques such as RF and AdaBoost. FIGUEIREDO et al. (2021) applied six unsupervised models to detect anomalous events in a production line, and their best-ranked model achieved an accuracy ranging from 97% to 100%. In addressing the scale deposition problem, YOUSEFZADEH et al. (2022) compared the performance of ten different intelligent algorithms, highlighting the performance of K-Nearest Neighbors and Ensemble Learning models. AL-HAJRI et al. (2020) used classification techniques such as DT and Gradient Boosting classifier to generate prediction results for scale

buildup, which are used as inputs for a probabilistic inhibition-design model. MONDAY and ODUTOLA (2021) employed both supervised and unsupervised learning algorithms to address hydrate formation, while GJELSVIK et al. (2023) conducted a systematic review on the use of intelligent techniques to tackle the gas hydrate problem.

Various models based on Support Vector Machines (SVMs), LSTM, and GANs have been presented in the literature for detecting anomalous behavior from pressure and temperature data gathered from subsea well sensors. These models can recognize undesirable events based on the short and long-term responses used for training. Time series novelty detection, or anomaly detection, is a challenging subject in data mining that refers to the automatic identification of new or abnormal events incorporated in the time series regular points. This subject is gaining increasing attention due to its enormous potential for immediate applications. One-class SVMs are a well-established method in literature, as demonstrated in the works of VARGAS et al. (2019), MA and PERKINS (2003), and SHAWE-TAYLOR and ZLICAR (2015). Random Forest (RF) algorithm is also employed for anomaly detection, as can be seen in the study by MARINS et al. (2021), who address different well production problems presented in the work of VARGAS et al. (2019).

The Long Short-Term Memory (LSTM) networks were proposed to create more robust Recurrent Neural Networks that avoid vanishing gradients. They have a sophisticated formulation that enables selective "remember and forget" configurations, allowing for the determination of the amount of previous data to be considered for predicting the next data. Several studies such as VÁVRA and HROMADA (2019), MARCHI et al. (2015), and MALHOTRA et al. (2015) have presented methodologies for detecting abnormal behavior in time series data by using only data from systems in regular operation. In MACHADO et al. (2022), LSTM and one-class SVM were successfully applied to detect two short and long-term problems in well production lines, namely, spurious valve closure and hydrate formation. The results are compared to tree-based classifiers such as DT and RF models.

Generative Adversarial Networks (GAN) use data from standard instances to train two interconnected neural networks, the generator and discriminator. The generator reproduces typical operating scenarios, and the discriminator can detect anomalies and classify the input data. Recent studies, such as LI et al. (2018),

SABOKROU et al. (2018), and MATTIA et al. (2019), have shown that using the GAN discriminator to detect abnormal system behavior produces good results.

The three anomaly detection methodologies discussed have unique characteristics that differentiate them. SVMs have pre-established configurations that make them easy to implement but lack the versatility of the other two methods. While they achieve an accuracy of 70% to 90% in detecting abnormal states according to MARINS (2018), changing the tolerance degree requires adjusting the SVM parameters, which is time-consuming. GAN-based networks are the most sophisticated approach but require a complex configuration and a significant amount of data for training. Although they are capable of accurately reproducing complex signals, their requirement for a robust computer infrastructure can make them impractical for real-time or embedded systems (LI et al. (2018)).

In contrast, LSTM networks are simple to train and can automatically configure for each well and valve state, being versatile in adjusting their configuration and tolerance for detecting anomalies. It is worth mentioning its ability to handle sequential data, considering non-linear and long-term dependencies, as it is observed in the pressure and temperature series collected. These datasets can exhibit complex patterns due to the evolving conditions of the reservoir and the well over time. The memory capability of LSTMs allows for the detection of anomalies that occur intermittently or over extended periods. Regarding the specific problem addressed in this paper, there is a limited availability of labelled anomalous data due to the rare occurrence of anomalies, which is the rationale for choosing a LSTM-based Autoencoder, which can be trained using only data labelled as normal (VÁVRA and HROMADA (2019), MARCHI et al. (2015), and MALHOTRA et al. (2015)).

With that said, the current work proposes a comprehensive anomaly detection methodology that combines LSTM autoencoders and a rule-based analytical approach to real-time anomaly detection in subsea well sensor pressure and temperature data. It is worth mentioning that the methodology relies solely on normal data for training and is capable of detecting anomalies, whether they have been previously mapped or not. It was integrated to a monitoring framework, and this system has been able to deliver a prompt response online well integrity monitoring, improving operational safety and reducing costs associated with non-productive time and failure repair in production/injection wells.

3.2 Methodology

Sensors installed to monitor production in oil wells are located at a few viable positions to monitor the behavior of a well during its operation, and regularly transmit data concerning pressure and/or temperature values along the depth. With an adequate treatment of these data, followed by pattern identification techniques, it becomes possible to evaluate if the well operates within normality or not, allowing operators and engineers to be capable of classifying normal and abnormal situations by analyzing the time series.

In the anomaly detection system, there is an entry point for the sensors data, from which checks are performed with the association of a Decision Diagram (DD) and a deep learning network, as illustrated in Figure 13. The system can map valve configurations and set its anomaly search mechanisms to suit the current valve status. The methodology is developed in such a way that the system is scalable to monitor simultaneously multiple wells.

Figure 13 - General methodology of the proposed dual process.

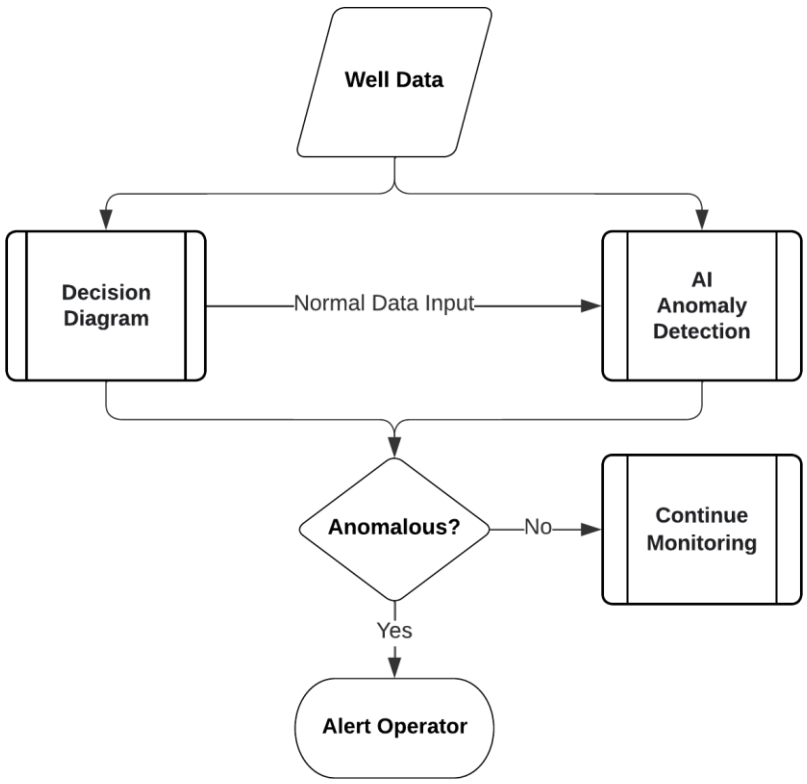

The anomalies detected by the DD can be classified as mapped and unmapped. For the first case, the tool has a portfolio of anomalies that contains the attributes of undesired scenarios in terms of pressure and temperature. The portfolio was designed based on the expected behavior of the well for a given valve configuration. Therefore, the attributes of each scenario are defined by rules and tolerances. As for the second group of anomalies, these are the cases that have not yet been mapped in the system but configure a scenario that does not correspond to the normality of the well in question, being detected due to the behavior patterns that the system attributes to the well for both analytical DD and deep learning approaches.

3.2.1 Analysis of pressure and temperature sensor data

One of the steps in data processing is grouping and synchronizing the pressure and temperature sensor data provided by the oil company. The time series of each sensor are stored in files, containing information gathered in different time intervals. The data were synchronized and grouped based on combinations of valve states in production. The first analysis considered the two main well valve combinations as output, which differ from each other by the open or closed state of the Master 2 valve (M2). Correlation studies are carried out to identify behaviors of well operation that differ from normal. Figure 14 illustrates the correlation between pressure and temperature values collected from sensors, comparing data from literature (VARGAS et al. (2019)) with industry data provided for both the open and closed M2 valve.

The red color indicates positive correlation (directly related variables), and the blue color negative correlation (inversely proportional variables). This study indicates that different valve status configurations should be investigated and taken into consideration during the development of methodologies for anomaly detection, as they influence the correlation between variables.

Figure 14 - Correlation matrices for sensor data.

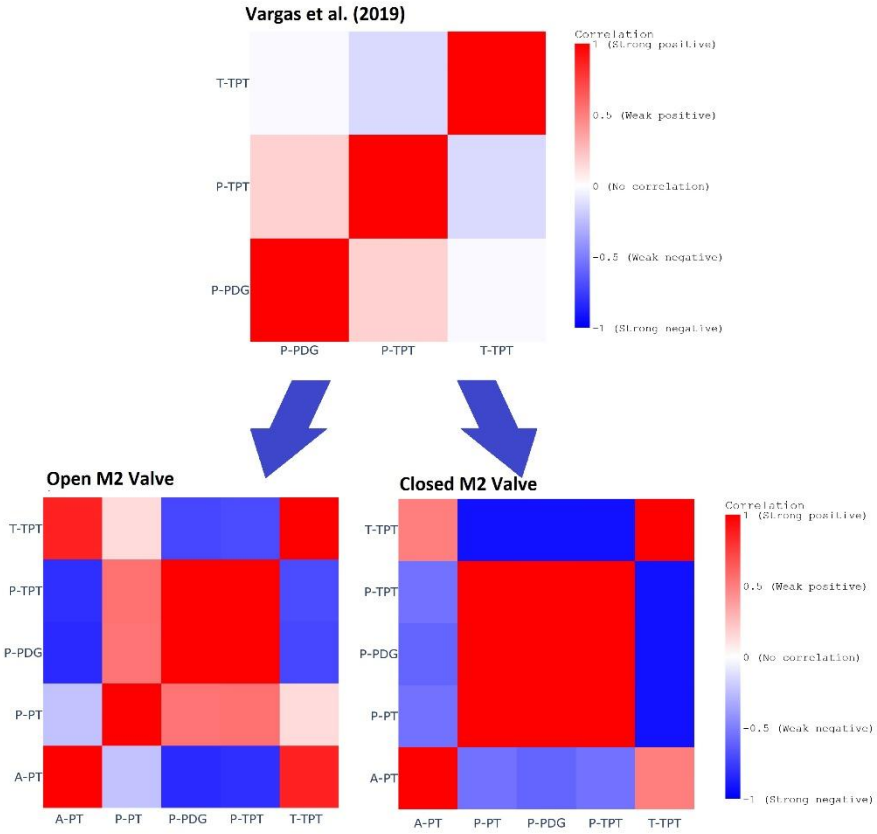

3.2.2 Anomaly detection using the DD

The methodology that defines an action to be taken by the DD consists of structuring a set of rules based on layers with nodes. Each node verifies a condition that determines the next node that the information will be passed to, until it reaches a leaf node. As decisions advance through the internal nodes, the data become increasingly specific. As a result, the DD can effectively manage the information to extract maximum benefits and indicate the occurrence of anomalies.

The first layer of the DD refers to the data of the monitored well, given the tool's capability to track multiple wells simultaneously. In the next layer, the type of well data is checked, determining if it is the initial data or if a valve change has occurred. In the case of initial well data, only the well data structure is created and stored in the database. However, if there has been a change in the state of the operating valves, the system enters standby mode until pressure and temperature levels are normalized. When the state of the valves remains the same, the system performs well behavior analysis to identify possible anomalies.

Finally, the well's state is reported, which can be categorized as either Normal when the pressure and temperature levels are within the expected range, or Analyzing when there is a change in the status of a valve, avoiding false alerts when the sensors are still stabilizing after a valve closure/opening. In addition to these, there are anomaly statuses, such as Anomalous, for when there is a significant change in pressure and temperature levels – greater than a previously set threshold, and the cases of M1/DHSV Closed, W1 Closed, M2 Closed and Tubing leakage. For example, in the case of a production well, if the M1/DHSV are supposed to be open according to the monitoring system, but the pressure at the PDG increases while the pressure at the TPT decreases, the DD alerts that the M1/DHSV valves might be closed. Another scenario is when the W1 valve is reported as open, but there is a sudden simultaneous increase in pressure readings from the TPT and PDG sensors with the same choke opening. In such a case, the monitoring system triggers an alert, suggesting that the W1 valve might be closed. Figure 15 displays the structure of the decision diagram.

Figure 15 - Structure of the Decision Diagram.

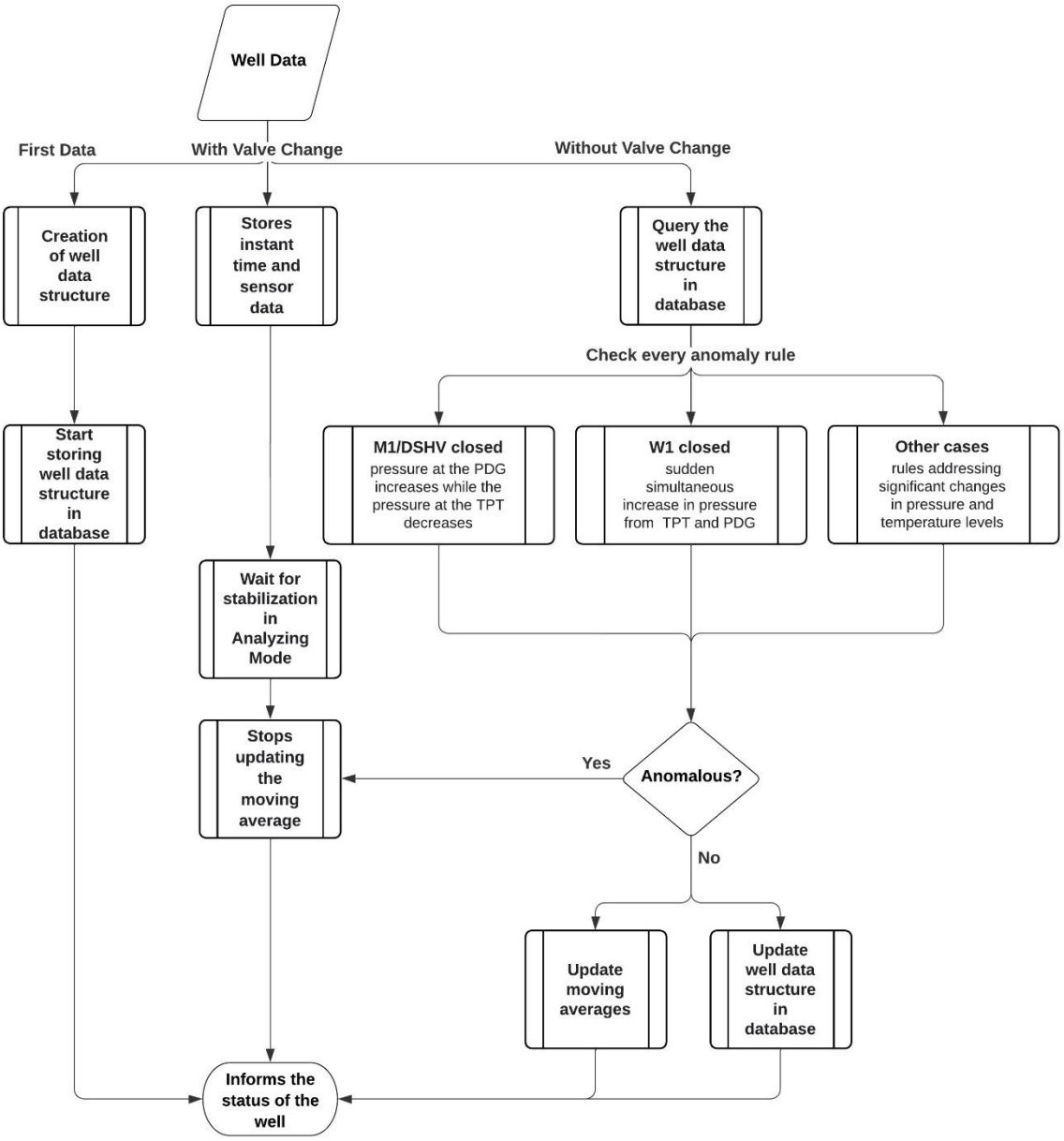

The data concerning pressure and temperature sensors PDG, TPT, and PT are first analyzed together with the state of the monitored valves – DHSV, M1, M2, W1, W2, XO, PXO and Choke valve – to develop the proposed methodology. The typical valve and sensors scheme for a subsea oil well is described in Figure 16. The data history is collected from wells and production vessels (FPSOs) in different oil basins. Initial studies are conducted to determine the behavior and correlations from the pressure and temperature data for the most common combinations of valve states. An

analytical rule-based approach is then developed to detect abnormal variations in the data, serving as a basis for classifying the anomaly based on a known portfolio.

Figure 16 - Oil well valves and sensors scheme.

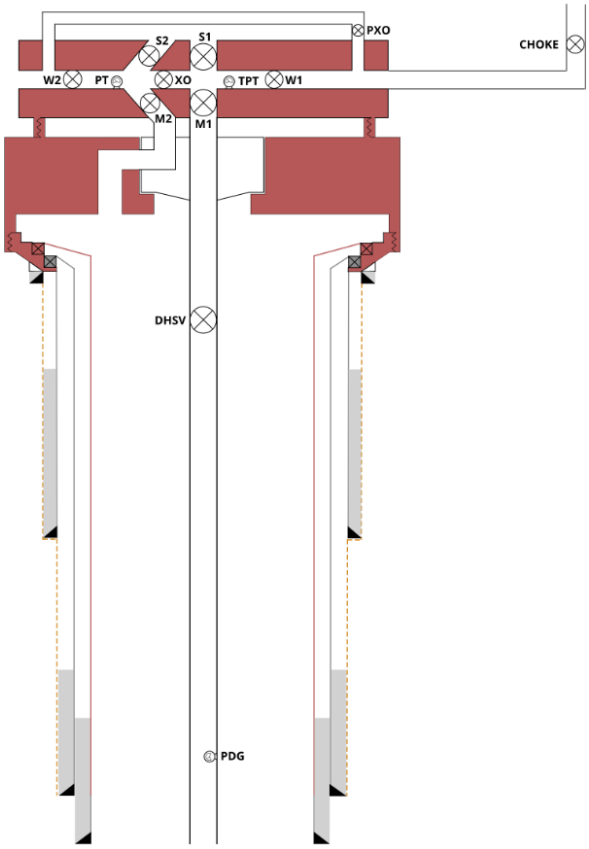

The response of this analytical system is applied to neural network training, also dedicated to anomaly detection. The trained models receive real-time data and monitor valve behavior using load conditions that may indicate abnormal events during oil production based on the current valve scheme. Multiple datasets from the literature (VARGAS et al. (2019)) were used to train and validate the proposed methodology.

After validating the joint application of the analytical and machine learning methodologies, an interface is developed using the Node-Red platform coupled with the python 3.7 code. This tool can receive data from different wells and perform simultaneous monitoring using advanced methods.

3.2.3 Anomaly Detection through Machine Learning

An important challenge for anomaly detection in the oil industry is that data of anomalies is scarce, so it is difficult to train an AI accurate enough to classify anomalies. So, the proposed methodology involves automatically learning what fits as a normal operation state, which happens most of the time, and constantly checking if the new data matches the previously trained. Once the system has learned what is considered normal, it can alert the operator when it detects an abnormal state. This means that for each oil well, the network must collect data and learn on its own without requiring operator interference. In this sense, two modules are developed: one for learning and the other for detection. The learning module stores sequential temporal data classified as normal by the DD formulation. The module enters the training mode after acquiring approximately 500 normal data points, which covers roughly 5,000 seconds of real time production, an amount determined through tests using industry data. It generates three outputs: 1) data normalization parameters, 2) neural network weights, and 3) anomaly tolerance calculated during training. After saving these three outputs, the detection module starts operating, detecting abnormal behaviors in newly acquired data. Networks based on different configurations were tested, and the LSTM-based autoencoder proposed by LARZALERE (2019) had the best results.

The LSTM autoencoder input consists of a multivariate time-series data capturing temperature and pressure readings from various sensors. Given that the model is an autoencoder, it is trained to reconstruct the input time series, after passing through several bottleneck hidden layers which first encode the original data in a lower dimension space, and then decode the original data. This reconstructed data is compared with the original input, yielding what we term as the reconstruction error. This error is then measured against a predefined threshold set during training. Consequently, the LSTM output categorizes the result as either Normal or Anomalous.

Figure 17 depicts the network developed, in which None refers to the batch size, that is not predefined on the model’s constructor, and ReLU refers to the Rectified Linear activation function. The LSTM features consist of pressure values from the sensors TPT, PT and PDG, as well as the temperature values from TPT and PDG.

Figure 17 - Network based on LSTM architecture.

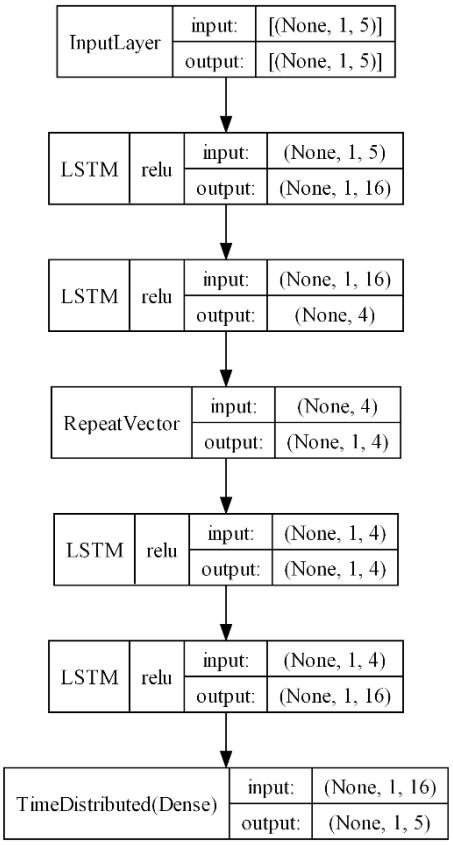

The Adam optimizer (KINGMA and BA (2014)), available in the Keras framework (CHOLLET et al. (2015)), is used to calculate the network weights. The Adam algorithm enhances the classical stochastic gradient descent procedure for optimization. Regarding the error metric, Mean Absolute Error (MAE) and Symmetric Mean Absolute Percentage Error (SMAPE) were applied and obtained similar results, leading to the choice of SMAPE as the main error metric, which is given by**:**

$$SMAPE = \frac{100\%}{n}\sum_{t=1}^{n}\frac{|F_t+A_t|}{(|A_t|+|F_t|)/2} \qquad (9)$$

where:

A_t- real value

F_t- model predicted value

In the studies, the number of epochs is 500 with a batch size of 100. Using a similar approach, the training of the deep network uses 500 instances of data labelled as normal in the DD. After training, the SMAPE value for each prediction is calculated, then approaching this error metric as a normal distribution of values.

Assuming that the reconstruction error follows a Gaussian distribution, the tolerance is evaluated by following equation, in terms of mean of the parameter and its standard deviation, defined as μ and σ, respectively:

$$tol_{AI} = \mu + k\sigma \qquad (10)$$

in which k controls the tolerance interval around the mean and can be set for each problem. In the current study, $k = 3$ was adopted in accordance with the database used, comprising about 99.7% of the normal data saved. The threshold for occurrence of an anomalous event is based in this tolerance. If a new data SMAPE value is under this tolerance, the new instance is a normal data. If SMAPE value exceeds tol_{AI} value, it can be associated with risk levels defined by the operator, supporting the real-time decision-making process. For the purpose of the system presented herein, values exceeding by 30%, 70% and 100% represent low-, medium-, and high-risk anomalies, respectively. Figure 18 illustrates the process flow diagram triggered on a fixed time interval for anomaly detection using the developed LSTM-based autoencoder.

Figure 18 - The process flow diagram for anomaly detection using the developed LSTM-based network.

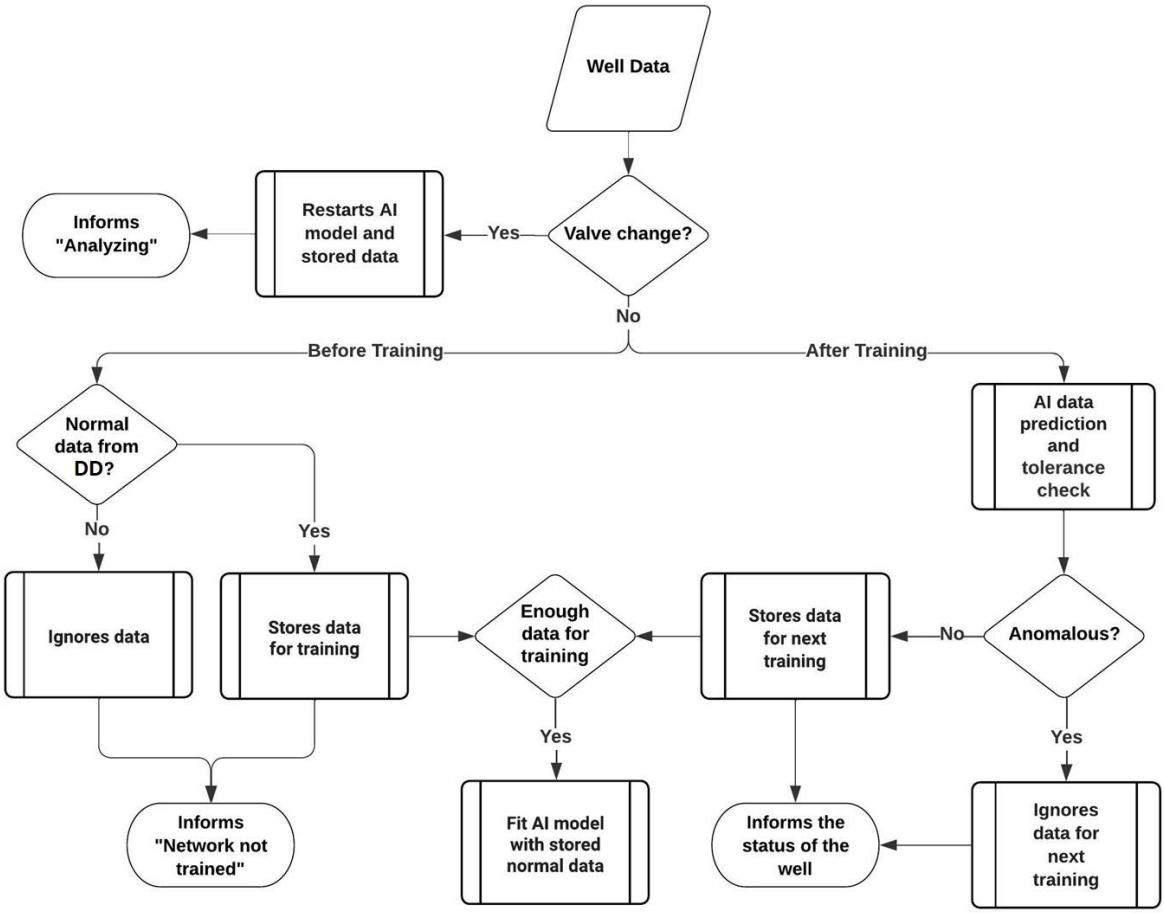

By using both literature VARGAS et al. (2019) and industry data, the autoencoder network was tested to verify its robustness when exposed to time series containing normal, transitional and anomalous points. It was able to correctly classify 98 to 99% of the anomalous data, indicating that the autoencoder network is capable of accurately detecting undesirable events in oil production.

Figure 19 shows an example of abnormal state using real data from a subsea well, in which it can be seen the pressure values gathered from PDG, PT, and TPT in the upper graph, the temperature values from PDG and TPT in the central graph, and the anomaly score value calculated by the neural network in the lower graph, compared to the tolerance line (threshold).

Figure 19 – Illustrative example of anomaly detection using AI.

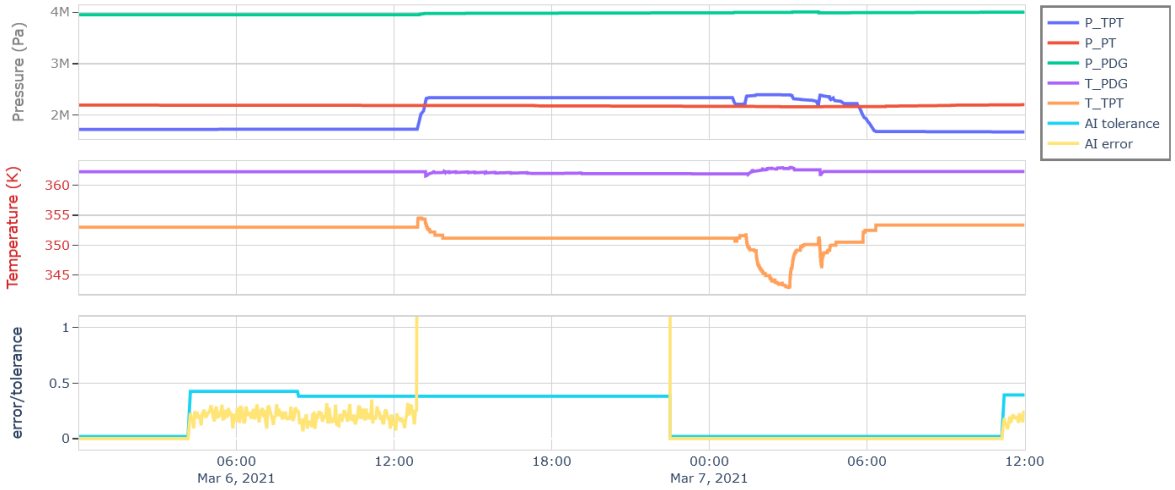

As previously stated, three parameters are obtained after the training: 1) data normalization parameters, 2) weights of neural networks, and 3) anomaly tolerance calculated during training. The first two are configuration parameters relevant to the transformation of input variables and network coefficients. As the monitoring is occurring in real time, and the conditions of the oil well operation are constantly changing, new training is performed every time 500 new instances are saved. The number of instances required for new training was determined via hyperparameter testing on real data, aiming to have enough data that minimizes hypersensitivity of the results without penalizing computational resources or causing overfitting. It should be noted that the weights, normalization parameters and tolerance depend on the valve schematics. If the operator changes the valve configuration, a new network is trained specifically for that new scheme. In other words, each valve configuration has its own deep network associated with it, which evolves over time by the acquisition of new data. It also allows the simulation of a lookahead scenario, to predict the system response to a specified action, such as a valve maneuver.

Before training a new network, the data is scaled to be between 0 and 1 using a min-max scaler, to ensure that each variable has the same order of magnitude, leading to more stable and expedited training. The procedure is described in following equation, in which x and x' refers to the original data point and its scaled value, respectively:

$$x' = \frac{x - \min(x)}{\max(x) - \min(x)} \quad (11)$$

This step is crucial to achieve accurate optimization results from the network. However, in some cases, the sensors installed in the wells may transmit data with low variation due to physical conditions or resolution limitations. This scenario can cause the network to become more sensitive, resulting in maximum and minimum values that are close together, so even minor variations may be unproperly classified as an anomalous event. To avoid this excessive sensitivity of the network from occasional low variation of the signal, randomly generated noise from a uniform distribution is added before scaling, as depicted in:

$$y = x' + \varepsilon \quad (12)$$

The noise level ε is set between 0 and 0.5% of the average of the received data. This procedure not only enriches the dataset by introducing variance but also ensures that the model is better equipped to distinguish between significant patterns and minor deviations, reducing the propensity for false positives.

3.2.4 Metrics applied for performance evaluation

Classification metrics are highlighted and used as a benchmark to evaluate the performance of classification algorithms. Therefore, a set of metrics was used to compare and evaluate the algorithms. Accuracy (ACC) considers all normal and fault samples. ACC can be calculated using:

$$ACC = \frac{TP+TN}{n_{total}} \quad (13)$$

where TP is the number of true positives, TN is the number of true negatives and n_{total} is the total number of samples. When dealing with unbalanced data, Accuracy (ACC) is not a suitable measure. Instead, it is recommended to utilize balanced accuracy ($ACCb$) as a more appropriate metric. The calculation for $ACCb$ can be estimated using following equation:

$$ACCb = \frac{REC+SP}{2} \quad (14)$$

where Recall (REC) indicates the proportion of anomalous data that is correctly detected from all anomalies. Typically, in industrial applications, REC is a prominent metric, as false negatives lead to much more harmful results than false alarms or false positives. The REC is given by:

$$REC = \frac{TP}{\mathrm{TP+FN}} \quad (15)$$

in which TP is the number of true positives, TN is the number of true negatives and FN is the number of false negatives. The Specificity (SP) estimates the ability of the algorithm to predict true negatives over false positives and can be calculated by:

$$SP = \frac{TN}{TN+FP} \quad (16)$$

where FP is the number of false positives.

The $\mathrm{F1-SCORE}$ consists in an important metric, especially in problems containing imbalanced data. It is defined as a harmonic mean between Recall (REC) and Precision (PR) and can be estimated in following equation:

$$\mathrm{F1-SCORE} = \frac{2(\mathrm{PR}*\mathrm{REC})}{\mathrm{PR+REC}} \quad (17)$$

Precision (PR) evaluates how many of the predicted positive instances were actually true positives. It is defined by the ratio of true positives to the sum of true positives and false positives, as defined in:

$$\mathrm{PR} = \frac{\mathrm{TP}}{\mathrm{TP+FP}} \quad (18)$$

Additionally, the Instances Identification Percentage (IIP) was calculated when the model was tested against instances of the same class of the target class. This metric is the percentage of the total instances of class in the test set for which the classifier successfully identified both phases: the normal and fault phases. A value of 1.0 indicates that the model correctly identifies both normal and fault occurrences in all tested instances.

3.3 Comparison to Other Methods

The proposed methodology has been validated against other classification techniques, addressing several datasets related to anomalies in subsea production/injection wells. To illustrate this process, the results of the present study were compared with those of previous works on the same type of anomaly using Random Forest (MARINS et al. (2021)), Decision Tree (TURAN and JASCHKE (2021)), and LTSM autoencoder (MACHADO et al. (2022)). This comparison refers to spurious DHSV closure events in 22 instances recorded in a public database (VARGAS et al. (2019)). The same type of anomaly is addressed in the Case Studies section – well #1 and well #3.

3.4 Case Studies

The proposed methodology was integrated to a real-time monitoring system of offshore wells, gathering data from sensors and the valve status of subsea production/injection wells. It has been implemented in more than 20 FPSOs, monitoring more than 250 wells in Santos and Campos basin, eastern Brazil, all equipped with multiplexed Wet Christmas Trees. An advantage of this system lies in its comprehensiveness in identifying anomalies related to well integrity for hundreds of subsea wells. These anomalies would be difficult for human operators to track. Some use cases are presented to illustrate the system's efficacy compared to human post-classification (class). Additionally, a web-based prototype was developed to provide a user-friendly experience for monitoring multiple wells simultaneously.

Three case studies are presented to illustrate the efficacy of the system in real monitoring situation:

Well #1 is an oil production well in the pre-salt area in Santos Basin, ultradeep water scenario, water depth 2041 m, drilled in five phases, directional trajectory, and final depth of 5870 m, equipped with downhole Interval Completion Valves, and producing in three different zones at 5432 m to 5774 m.

Well #2, is an oil production well in the pre-salt area in Santos Basin, water depth of 2125 m, drilled in four phases with directional trajectory and final depth of

5552 m, equipped with downhole Interval Completion Valves, and producing in two different zones at 5137 m to 5418 m.

Well #3, is a water alternating gas injection well in the pre-salt area in Santos Basin, in water depth of 1946 m, drilled in four phases, vertical trajectory and Final depth of 6197 m, equipped with downhole Interval Completion Valves, and injecting in three different zones at 5437 m to 5738 m.

3.5 Results and discussions

As mentioned above, the proposed methodology was applied to analyze 22 instances recorded in public database to demonstrate its validity. It was also applied in three case studies selected from the real-time monitoring system, to which the methodology was integrated, aiming to illustrate its efficacy. The results of these analyses are presented and discussed in this section.

3.5.1 Comparison to other methods

Table 10 presents the summarized results for the four classifiers applied to spurious DHSV closure data. RF was used for the Random Forest results of MARINS et al. (2021), DT for the Decision Tree model presented in TURAN and JASCHKE (2021), and LTSM refers to the results obtained by MACHADO et al. (2022) using LSTM autoencoder. Finally, DD+LSTM stands for the present study and the comparison is performed in terms of ACC , $\mathrm{F1-SCORE}$ and IIP metrics.

Table 10 - Comparison of metrics between literature and the proposed method for identifying spurious closure events of DHSV from public database (Vargas et al., 2019).

Classifiers	Accuracy (ACC)	$\mathrm{F1-SCORE}$	IIP
RF	0.8708	-	0.58
DT	0.6000	0.4900	-
LSTM	0.9992	0.9360	1.0
DD+LSTM	0.9894	0.9917	1.0

From Table 10, the results obtained are in line with other works in literature. The Accuracy achieved is around 98.9%. On the same dataset, MACHADO et al. (2022) report 99.9% accuracy by using LSTM autoencoder, MARINS et al. (2021) present 87.1% by using Random Forest, and TURAN and JASCHKE (2021) report 60% with Decision Tree method. Looking at $\mathrm{F1-SCORE}$ values, DD+LSTM performs the best, followed by the LSTM model, both of which are significantly superior to the Decision Tree. The IIP values indicate that both DD+LSTM and LSTM models successfully identified both normal and anomaly instances, in contrast to the RF results for this metric.

The coupled method has demonstrated good performance compared to using the Decision Diagram alone. To illustrate this, the results obtained by using DD model are compared with the ones provided by the comprehensive model (DD+LSTM). Table 11 presents the average values for accuracy (ACC), balanced accuracy ($ACCb$), and $\mathrm{F1-SCORE}$, allowing for a direct comparison between the models developed herein.

Table 11 - Metrics obtained for DD model and the complete model (DD+LSTM) for identifying spurious closure events of DHSV from public database (Vargas et al., 2019).

	ACC	$ACCb$	$\mathrm{F1-SCORE}$	IIP
DD	0.9727	0.9615	0.9758	1.0
DD+LSTM	0.9894	0.9771	0.9917	1.0

3.5.2 Case Studies

The dual system proposed was applied to the three case studies and the results were compared with human post classification (class), as presented in Figure 20 to Figure 23. It can be noticed that the occurrence of anomalies happens abruptly in all case studies. In these figures, the bottom graphics represents the statuses of the DD and LSTM methods, which can be: Analyzing, for both methods, which is triggered when there is a change of a valve status (e.g., M1 has closed), that will cause temporary fluctuations in the pressures and temperatures measured by the sensors, so the system awaits some time for these readings to stabilize before resume monitoring; Network not trained, exclusive to LSTM, reported just after Analyzing while

there are not enough data classified by the DD as normal for the LSTM to train; Normal/Anomalous, for both methods, regarding anomaly detection; and some others exclusive to DD, such as DHSV/M1 closed, reported when according to sensors those valves should be open but the DD detects that they might actually be closed.

The analyzed data from well #1 is presented in Figure 20 and shows data from the PDG, PT, TPT and valve status sensors along with the results of analyses and classifications for a specific time window on 08/01/2022. All the valves have a binary open or closed status except for the choke, which reports a partial opening indication. Two anomalous events were identified in the period. The first at 1:16AM (curve Analytical Status curve) related to a spurious closure of the DHSV, corrected by the operator in the sequence with valve cycling performed from 1:39AM to 1:52AM. Only the analytical approach captured this anomaly, whereas the AI did not have time to identify it because the system went into analysis mode due to the change in parameters. A few hours later (Figure 21) a second event at 8:48AM also occurred, being identified by the model (curves LSTM Status and Analytical Status) and promptly corrected by the operator. In this case, the analytical model correctly classified, after detecting the anomaly, as spurious closure of the DHSV or the M1 and the LSTM model correctly identifies the anomalous event.

Figure 20 - Results for well #1 for the first anomalous event detected – PDG, PT and TPT sensors, valve status and comparison between model classification (LSTM Status and Analytical Status) and fault classification (class).

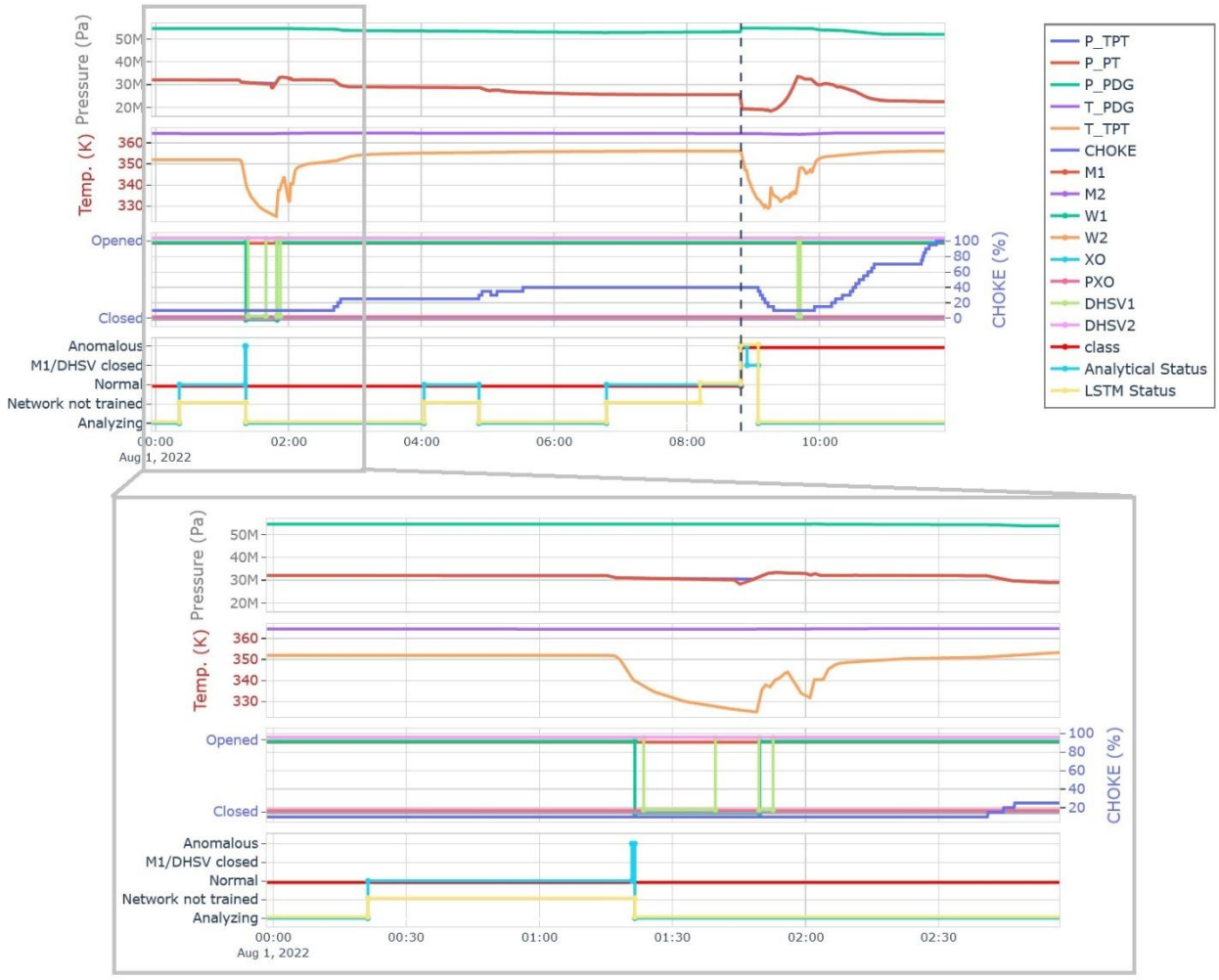

Figure 21 - Results for well #1 for the second anomalous event detected – PDG, PT and TPT sensors, valve status and comparison between model classification (LSTM Status and Analytical Status) and fault classification (class).

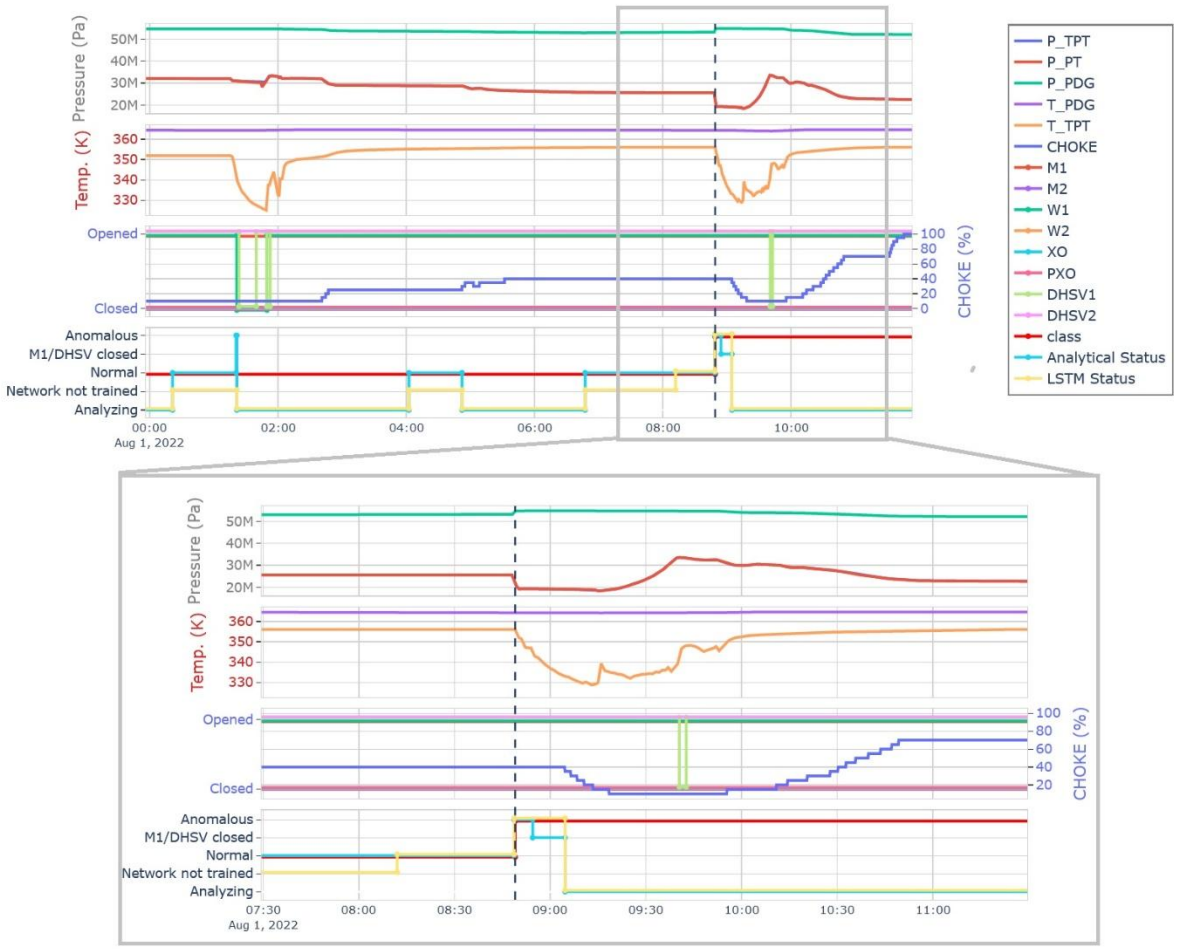

The following example refers to well #2, In this well, the developed system was applied in a retroanalysis to identify an anomaly event at 2:37 PM on 06/06/18 (curves LSTM Status and Analytical Status). In the field, the problem was only detected sometime later in a light workover intervention; the cause was the pressure communication by the gas lift valve with the subsea well closed. Figure 22 presents the data from the PDG, PT, TPT and valve status sensors along with the results of the analyses and classifications. It is important to mention that in this well, if the developed methodology had already been implemented at that time, the identification and correction of the problem would have been anticipated, avoiding non-productive time (NPT), so bringing enormous gains in oil production.

Figure 22 - Results for well #2 – PDG, PT and TPT sensors, valve status and comparison between model classification (LSTM Status and Analytical Status) and fault classification (class).

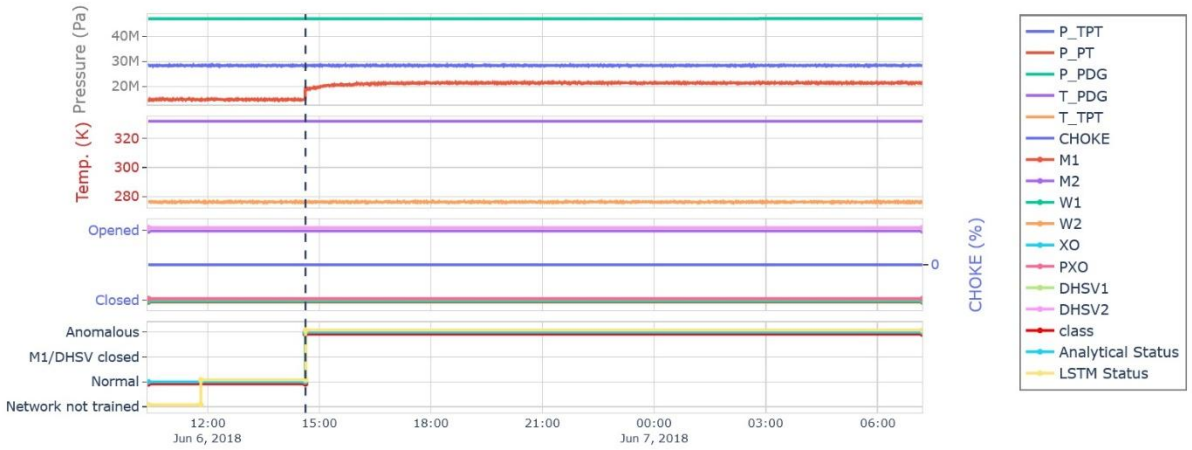

Figure 23 presents data and results for well #3, on 10/18/2022. The dual model identified the anomaly at 2:10AM (curves LSTM Status and Analytical Status) and correctly classified it in the sequence as spurious closure of DHSV or M1. It is important to note that the operator then closed the well, proceeded with the valve cycling and reopening procedure, resuming production in safe condition. After reopening well at 7:14AM, the system restarts to analyze and returns after some time to normal condition at 8:29AM.

Figure 23 - Results for well #3 – PDG and TPT sensors, valve status and comparison between model classification (LSTM Status and Analytical Status) and fault classification (class).

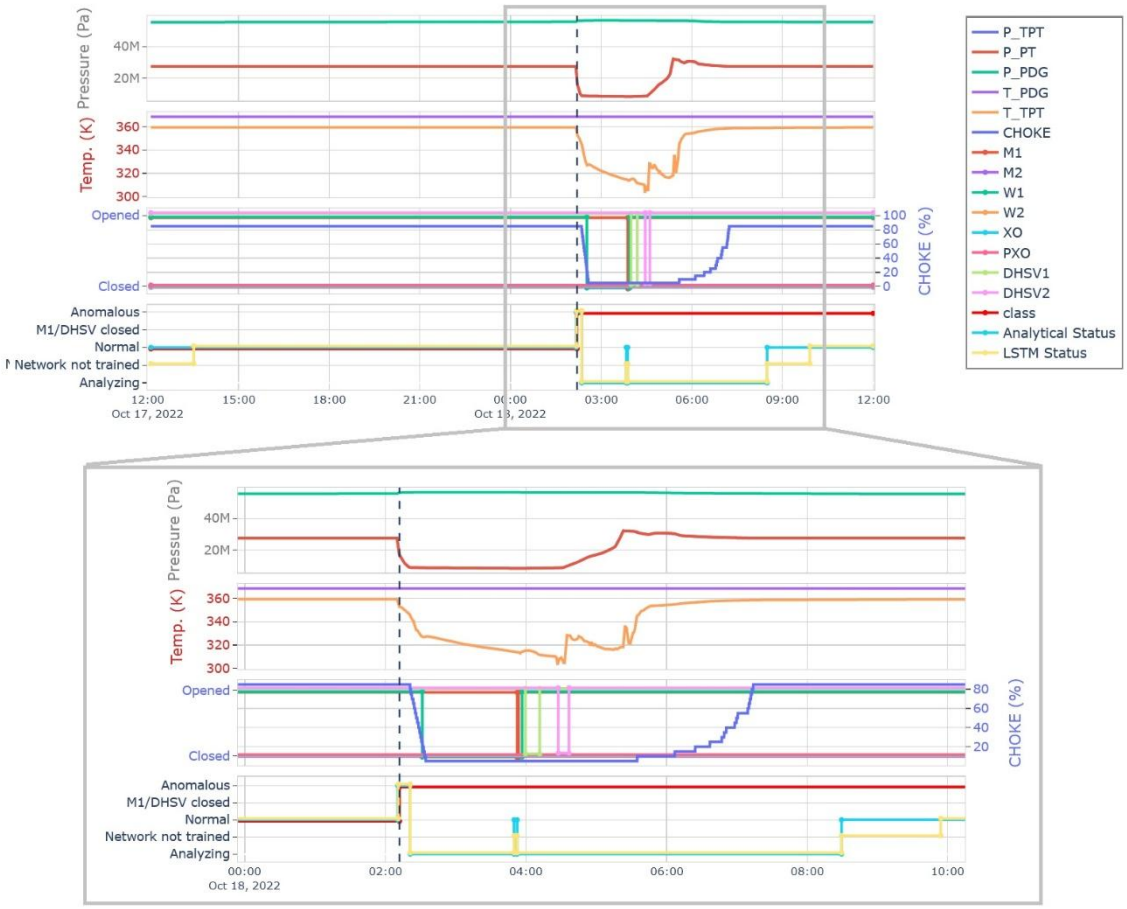

Table 12 presents the $SMAPE$ values, balanced accuracy ($ACCb$) and $\mathrm{F1-SCORE}$ values calculated for the cases studied when compared with the human post classification (class).

Table 12 - Comparison of metrics between literature methods and the proposed method for the three case studies.

	$SMAPE$	$ACCb$	$\mathrm{F1-SCORE}$
well #1 – 1st event	39.148	*	*
well #1 – 2nd event	48.312	0.9987	0.9987
well #2	33.136	0.9998	0.9998
well #3	23.390	0.9968	0.9991

* Human post classification did not identify the anomalous event.

The dual model consistently exhibits superior performance across all metrics when contrasted with the standalone DD model. This is further evident in the

detection results presented in Table 13, where $ACCb$ and $\mathrm{F1-SCORE}$ are compared for the case studies. Although the DD model on its own already produces impressive results, the combined model surpasses it.

Table 13 – Metrics obtained for DD model and the complete model (DD+LSTM) for the three case studies.

	DD		DD+LSTM	
	$ACCb$	$\mathrm{F1-SCORE}$	$ACCb$	$\mathrm{F1-SCORE}$
well #1 – 2nd event	0.9800	0.9306	0.9886	0.9373
well #2	0.9990	0.9998	0.9998	0.9998
well #3	0.9988	0.9983	0.9995	0.9993

3.5.3 Some comments on the proposed system

The proposed system performs well on the task of anomaly detection, presenting detection rates exceeding 90% in the real field production scenarios studied. Changes in well and reservoir conditions over time impose concept and data drift in time series, which are challenging factors for machine learning models. The dual approach enables the handling of these aspects, albeit generating the need for recurrent training of LSTM autoencoder, which can result in increased computational cost. The DD part serves the specific and valuable purpose of describing the normal state of the well under different valve states. However, due to its analytical basis, it exhibits lower sensitivity compared to LSTM, resulting in a lower detection rate.

DD is primarily employed to assess the system's status under different valve schemes, relying on predefined rules and up to a predetermined threshold of 5%. However, in some cases, minor variations can result in false positives, making it a complementary method to LSTM. In contrast, LSTM exhibits dynamic sensitivity that adapts with each training, enabling it to detect subtle changes that the analytical method may occasionally miss.

3.5.4 Prototype development

Aiming to provide an agile and accurate monitoring experience, a web-based computational system has been developed, allowing to handle multiple wells simultaneously. From the main dashboard, the operator can set a specific well, whose graphical interface is presented in Figure 24. The center of the screen displays two graphs on the left that represent the absolute values of the sensors, as well as two first graphs on the right that display the relative error of the moving average calculated from previous data. The lower right graph shows the reconstructed error and tolerance from the AI approach. On the sides, the latest absolute values received from the sensors are displayed on the left, while the latest calculated relative errors are displayed on the right. At the top of the screen, the well status evaluated by the analytical approach and the neural network is shown, along with some real-time monitoring control buttons.

Figure 24 – Illustrative example of the developed prototype: parameters and system response during to a tubing to annular communication anomalous event.

In addition to searching for anomalies, the system has some functionalities that help prevent false positives. One of them is the detection of frozen sensors, which evaluates the repetition of values from the sensors for a certain period of time. If detected, the frozen sensors are reported at the system output. Another functionality is the identification of invalid data, so that inconsistent data, such as non-numeric or

null values for sensors, is not included in the analysis. Changes in the valve status can significantly alter the well behavior. Therefore, the system has an analyzing mode whose objective is to provide adequate time for pressure and temperature levels to stabilize, thus ensuring that planned changes are not mistaken for anomalous events. With these functionalities, the system becomes more robust and capable of providing more security during monitoring.

3.6 Conclusions

The presented work describes a system for real-time monitoring and anomaly detection using production sensor data from oil wells. The system utilizes a combination of deep learning autoencoder and a rule-based analytic approach for detecting unexpected events, with the goal of improving operational safety and reducing costs associated with non-productive time and failure repair.

Initial studies were conducted to determine the behavior and correlations of pressure and temperature values for the most common combinations of well valve states. The proposed methodology uses pressure and temperature sensor data to classify the well status via a Decision Diagram, which is then used to train autoencoders based on LSTM deep networks devoted to anomaly detection. This coupling enables the deep neural network to evolve constantly through the normal data collected by the analytical method. It makes the system versatile enough to adapt itself to variations of the valve scheme, while also allowing new anomalies to be added to the rule-based analytical approach's cataloged portfolio.

A comparison to other approaches using the same public dataset, focusing on spurious DHSV closure events, is provided. Evaluating metrics such as Accuracy, F1-SCORE and IIP indicates that the proposed system either performs comparably or outperforms other Machine Learning techniques.

The developed system exhibits high accuracy, with true positive detection rates exceeding 90% in the early stages of anomalies identified in both simulated and actual well production scenarios. From these latter, it can be highlighted the enhancement of detection process, typically carried out by humans. For the case studies presented, all three wells had a short transitional phase, and the model performed well with balanced accuracy higher than 98.0%.

The system is implemented in more than 20 FPSOs, monitoring more than 250 production/injection subsea wells, and can be applied in both real-time operation and in testing scenarios. The continuous acquisition of data through sensors combined to the adaptability of the detection model ensures robustness over time, along with the changes in well, reservoir and operation conditions. It is worth mentioning the limited computational infrastructure available at rig site, which require expedited models to provide a quick response to the data flow. By observing the performance of the proposed system on the massive simultaneous monitoring, it has consistently delivered a prompt response in online well integrity monitoring.

In summary, the proposed system for online monitoring and anomaly detection has been successfully validated and applied to the analysis of real-time data. It exhibits high accuracy rates in detecting anomalies, making it a valuable tool for supporting the decision-making process in oil well monitoring.

However, there is still room for future research such as a rigorous study on how accurately the proposed method can perform early-stage anomaly detection and to address persistent challenges related, for example, to valve performance and tightness. While the current work focuses on the field application, future research could explore the use of other deep learning architectures, such as GRUs or Transformer neural networks, which are known for their efficiency in processing sequential data.

CHAPTER 4 – A TRANSFORMER-BASED APPROACH FOR ANOMALY DETECTION IN INTELLIGENT WELL COMPLETIONS

4.1 Introduction

In the initial development phases of the Pre-Salt Cluster in the Santos Basin, Intelligent Well Completions (IWC) emerged as a crucial design for Production Development projects. This technology not only enhances reservoir management but also addresses uncertainties, particularly vital in carbonate reservoirs. The complexity associated with IWC poses a challenge for well engineering teams, especially in ultra-deepwater, where minimizing construction costs is paramount. Successful and efficient IWC deployment becomes pivotal for the budgetary success of projects, with over 200 IWCs deployed in the last 15 years (SCHNITZLER et al. (2015); SCHNITZLER et al. (2019)).

The typical IWC design in Pre-Salt fields involves a combined 10 ¾" × 9 ⅞" production casing. Perforation operations are carried out before running the completion string in-hole (RIH) using techniques such as tubing-conveyed perforation (TCP) shoot-and-pull runs or wireline-conveyed methods (SCHNITZLER et al. (2019)).

In more recent wells, open-hole completions are often employed alongside multi-position, hydraulically controlled interval control valves (ICVs), as illustrated in Figure 25. These ICVs enable remote control of production or injection across 2–3 zones. The valves are operated via 3 or 4 dedicated control lines, one of which is common to all valves, known as the common close line, while the remaining lines are assigned to open individual valves. Given the shared control line, a specific operational logic must be adhered to in order to prevent undesired valve movements.

Each interval and the completion string are equipped with dedicated pressure and temperature (P&T) sensors, along with downhole chemical injection systems. A multiplex-controlled Wet Christmas Tree (WCT) interfaces with the downhole control lines, providing power and communication to the P&T sensors, ensuring efficient monitoring and control of well operations.

Figure 25 - Typical Pre-salt well design with in-line ICVs flow path – open hole (left) and casing perforated (right)

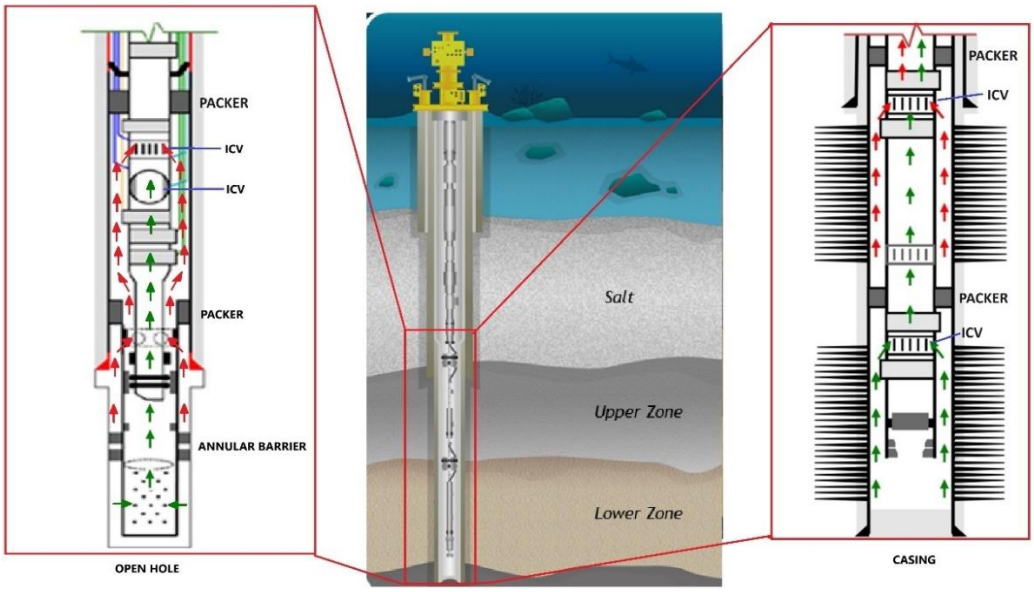

Despite initial challenges, the majority of IWC systems were successfully installed, with over 200 wells in production in the Santos Basin Pre-Salt Cluster. These systems play a versatile role in proactive and reactive reservoir management, addressing various aspects such as gas injection, managing water and gas ratios, performing WAG (Water Alternating Gas) cycles, optimizing drainage, balancing production/injection, integrity tests, using ICVs as temporary barriers, injecting tracers for reservoir behavior studies, and eliminating hydrates in flowlines (SCHNITZLER et al. (2019)).

During the production phase, some anomalies and failures have been detected in IWC systems. Common issues include undesired movements on ICVs, valve cycling difficulties, hydraulic module malfunctions, scale occurrence risks, stuck or leaking ICVs, and gas migration through control lines causing blockages due to hydrate formation Figure 26. All these issues with ICVs during production result in a loss of oil production, reservoir management problems, intervention costs with drilling rigs for workover operations, and other issues such as increase in carbon dioxide (CO2) emissions (SCHNITZLER et al. (2019)).

Figure 26 - Example of hydrates blockage on IWC control lines on WCT stab plate

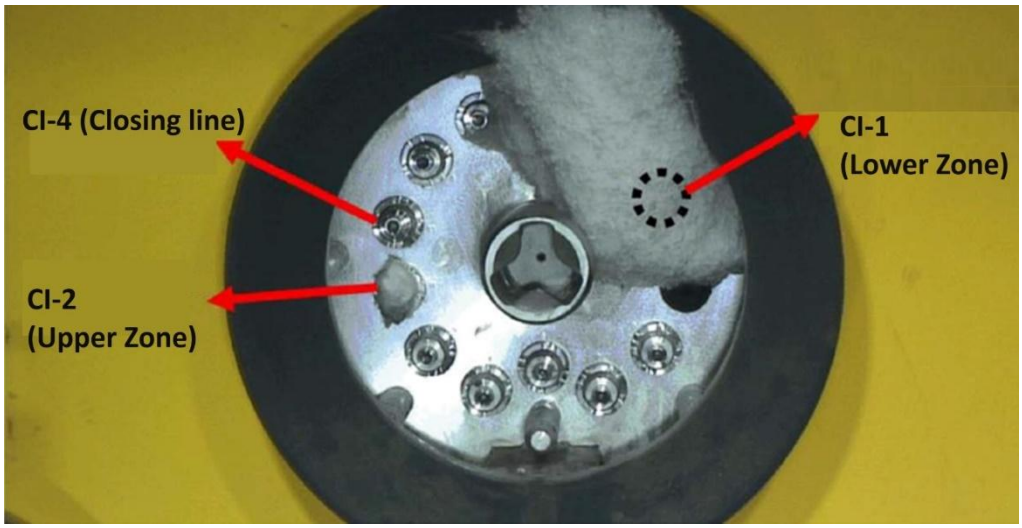

Machine learning models applied to anomaly detection addressing issues that traditional digital twin technology struggles to capture. While digital twins effectively monitor real-time well integrity by capturing thermo-mechanical behavior and loads on well components, they fall short in addressing all potential subsurface or control system-related anomalies such as wear, column holes, equipment malfunctions, or spurious valve closures (ANJOS et al. (2020); ARANHA et al. (2022)). This highlights the critical need for advanced machine learning techniques that can proactively anticipate these issues and prevent operational losses. Early detection of anomalies in offshore wells is particularly crucial due to the high costs associated with rig interventions, making machine learning a key component in minimizing production loss and ensuring well integrity.

Recent advancements focus on reconstruction-based time-series anomaly detection methods, which transform time-series data into a latent vector and reconstruct it to detect anomalies through high reconstruction errors. MALHOTRA et al. (2015) used autoencoders for learning the distribution of normal data, while others advanced this approach with TadGAN (GEIGER et al. (2020)), leveraging generative adversarial networks (GANs) for time-series anomaly detection.

Other studies have investigated the potential of machine learning in the domain of oil production but have not specifically addressed the challenges associated with ICVs in Intelligent Completion Wells. These studies highlight several limitations in existing approaches that necessitate further exploration. For instance, K-Nearest Neighbors (K-NN) and sliding window algorithms have been employed to detect issues

such as DHSV closure, production loss, line obstructions, and control valve closure. While real and simulated data demonstrated the feasibility of these methods in practical applications, they struggle with the complexities of ICV failures, which often involve intricate interactions with reservoir dynamics (VARGAS et al. (2017)). Moreover, Condition-Based Monitoring (CBM) using Random Forest and Bayesian models has classified eight operational problems with over 94% accuracy. However, these models exhibit minimal detection delays that may not suffice in scenarios requiring immediate response to ICV malfunctions, emphasizing a gap in timely mitigation for complex failures (MARINS et al (2021)).

Some studies evaluated various machine learning algorithms, highlighting Decision Trees as effective in classifying failures, yet they fall short in accurately detecting spurious DHSV closures. An anomaly detection model utilizing an LSTM (Long Short-Term Memory) autoencoder and Support Vector Machines (SVM) classifier showed improved performance for faults with slow dynamics, but these approaches may not adequately address the multifaceted nature of ICV failures within IWCs (TURAN and JASCHKE, (2021); MACHADO et al. (2022)).

Recent evaluations of techniques such as Isolation Forest, One-class Support Vector Machine (OCSVM), Local Outlier Factor (LOF), Elliptical Envelope, and Autoencoder (both feedforward and LSTM architectures) showcased the Local Outlier Factor as the top performer in various scenarios (FERNANDES, et al. (2024)). However, while they demonstrated competitive accuracy for general anomaly detection, they did not specifically target ICV problems in IWCs, leaving a significant gap in the literature (VARGAS, et al. (2019)).

Additionally, the use of unsupervised machine learning algorithms, particularly the Local Outlier Factor (LOF), has shown promise in detecting anomalies in multivariate oil production time series data. Despite its competitive accuracy in identifying spurious DHSV closures, it has not successfully identified ICV issues within IWCs (ARANHA, et al. (2024a)). A recent study employed a combination of deep learning autoencoder and a rule-based approach for anomaly detection, which demonstrated potential in enhancing operational safety and reducing costs associated with Non-Productive Time (NPT) and repairs. However, it failed to capture the effects of malfunctioning ICVs in the context of reservoir zones in intelligent well completions (ARANHA, et al. (2024b)).

In contrast, the Transformer method, originally developed for natural language processing, has proven effective in sequential data analysis across various domains (DOSOVITSKIY, et al. (2021); HUANG, et al. (2019)). Its superior performance in long sequence time-series forecasting positions it as a promising tool for addressing the complexities inherent in anomaly detection (WU, et al. (2020); ZHOU, et al. (2021); KIM, et al. (2023)). Transformer algorithms present significant advantages in time-series anomaly detection, primarily due to their ability to handle data drift and capture complex patterns effectively. Their self-attention mechanism allows these models to adapt to shifts in data distribution over time, ensuring resilience against changes that can occur in time-series data. Additionally, Transformers excel at identifying intricate temporal dependencies and long-range interactions, which are often challenging for traditional models. Unlike recurrent neural networks, Transformers can process entire sequences in parallel, leading to faster training and inference times, making them suitable for large datasets. Their flexibility in input representation accommodates various feature types, enhancing the modeling of complex time-series data. Furthermore, the rich contextual information that Transformers gather through their attention mechanism aids in accurately identifying anomalies that may otherwise go unnoticed, making them a powerful tool for detecting unusual patterns and behaviors in time-series data.

This research aims to evaluate Transformer models specifically for time series anomaly detection, targeting malfunction events in interval control valves (ICVs) within Intelligent Well Completions (IWC). By addressing the limitations of existing models that fail to capture the intricacies of ICV failures, this study seeks to fill a critical gap and provide significant advancements in anomaly detection methodologies.

4.2 Methodology

As described in the introductory section, this work aims to apply transformer models anomaly detection in wells, addressing the limitations of existing models that fail to capture the intricacies of ICVs failures in IWC. Additionally, the model is designed to operate in environments with low computational availability and to provide timely responses for operational personnel. The following sections present the transformer model, the training and anomaly detection processes implemented, as well as considerations regarding hyperparameters and metrics used.

4.2.1 Transformer Networks for Time Series

In this study, we propose a time-series anomaly detection method based on a Transformer networks for time series prediction model (KIM, et. al (2023)). The model comprises an encoder that learns a hierarchical representation from multiple Transformer encoder layers and a decoder that integrates this representation. Figure 27 illustrates the architecture of our prediction model. The goal is to minimize the prediction error between predicted and actual sequences, thereby learning the distribution of normal data prevalent in the training set.

The self-attention mechanism is a key feature of the Transformer, allowing the model to weigh the importance of different time steps in a series when encoding a particular time step. This mechanism helps the model to capture dependencies between distant points in the time series, which is crucial for understanding trends and seasonal patterns. Self-attention computes a weighted sum of all time steps in the series for each time step, enabling the model to focus on the most relevant information.

In time-series data, each timestamp's input (e.g., temperature, pressure, valves sensor readings) has dependencies on past and future timestamps. The self-attention mechanism allows the model to compute these dependencies flexibly:

Key Idea: Every timestamp in the series attends to every other timestamp, weighting their contributions based on similarity (measured by dot products of query and key vectors).

Benefit: This removes the need for sequential processing (as in RNNs), enabling parallel computation and capturing long-range dependencies more effectively.

Figure 27 - Architecture of proposed model

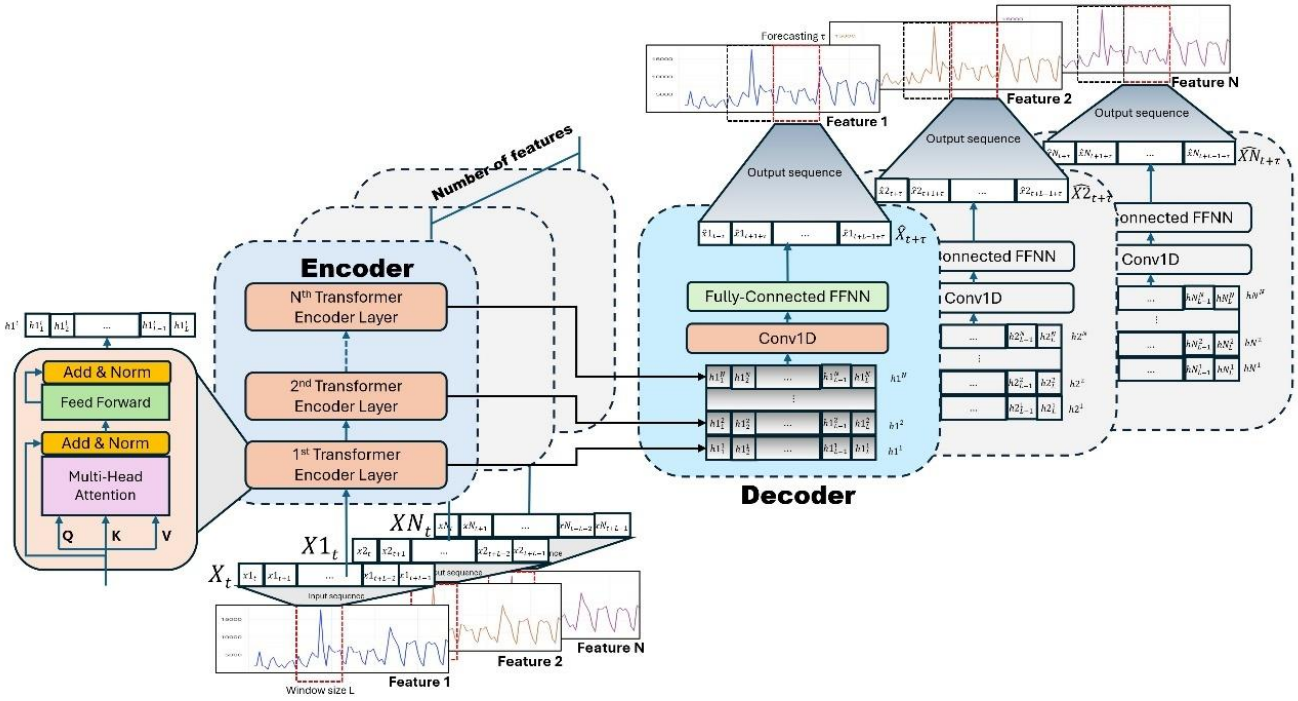

A sequence of vectors, where each vector represents a token (timestamp) in the input sequence. For example, for a sequence of length n, there are n vectors, each of dimension d.

For each input vector, three different linear projections are created:

Query (Q): Represents the current element asking for information from others.

Key (K): Represents the information provided by other elements.

Value (V): Represents the content to be aggregated.

These projections are learned during training.

For each query, its compatibility with all keys is computed as a dot product:

$$Attention\ Score = Q.K^T \qquad (19)$$

This results in a matrix of scores, one for every pair of elements in the sequence. The scores are normalized using a softmax function to obtain attention weights. These weights indicate how much attention each token should pay to others.

Using the attention weights, a weighted sum of the value vectors is computed for each query:

$$Output_i = \sum_j Attention\ Weight_{ij}.V_j \qquad (20)$$

This results in a new representation of the sequence.

Multi-head attention extends the self-attention mechanism by allowing the model to focus on different aspects of the time series data simultaneously. Each "head" in the multi-head attention mechanism learns to capture different types of temporal relationships or patterns within the data. For example, while some heads may attend to long-term trends, others may focus on short-term fluctuations or seasonal patterns.

Mechanism: Each head operates independently with different learned projection matrices for queries, keys, and values. The outputs from these heads are then concatenated and linearly transformed, resulting in a richer representation of the time series.

Application in Time-Series: The multi-head attention mechanism is particularly beneficial in time-series modeling as it allows the model to capture diverse temporal dynamics. Different heads can focus on distinct temporal patterns, such as seasonal versus short-term trends, enabling the model to learn more complex relationships. For instance, some heads may prioritize recent timestamps for immediate context, while others might attend to distant timestamps to understand overarching trends.

To prepare the time-series data for continuous prediction, we segment the input X$total$ = {$\mathbf{x}$0, $\mathbf{x}$1,⋯, $\mathbf{x}T$ }, $where$ $\mathbf{x}l$ ∈ Rdx, into windows of length L. These windows are created using a sliding mechanism with a step size of 1, resulting in Xt = {$\mathbf{x}t$, $\mathbf{x}t$+1,⋯, $\mathbf{x}t$+L−1} starting at time t.

Each window Xt = {$\mathbf{x}t$, $\mathbf{x}t$+1,⋯, $\mathbf{x}t$+L−1}, $where$ $\mathbf{x}l$ ∈ Rdx, undergoes processing through N Transformer encoder layers. For each layer i, the sequence is transformed as follows:

$$h^1 = TransformerEncoder^1(X_t) = \{h_1^1, h_2^1 \dots., h_L^1\} \quad (21)$$

$$h^i = TransformerEncoder^i\left(h^{i-1}\right) = \{h_1^i, h_2^i \dots., h_L^i\} \quad (22)$$

Here, hi t ∈ Rd, and d denotes the Transformer encoder's dimension. Each layer employs masked multi-head self-attention to capture dependencies within the sequence, ensuring no future information leakage by masking the upper triangular

elements of the attention matrix. To effectively capture features relevant to tasks such as identifying ICV failure time-series characteristics, we aggregate the features learned across the Transformer layers. To aggregate the features learned across Transformer layers, the representations $h1$, $h2$,…. hN are stacked to form the final encoder output h^{encoder_output} :

$$h^{encoder\_output} = stack(h^1, h^2, \dots, h^N) \in R^{(d\dot{N})xL} \quad (23)$$

This approach integrates both local details from lower layers and global dependencies from higher layers within the sequence.

The decoder receives h^{encoder_output} and utilizes a 1-dimensional convolutional neural network (1D CNN) to combine hierarchical information:

$$h^{conved} = Conv(h^{encoder\_output}) \in R^{dxL} \quad (24)$$

The 1D CNN efficiently captures time-invariant characteristics with fewer parameters compared to traditional RNNs, enhancing its suitability for time-series modeling. From h$conved$, a fully-connected layer generates predictions $\hat{X}_{t+\tau}$:

$$\hat{X}_{t+\tau} = Linear(h^{conved}) \in R^{d_x xL} \quad (25)$$

This comprehensive connection between the encoding and decoding processes, alongside the attention mechanisms, enhances the model's ability to capture and predict ICV failure time-series features, ultimately improving its effectiveness in anomaly detection tasks.

4.2.2 Training Process and Anomaly Detection

In this study, the prediction model is trained using the mean squared error (MSE) as the loss function, which measures the discrepancy between the actual values value Xt+τ = {$\mathbf{x}t$+τ , $\mathbf{x}t$+1+τ ,⋯, $\mathbf{x}t$+L−1+τ} and the predicted values $\hat{X}t$+τ = {$\hat{x}$t+τ , $\hat{x}t$+1+τ ,⋯, $\hat{x}t$+L−1+τ} across N sequences in the training data. The loss function is formulated as follows:

$$Loss(X_{t+\tau}, \dot{X}_{t+\tau}) = \frac{1}{L}\frac{1}{d_x}\sum_{l=1}^{L}\sum_{m=1}^{d_x}(x_{m,t+l-1+\tau} - \hat{x}_{m,t+l-1+\tau})^2 \qquad (26)$$

This function averages the squared differences between corresponding elements of the actual and predicted sequences, normalized by the sequence length L and the dimensionality d_x. After training, the prediction model learns to approximate the distribution of normal data from the training set. The overall loss across N sequences is computed as:

$$Total\ Loss = \frac{1}{N}\sum_{n=1}^{N} Loss(X_{t+\tau}^{n}, \hat{X}_{t+\tau}^{N}) \qquad (27)$$

Where $X_{t+\tau}^{n}$ and $\hat{X}_{t+\tau}^{N}$ represent the actual and predicted sequences, respectively, for the n-th sequence.

To detect anomalies in real-time, the prediction error for each timestamp t is quantified as the anomaly score. This score is defined by the Euclidean distance between the actual x_{mj} and predicted $\hat{x}_{mJ}$ values across all dimensions d_x:

$$Anomaly\ Score\ of\ x_t = s_1 = \sum_{n=1}^{d_x}\sqrt{((x_{mj} - \hat{x}_{mJ})^2} \qquad (28)$$

During the inference phase, the model processes the most recent L timestamps X$t-L$+1 = {$\mathbf{x}t-L$+1, $\mathbf{x}t-L$+2,⋯, $\mathbf{x}t$} as input and predicts the sequence τ time steps into the future X$t-L$+1+τ = {$\mathbf{x}t-L$+1+τ , $\mathbf{x}$ t−L+2+τ ,⋯, $\mathbf{x}t$+τ}. The anomaly score is calculated in real-time based on the last τ predicted values. To determine if a data point is anomalous, a threshold (tol_{AI}) is set based on the mean μ and standard deviation σ of the reconstruction errors, following a Gaussian distribution assumption. The threshold is defined as:

$$tol_{AI} = \mu + k\sigma \qquad (29)$$

Where, k is a parameter that determines the tolerance interval around the mean. The acceptance criteria, which are based on tolerance intervals around the mean, can be applied to both sequential and non-sequential datasets, as this method aims to encompass a specified proportion of the population with a defined level of confidence. Employing the properties of the normal distribution in this manner is a well-

established and widely recognized approach in the scientific domain of anomaly detection (SATHE and AGGARWAL (2016); NAKAO, et al. (2021)). By establishing a threshold using the mean plus three standard deviations ($k = 3$) , any data point (or reconstruction error in the context of autoencoders) that lies outside the central 99.7% range can be identified as an anomaly. An instance is flagged as anomalous if its anomaly score exceeds tol_{AI}. This methodology allows for effective real-time anomaly detection by leveraging the trained prediction model to continuously monitor and evaluate incoming time-series data against learned normal patterns. Despite its simplicity, it yielded consistent results and does not impose computational overhead on real-time monitoring.

One characteristic that Transformer models enable us easy to evaluate, beyond available attributes, is the use of calculated features, such as the differential pressure between the annular PDGs in front of reservoir zones, as well as the PDG within the column. This type of calculated variable can yield more significant results as it provides a physical interpretation of the variations, or lack thereof, in differential pressures across different reservoir zones. These variations can be correlated with changes in flow, indicating a shift in the position or closure of one or more ICVs. In contrast, analyzing sensor data as a separate feature could not capture this physical phenomenon effectively.

4.2.3 Metrics for performance evaluation

In evaluating the performance of classification algorithms, several key metrics play pivotal roles. Accuracy (ACC) is fundamental, representing the proportion of correctly classified samples both normal and fault out of the total dataset. It is calculated using the Eq. 30:

$$ACC = \frac{TP + TN}{n_{total}} \tag{30}$$

Where TP (true positives) and TN (true negatives) are the correctly identified instances of normal and fault conditions, respectively. Precision (PR) presented in Eq. 31 assesses the proportion of true positives among all predicted positives, helping to gauge the algorithm's exactness in identifying faults:

$$PR = \frac{TP}{TP + FP} \tag{31}$$

Where FP (false positives) denotes instances incorrectly flagged as faults. Recall (REC) presented in Eq. 32, on the other hand, measures the ratio of true positives to all actual positives, crucial in industrial applications where missing true faults (false negatives) can lead to significant consequences:

$$REC = \frac{TP}{TP + FN} \tag{32}$$

Where FN (false negatives) represents fault instances incorrectly classified as normal. Furthermore, Specificity (SP) in Eq. 33 evaluates the algorithm's ability to correctly identify true negatives among all actual negatives, complementing the evaluation of false positives:

$$SP = \frac{TN}{TN + FP} \tag{33}$$

The F1 Score, a harmonic mean of Precision and Recall presented in Eq. 34, offers a balanced measure especially useful in scenarios with class imbalance:

$$F1 = \frac{2(PR \cdot REC)}{PR + REC} \tag{34}$$

For cases of unbalanced data, where accuracy might not reflect true performance, balanced accuracy (ACCb) provides a more suitable alternative as presented in Eq. 35:

$$ACCb = \frac{REC + SP}{2} \tag{35}$$

Additionally, the Instances Identification Percentage (IIP) measures the classifier's ability to correctly identify instances of a specific class across both normal and fault phases in the test set. A value of 1.0 indicates perfect identification across all instances tested.

4.2.4 Model parameterization

In this study, we aimed to optimize the performance of predictive algorithms using public datasets and real-world monitoring system data. The focus was on

exploring various hyperparameter combinations without exhaustively testing every possibility due to computational constraints. The study leveraged Python 3.9 for implementation and employed a MinMax scaler to normalize the data. For the public datasets, we began by defining a training window and forecasting window approach. The training window consisted of 60 samples for each attribute, with a time interval of 60 seconds (1 minute) between samples. Subsequently, the forecasting window spanned the next 60 seconds. This setup allowed us to evaluate model performance under controlled conditions with well-defined intervals.

In contrast, the data from the monitoring system arrived at a lower frequency, with data points collected every 30 seconds. Consequently, the training period comprised 60 samples per attribute, corresponding to a 30-minute window. The subsequent test period utilized 60 samples to evaluate performance over the subsequent 30 minutes. This approach accommodated the inherent differences in data frequency and temporal dynamics compared to the public datasets.

For determining the Number of Layers and Number of Heads, we employed a grid search method. In contrast, the selection of other hyperparameters, such as learning rates and batch sizes, was guided by considerations of computational feasibility and the loss criteria for the validation dataset. Each parameter combination was evaluated based on performance metrics, including accuracy and F1-score. Table 14 presents the hyperparameters utilized in the public datasets and the specific cases studied.

Table 14 - Hyperparameters used for Transformer model training and tests for different databases.

	Number of Layers	Number input size	Number of heads	Window size L	Forecasting τ	Learning rate	Epochs
Public dataset	16	3	3	60	60	0.001	20
IWC Case Studies	16	4 to 12	4 to 12	60	60	0.001	10

4.3 Case studies

To evaluate the application of the transformer model, utilizing hyperparameters, training processes, and anomaly detection as presented in the methodology section, case studies were conducted starting with publicly available datasets (VARGAS, et al. (2019)) for an initial assessment of the model's capability compared to existing literature models. Subsequently, the focus expanded to wells with Intelligent Well Completions (IWC) in the Pre-Salt Cluster of the Santos Basin, where Decision Diagram + LSTM (ARANHA, et. al, (2024b)) and LOF (ARANHA, et. al, (2024a)) models may not achieve satisfactory results. This approach aims to demonstrate the effectiveness of the transformer model in complex scenarios where literature methods may not yield satisfactory results.

4.3.1 Comparison to Other Methods

There is a lack of public data available for events related to Intelligent Completion Systems and ICVs. To initially train and validate our methodology, we utilized well data from the public database (VARGAS, et al. (2019)) under normal production conditions (class 0 in the public base). Subsequently, we compared our methodology with other techniques, focusing on spurious DHSV (Downhole Safety Valve) closure events (class 2 in the public base) obtained from the public database. Automatic detection of these closures can enable timely corrective actions, preventing production losses and additional costs. Key sensors used include pressure and temperature sensors at the TPT (Temperature/Pressure Transducer) of the Wet Christmas Tree and the PDG (Pressure Downhole Gauge) the description and units are presented in Table 15. Data is available at one-second intervals, when building the public database the authors classified each event instance in addition to failure periods. The transient and steady states of failure were unified as a single anomalous state, that is, a binary classification (normal and failure) was performed. There is no not-a-number (NaN) value in the variable monitoring data. However, there are few data points without labels (NaN values in the class column). For these samples, the data located between the transient and steady-state periods of failure were considered a failure, and the rest as normal.

Figure 5 shows a schematic view of an offshore well connected to the production platform and the position of the TPT sensors, the PDG (Pressure Downhole Gauge), and the Downhole Safety Valve (DHSV) in an offshore well.

Table 15 - Available attributes in the database with descriptions and units.

Name	Description	Unit
P-TPT	Pressure on temperature/pressure transducer (TPT)	Pa
T-TPT	Temperature on temperature/pressure transducer (TPT)	ºC
P-PDG	Pressure on Pressure Downhole Gauge (PDG)	Pa

To clarify the process, we aligned our study results with previous research on similar anomalies, using methodologies like Random Forest (MARINS, et al. (2021)), Decision Tree (TURAN and JASCHKE, 2021), LSTM autoencoder (MACHADO, et al. (2022)), Decision Diagram + LSTM (ARANHA, et. al, (2024b)) and LOF (ARANHA, et. al, (2024a)). This comparative analysis provided initial insights into the effectiveness and reliability of our proposed methodology. We are also preparing the methodology for integration with additional variables/sensors from IWC systems, enhancing its adaptability. Notably, the DD+LSTM (ARANHA, et. al, (2024b)) and LOF(ARANHA, et. al, (2024a)) methods showed satisfactory results for spurious DHSV closure events. However, further investigation is needed for a comprehensive comparison with other methods on public datasets and to extend the methodology to more complex problems where DD+LSTM and LOF might not perform well.

4.3.2 Real Dataset – Brazil's Intelligent Well Completion in a Pre-salt offshore cluster

Following the model's evaluation using a public database, it was deployed in production and injection subsea wells located in Brazil's Santos basin, equipped with multiplexed Wet Christmas Trees and IWC (Intelligent Well Completion) (CARPENTER, 2020). For training, relevant data from three months of each well's operation was used, focusing on periods two hours before and after well openings, closings, or changes in production/injection flow rates under normal conditions. Extended steady-state production periods were excluded to prioritize capturing anomalies during valve operations in downhole control valves (ICVs). Separate training sets were prepared for production and injection wells due to their distinct flow regimes

and feature behaviors. Training utilized 80% of the data for minimizing loss, with 20% reserved for validation. As it has been used in reservoir model studies and infrastructure for real time monitoring (PARI, et al. (2009); KLUTH, et al. (2000)) key sensors included pressure and temperature sensors in the Wet Christmas Tree's TPT, PDGs and surface pressure and choke position in the production/injection line are presented in Table 16, with data recorded at 30-second intervals.

Based on the real-time sensors presented in Table 16, pressure differential values were calculated between the following sensors: P-TPT and P-PDG, P-PDG and P-L-PDG, P-PDG and P-U-PDG, P-L-PDG and P-U-PDG. In cases where the well has three producing/injection zones, differentials were also calculated for P-PDG and P-I-PDG, P-L-PDG and P-I-PDG, and P-I-PDG and P-U-PDG, Table 17 presents the calculated attributes available.

The differential pressure calculated between the annular PDGs situated in front of reservoir zones, along with the PDG within the column, can provide valuable insights by demonstrating how differential pressures fluctuate, or remain stable, across various reservoir zones. These fluctuations can be linked to changes in flow, suggesting possible movements or closures of one or more ICVs. Additionally, this approach may be more effective for use in machine learning models, as it could be less sensitive to noise originating from the sensors.

Given that the Transformers model allows for the use of multiple features, we evaluated several configurations:

- Model TRANS-A: Considered all sensors presented in Table 16 (total of 12 features).
- Model TRANS-B: Included only the pressure sensors on the WCT and the bottom hole PDGs (total of 4 or 5 features, depending on whether the well has two or three zones, respectively).
- Model TRANS-C: Included the pressure sensor data and the calculated pressure differential data (8 or 12 features, depending on whether the well has two or three zones, respectively).
- Model TRANS-D: Considered only the calculated pressure differential presented in Table 17 data (4 or 7 features, depending on whether the well has two or three zones, respectively).

Table 16 - Available attributes in the IWC wells

Name	Description	Unit
P-TPT	Pressure on temperature/pressure transducer (TPT)	Pa
T-TPT	Temperature on temperature/pressure transducer (TPT)	ºC
P-PDG	Pressure on Pressure Downhole Gauge (PDG)	Pa
P-U-PDG	Pressure in front Upper Zone - Pressure Downhole Gauge (PDG)	Pa
P-I-PDG	Pressure in front Intermediate Zone - Pressure Downhole Gauge (PDG)	Pa
P-L-PDG	Pressure in front Lower Zone - Pressure Downhole Gauge (PDG)	Pa
T-PDG	Temperature on Pressure Downhole Gauge (PDG)	ºC
T-U-PDG	Temperature in front Upper Zone - Pressure Downhole Gauge (PDG)	ºC
T-I-PDG	Temperature in front Intermediate Zone - Pressure Downhole Gauge (PDG)	ºC
T-L-PDG	Temperature in front Lower Zone - Pressure Downhole Gauge (PDG)	ºC
P-SURFACE	Surface Pressure in the well production/injection line	Pa
CHOKE	Choke position in the well production/injection line	%

Table 17 - Calculated attributes in the IWC wells

Feature Name	Description	Unit
DP1	Differential Pressure between Pressure transducer (TPT) and Pressure Downhole Gauge (PDG)	Pa
DP2	Differential Pressure between Pressure Downhole Gauge (PDG) and Upper Zone - Pressure Downhole Gauge (PDG)	Pa
DP3	Differential Pressure between Pressure Downhole Gauge (PDG) and Lower Zone - Pressure Downhole Gauge (PDG)	Pa
DP4	Differential Pressure between Upper Zone - Pressure Downhole Gauge (PDG) and Lower Zone - Pressure Downhole Gauge (PDG)	Pa
DP5	Differential Pressure between Pressure Downhole Gauge (PDG) and Intermediate Zone - Pressure Downhole Gauge (PDG)	Pa
DP6	Differential Pressure between Lower Zone - Pressure Downhole Gauge (PDG) and Intermediate Zone - Pressure Downhole Gauge (PDG)	Pa
DP7	Differential Pressure between Intermediate Zone - Pressure Downhole Gauge (PDG) and Upper Zone - Pressure Downhole Gauge (PDG)	Pa

The model was successfully implemented across more than 200 IWCs in the Pre-salt Santos Basin. However, the infrequency of ICV-related issues presents challenges in obtaining representative case examples. To address this, an analysis was conducted from late 2022 to 2024, obtaining eight case studies from six wells in Brazil's Santos Basin to evaluate the effectiveness of ICV fault detection and to validate the applicability of the Transformer model. These case studies demonstrate the efficacy of the developed monitoring model in detecting anomalous events:

Well #1: An oil production well in ultradeep water (2,119 m depth), drilled vertically to a depth of 5,243 m. Equipped with Interval Completion Valves, it produces from 4,898 m to 5,129 m.

Well #2: A water injection well with a water depth of 2,128 m, drilled vertically to 5,275 m. Also equipped with Interval Completion Valves, it injects water into zones from 4,917 m to 5,180 m.

Well #3: A water alternating gas injection well in 1,900 m of water, drilled directionally to a depth of 6,111 m. It uses Interval Completion Valves for injection across three zones from 5,585 m to 5,895 m.

Well #4: Similar to Well #3, this water alternating gas injection well is in 2,027 m of water, drilled vertically to 5,933 m, with Interval Completion Valves used for injection from 5,591 m to 5,871 m.

Well #5: Another oil production well in ultradeep water (2,125 m depth), open hole completion, drilled directionally to 5,343 m. Equipped with Interval Completion Valves, it produces from 5,152 m to 5,255 m.

Well #6: A water alternating gas injection well in ultradeep water (2,183 m depth), open hole completion, drilled directionally to 5,538 m. It uses Interval Completion Valves for injection into zones from 5,362 m to 5,530 m.

The diverse conditions presented by these wells highlight the model's robustness in varying depths, trajectories, and operational configurations. The performance of the monitoring model can be compared across different well types—oil production versus water injection and gas injection—allowing for a comprehensive analysis of its efficacy in detecting anomalies.

The case studies reveal that four anomalies were detected in production well scenarios (Wells #1 and #5), while the remaining four spurious anomalies were identified in injection well scenarios (Wells #2, #3, #4, and #6). This distinction underscores the model's capability to adapt to distinct operational environments, demonstrating its reliability and effectiveness in pre-salt offshore conditions.

A critical advantage of the fast anomaly detection provided by the Transformer model is the ability for operators to swiftly address issues related to production or injection. The main impacts of ICV closure include reductions in production or injection rates, which, over time, can compromise reservoir management and well integrity, potentially necessitating costly workover interventions. In the context of the production wells studied, the flow rate for each reservoir interval is approximately 3,000 m^3/d. Without the Transformer model, human detection of anomalies could take more than a day in some cases, leading to significant economic consequences. Each

successfully identified and corrected anomaly could incur an impact of approximately $1.4 million USD.

In summary, the model's performance across various well types and operating conditions in the Santos Basin illustrates its robustness and adaptability, reinforcing its potential as a valuable tool for monitoring and ICV fault detection in complex offshore environments. The ability to quickly identify and rectify issues not only enhances operational efficiency but also safeguards the long-term integrity and productivity of the wells.

4.4 Results and discussions

As mentioned above, the proposed methodology was applied in a public database to demonstrate its validity. It was also applied in case studies selected from the real-time monitoring system, to which the methodology was integrated, aiming to illustrate its efficacy. The results of these analyses are presented and discussed in this section.

4.4.1 Evaluation of the proposed model using a public database

Table 18 presents the summarized results of TRANS model for the public database (VARGAS, et al. (2019)) for spurious DHSV closure, in terms of ACC , $F1-SCORE$ and $ACCb$ metrics. Table 19 presents the summarized results for the five literature classifiers applied to spurious DHSV closure data of the public database and the proposed transformer model applied. RF was used for the Random Forest results (MARINS, et al. (2021)), DT for the Decision Tree model (TURAN and JASCHKE, 2021), LSTM refers to the results using LSTM autoencoder (MACHADO, et al. (2022)), DD+LSTM for Decision Diagram coupled with LSTM autoencoder (ARANHA, et. al, (2024b)) and LOF for the Local Outlier Factor model (ARANHA, et. al, (2024a)). Finally, TRANS stands for the present study and the comparison is performed in terms of ACC , $\mathrm{F1-SCORE}$ and IIP metrics.

From Table 19, the results obtained are in line with other works in the literature. The Accuracy achieved TRANS model is around 98.6%. On the same dataset report a 99.9% accuracy by using LSTM autoencoder and LOF. DD+LSTM also perform good result (98.9%), RF present 87.1% and DT report 60%. Looking at

$\mathrm{F1-SCORE}$ values, LOF and DD+LSTM perform the best, followed by the TRANS model and LSTM model, both of which are significantly superior to the Decision Tree. The IIP values indicate that both DD+LSTM and LSTM models successfully identified both normal and anomaly instances, in contrast to the RF results for this metric.

Table 18 - Summary of data results for TRANS model for identifying spurious closure events of DHSV from public database (VARGAS, et al. (2019)).

Id Dataset	Name of Dataset	ACC	F1-SCORE	ACCb
1	WELL-00002_20131104014101.csv	0.9932	0.9942	0.9861
2	WELL-00003_20141122214325.csv	0.9936	0.9957	0.9832
3	WELL-00003_20170728150240.csv	0.9912	0.9934	0.9806
4	WELL-00003_20180206182917.csv	0.9879	0.9932	0.9420
5	WELL-00009_20170313160804.csv	0.9913	0.9909	0.9827
7	WELL-00011_20140515110134.csv	0.9716	0.9855	0.9500
8	WELL-00011_20140530100015.csv	0.9695	0.9802	0.9377
10	WELL-00011_20140720120102.csv	0.9949	0.9939	0.9957
11	WELL-00011_20140726180015.csv	0.9825	0.9883	0.9666
13	WELL-00011_20140916060300.csv	0.9971	0.9958	0.9978
14	WELL-00011_20140921200031.csv	0.9816	0.9877	0.9640
15	WELL-00011_20140928100056.csv	0.9892	0.9852	0.9915
16	WELL-00011_20140929170028.csv	0.9777	0.9828	0.9692
17	WELL-00011_20140929220121.csv	0.9917	0.9844	0.9944
18	WELL-00011_20141005170056.csv	0.9939	0.9947	0.9929
19	WELL-00011_20141006160121.csv	0.9893	0.9865	0.9912
20	WELL-00012_20170320033022.csv	0.9647	0.9686	0.9611
21	WELL-00012_20170320143144.csv	0.9820	0.9805	0.9835
22	WELL-00013_20170329020229.csv	0.9942	0.9954	0.9921
	mean	0.9861	0.9882	0.9769

Table 19 - Comparison of metrics between literature and the proposed method for identifying spurious closure events of DHSV from public database.

Classifiers	Accuracy (ACC)	$\mathrm{F1}-\mathrm{SCORE}$	IIP
RF	0.8708	-	0.58
DT	0.6000	0.4900	-
LSTM	0.9992	0.9360	1.0
DD+LSTM	0.9894	0.9917	1.0
LOF	0.9991	0.9969	1.0
TRANS	0.9861	0.9882	1.0

4.4.2 Application in Brazil's pre-salt offshore wells

The TRANS models were applied to eight case studies, and their results were compared with human post-classification (class). As illustrated in Table 20, the four transformer model approaches, using different feature inputs were evaluated. The results are consistent across the wells evaluated, demonstrating the superiority of TRANS-D compared to the other three approaches. The calculated differential pressure between the annular PDGs in front of reservoir zones, as well as the PDG within the column, can yield more significant insights, as they provide a physical interpretation of the variations, or lack thereof, in differential pressures across different reservoir zones. These variations can be correlated with changes in flow, indicating a shift in the position or closure of one or more ICVs. In contrast, analyzing sensor data as a separate feature could not capture this physical phenomenon effectively. Subsequently, the results obtained by TRANS-D are presented in Figure 28 to Figure 33, using pressure differentials calculated between the well sensors as a feature.

The analysis of events in Well #1, presented in Figure 28, illustrates the effectiveness of the model in detecting anomalies related to the lower interval completion valve (ICV), alongside human post-classification efforts. In the 1st event in Figure 28 the model, represented by the blue curve, accurately identified an anomaly at 10:29 PM on 09/10/22 based on differential pressures calculated and predicted. Subsequently, the operator performed ICV valve cycling to address the issue, with

human classification confirming the event at 01:04 AM on 09/11/22. This event demonstrates the model's prompt detection capability, facilitating timely operator intervention to mitigate potential production disruptions. In the second instance (2nd event in Figure 28) on 02/25/23, the model detected an anomaly at 02:17 PM before it was visually confirmed and addressed in the field. The operator initiated valve cycling to rectify the issue, and human post-classification identified the anomaly at 4:24 PM on the same day. This scenario underscores the model's ability to preemptively signal anomalies, enabling proactive maintenance actions to uphold operational continuity. During the event on 09/29/23 (3rd event in Figure 28), the model detected an anomaly at 11:28 PM, aligning closely with human classification at 10:20 PM. Both identifications confirmed a spurious closure event of the lower ICV. This synchronization highlights the model's consistency in identifying critical anomalies, reinforcing its reliability in real-time monitoring applications. In this specific case, the detection of the anomaly resulted in savings of approximately 400 thousand dollars by preventing a 4-hour interruption in production loss at a well with a flow rate of about 3500 m^3/d.

Figure 29 depicts anomalous events from 02/25/23 to 02/27/23 in Well #2. The model identified an anomaly at 07:30 PM on 02/26/23, correctly classifying it as a spurious closure event. The human post-classification confirmed the event at 8:28 PM on 02/26/23, prompting the operator to initiate valve cycling and reopening procedures to restore safe production conditions.

In Well #3, spanning from 07/05/23 to 07/08/23 (Figure 30), the model detected an anomaly at 3:13 PM on 07/06/23, identifying it as a spurious closure of the lower intelligent completion valve. Although the field detection occurred later, human post-classification verified the event at 4:47 PM on 07/06/23, underscoring the model's early detection capability in operational scenarios.

Figure 31 presents data and results for Well #4 between 02/28/23 to 03/03/23. Here, the model identified an anomaly at 2:45 PM on 03/01/23, indicating a potential issue with the ICV. The operator subsequently confirmed and addressed the anomaly with valve cycling, with human post-classification marking the event's identification at 6:25 PM on 03/01/23. This sequence illustrates effective collaboration between automated detection and manual intervention to maintain operational integrity.

Figure 28 - Results for well #1 for the anomalous events detected - Differential Pressures Calculated and Predicted, comparison between TRANS-D model (classification) and fault classification (class).

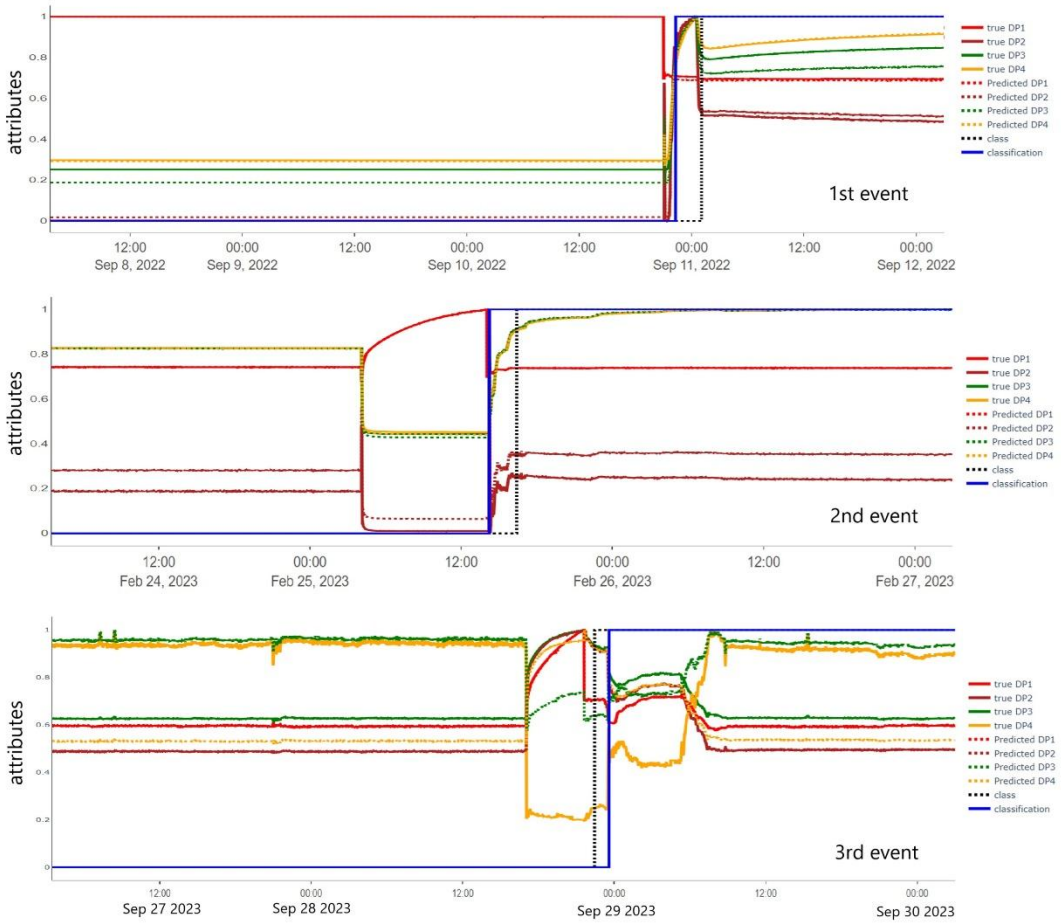

Figure 29 - Results for well #2 for the anomalous event detected – Differential Pressures Calculated and Predicted, comparison between TRANS-D model (classification) and fault classification (class).

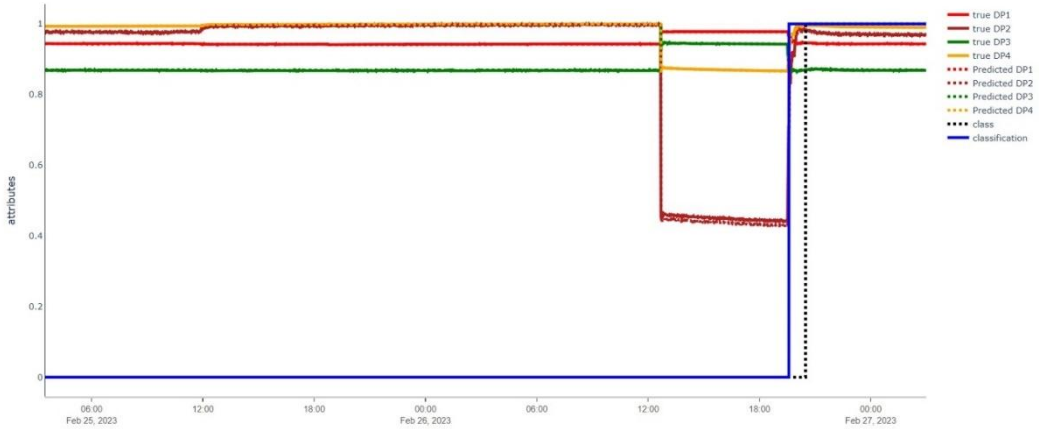

Figure 30 - Results for well #3 for the anomalous event detected – Differential Pressures Calculated and Predicted, comparison between TRANS-D model (classification) and fault classification (class).

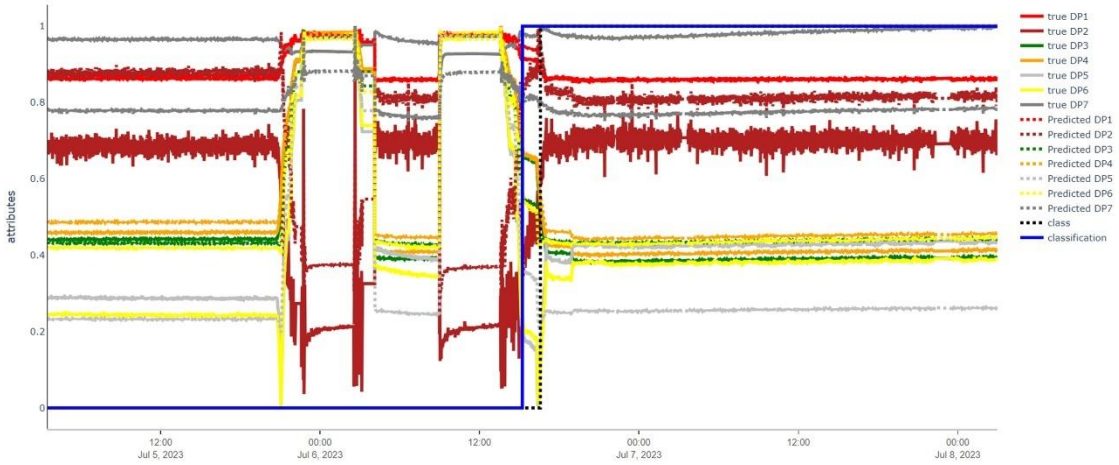

Figure 31 - Results for well #4 for the anomalous event detected – Differential Pressures Calculated and Predicted, comparison between TRANS-D model (classification) and fault classification (class).

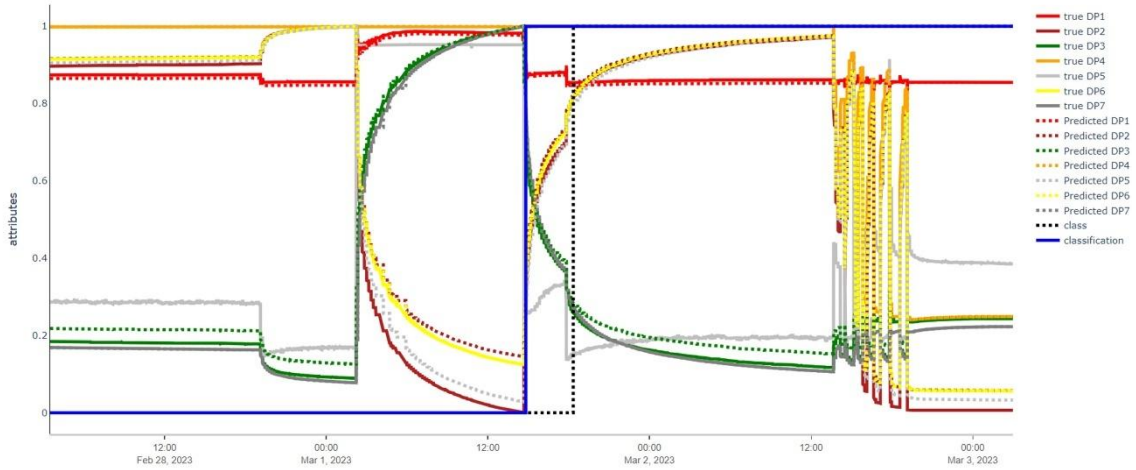

Analyzed data from Well #5, spanning 04/17/23 to 04/19/23 (Figure 32), shows the model accurately identifying an event at 4:36 AM on 04/18/23, signaling a spurious closure. The operator responded with ICV valve cycling, and human post-classification validated the event at 05:00 AM on 04/18/23, ensuring swift corrective actions and minimizing production disruptions.

Figure 32 - Results for well #5 for the anomalous event detected – Differential Pressures Calculated and Predicted, comparison between TRANS-D model (classification) and fault classification (class).

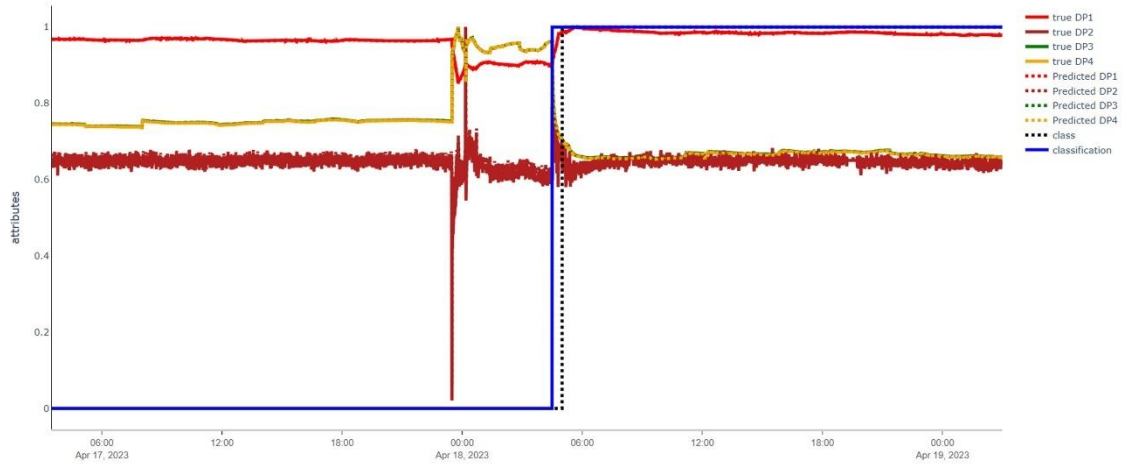

Finally, in Well #6 (Figure 33), the model identified an event at 2:16 PM on 01/21/24, highlighting a potential ICV anomaly. The operator promptly addressed the issue through valve cycling, and human post-classification confirmed the event at 3:43 PM on the same day. This example underscores the model's reliability in detecting and prompting timely corrective measures to uphold operational efficiency in complex offshore environments.

Figure 33 - Results for well #6 for the anomalous event detected – Differential Pressures Calculated and Predicted, comparison between TRANS-D model (classification) and fault classification (class).

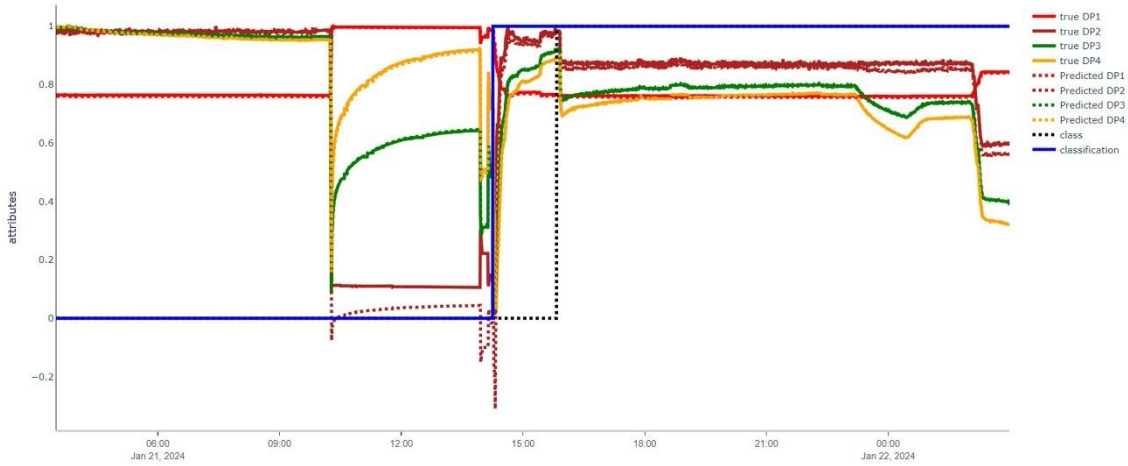

The analysis of data from various events across wells in the Santos Basin highlights the efficacy of the developed monitoring model in detecting and classifying anomalous events, particularly spurious closures of intelligent completion valves (ICVs). In Well #1, for instance, three specific events were identified and corrected following the model's detection, with human verification confirming these anomalies as ICV-related spurious closures. Similar successful detections were observed in Well #2, Well #3, Well #4, Well #5, and Well #6, each illustrating instances where the model correctly identified anomalies ahead of manual confirmation and corrective actions by operators. This contributes to well integrity management and helps in better defining operating conditions and extending the well's lifespan (MOREIRA, et al., (2024)). Notably, a comparative study involving DD+LSTM (ARANHA, et. al, (2024b)), LOF (ARANHA, et. al, (2024a)) and TRANS-D models, using differential pressures as input features, indicated superior performance of the TRANS-D model in detecting IWC spurious closures, achieving detection rates exceeding 90% in real-world production scenarios with comprehensive results summarized in Table 21. The TRANS-D performance metrics: achieving a balanced accuracy (ACCb) of 0.9694 and an F1-score of 0.9574 in predicting ICV closure or partial closure events indicates the model's efficacy in accurately identifying critical operational anomalies, crucial for maintaining production efficiency and preventing costly downtime where DD+LSTM (ARANHA, et. al, (2024b)) and LOF (ARANHA, et. al, (2024a)) previous developed models do not yield satisfactory results.

Despite demonstrating positive results in the eight anomaly cases studied and being implemented in around 200 wells with intelligent completion, the model has limitations. It requires a reasonable initial operating period with well opening and closing conditions, as well as a stable operating period, to be used for training. Additionally, the model needs several hours for training with the well's data. So far, we have not developed a general and generic model; the trained model requires specific data from the production or injecting well to understand the normal operating conditions. This necessity limits its applicability to other scenarios involving wells with ICVs, given the varying reservoir conditions, fluids, and column configurations.

Table 20 - Comparison of metrics Transformer modes for case studies

	model	ACC	$ACCb$	$\mathrm{F1-SCORE}$
well #1 – 1st event	TRANS-A	0.9518	0.9709	0.9274
	TRANS-B	0.9519	0.9709	0.9276
	TRANS-C	0.9508	0.9702	0.9258
	TRANS-D	0.9642	0.9794	0.9475
well #1 – 2ndevent	TRANS-A	0.9145	0.9235	0.9245
	TRANS-B	0.8218	0.8331	0.8488
	TRANS-C	0.9122	0.9213	0.9225
	TRANS-D	0.9625	0.9703	0.9692
well #1 – 3rd event	TRANS-A	0.9377	0.9595	0.9407
	TRANS-B	0.9108	0.9370	0.9108
	TRANS-C	0.9333	0.9558	0.9357
	TRANS-D	0.9702	0.9791	0.9787
well #2	TRANS-A	0.9696	0.9884	0.9318
	TRANS-B	0.8265	0.9046	0.6244
	TRANS-C	0.8265	0.9046	0.6244
	TRANS-D	0.9704	0.9889	0.9346
well #3	TRANS-A	0.7997	0.8125	0.8318
	TRANS-B	0.8005	0.8133	0.8324
	TRANS-C	0.7459	0.7602	0.7946
	TRANS-D	0.9740	0.9816	0.9806
well #4	TRANS-A	*	*	*
	TRANS-B	0.6615	0.6455	0.4508
	TRANS-C	0.9039	0.9316	0.9243
	TRANS-D	0.9026	0.9303	0.9231
well #5	TRANS-A	0.4656	0.5070	0.6362
	TRANS-B	0.8744	0.8918	0.8885
	TRANS-C	0.8916	0.9080	0.9036
	TRANS-D	0.9788	0.9900	0.9885
well #6	TRANS-A	0.9083	0.9314	0.9295
	TRANS-B	0.9000	0.9233	0.9218
	TRANS-C	0.9000	0.9233	0.9218
	TRANS-D	0.9128	0.9358	0.9375

*model did not identified the anomaly

Table 21 - Comparison of metrics between literature methods DD+LSTM (ARANHA, et. al, (2024b)), LOF (ARANHA, et. al, (2024a)) and the proposed method TRANS-D for IWC wells with ICV spurious movement events.

	DD+LSTM			LOF			TRANS-D		
Cases	ACC	$ACCb$	F1 − SCORE	ACC	$ACCb$	F1 − SCORE	ACC	$ACCb$	F1 − SCORE
well #1 – 1st event	0.6306	0.7012	0.5611	0.6821	0.7810	0.6363	0.9642	0.9794	0.9475
well #1 – 2nd event	0.8167	0.8119	0.7686	0.8286	0.8341	0.8539	0.9625	0.9703	0.9692
well #1 – 3rd event	0.7625	0.7326	0.7696	0.7060	0.7532	0.7339	0.9702	0.9791	0.9787
well #2	0.3829	0.2242	0.0	0.3086	0.5968	0.2953	0.9704	0.9889	0.9346
well #3	0.8143	0.7753	0.8638	0.8927	0.8472	0.9267	0.9740	0.9816	0.9806
well #4	0.7271	0.7339	0.7344	0.4729	0.5000	0.6428	0.9026	0.9303	0.9231
well #5	0.6697	0.6891	0.7393	0.4840	0.5102	0.6496	0.9788	0.9900	0.9885
well #6	0.7050	0.7130	0.7667	0.7681	0.7757	0.8179	0.9128	0.9358	0.9375
mean	0.6886	0.6726	0.6504	0.6428	0.6997	0.6945	0.9544	0.9694	0.9574

4.5. Conclusions

This study details the development and implementation of a Transformer models designed to detect anomalies in multivariate time-series data related to oil production. The model targets identifying spurious events involving ICVs in IWC and DHSVs. Testing results indicate that TRANS-D outperformed previous models, achieving a balanced accuracy (ACCb) of 0.9694 and an F1-score of 0.9574 for predicting ICV closure or partial closure events, representing a 38.5% accuracy increase over existing models. These outcomes highlight the model's precision and reliability, showing significant advancements over earlier approaches like DD+LSTM and LOF. Additionally, the transformer model exhibited good accuracy in detecting spurious DHSV closure events, reaching approximately 98.6% accuracy using a publicly available database, comparable to or exceeding other documented models.

The model's capacity to handle diverse and complex data patterns establishes it as a robust tool for anomaly detection in critical offshore well operations. A notable advantage of the TRANS algorithm is its resilience to concept and data drift, common in dynamic offshore settings. By maintaining high detection rates as reservoir

conditions evolve, TRANS ensures consistent and reliable anomaly detection, crucial for minimizing production interruptions and ensuring well integrity over time.

Spurious closure events of ICVs are rare, despite being implemented in around 200 wells; the analysis after nearly two years identified eight positive events. Four anomalies were detected in production well scenarios (Wells #1 and #5), and the remaining four in injection well scenarios (Wells #2, #3, #4, and #6). This distinction highlights the model's adaptability to different operational environments, demonstrating its reliability and effectiveness. Rapid anomaly detection enables operators to quickly address issues related to production or injection, mitigating the impacts associated with ICV closure. Without the transformer model, human detection of anomalies could take over a day, resulting in significant economic consequences. Each successfully identified anomaly could incur an impact of approximately $1.4 million USD.

Future research should expand the transformer-based approach from anomaly detection to anomaly prediction, enhancing its utility in proactive operational management through continuous feedback mechanisms. A key development would be designing a general model that can be trained using data from multiple wells, broadening its applicability. Integrating the TRANS model into digital twin frameworks also represents a promising avenue for enhancing well integrity monitoring. Digital twins provide synthetic sensors for real-time simulation and monitoring, allowing the advanced anomaly detection of TRANS to enhance predictive maintenance strategies. This integration would enable continuous adaptation to shifting operational environments, amplifying the model's contribution to sustainable and efficient offshore well operations.

The industrial impact of this study is significant, with prospects for large-scale adoption in intelligent well completion systems and potential adaptation to other complex well control systems or multivariate fault detection scenarios. The TRANS model not only enhances operational efficiency but also serves as a critical tool for ensuring the economic viability and safety of offshore oil and gas operations.

CHAPTER 5 – CONCLUSIONS

The developed methodologies presented are capable to predict anomalies related to well integrity events in oil wells based on a data-driven approach using machine learning methods, with minimal or no reliance on detailed geological information, fluid properties, or well-specific details.

From Chapter 2, it is possible to conclude that the unsupervised machine learning algorithm for anomaly detection obtained highly accurate anomaly detection with a balanced accuracy (ACCb) of 0.9910 and an F1-SCORE of 0.9969 when predicting spurious DHSV closure events, addressing the challenge of unbalanced databases. The proposed LOF-based method exhibits good accuracy, with over 90% detection rates in offshore well production scenarios. This early anomaly identification minimizes non-productive time (NPT) and significantly boosts oil production. The model's applicability was validated in ultradeep water subsea wells in the pre-salt area of the Santos Basin, demonstrating its potential to enhance anomaly prediction in offshore wells, ultimately reducing costly equipment malfunctions and safeguarding well integrity. In summary, the research presented in Chapter 2 introduces an innovative approach to anomaly detection in offshore well production scenarios, offering high accuracy, robustness, and real-world applicability.

The sequence of development presented in Chapter 3 describes a system for real-time monitoring and anomaly detection. The system utilizes a combination of deep learning autoencoder and a rule-based analytic approach for detecting unexpected events, with the goal of improving operational safety and reducing costs associated with non-productive time and failure repair. The proposed methodology uses pressure and temperature sensor data to classify the well status via a Decision Diagram, which is then used to train autoencoders based on LSTM deep networks devoted to anomaly detection. This coupling enables the deep neural network to evolve constantly through the normal data collected by the analytical method. It makes the system versatile enough to adapt itself to variations of the valve scheme, while also allowing new anomalies to be added to the rule-based analytical approach's cataloged portfolio. The developed system exhibits high accuracy, with true positive detection rates exceeding 90% in the early stages of anomalies identified in both simulated and actual well production scenarios. From these latter, it can be highlighted the

enhancement of detection processes, typically carried out by humans. For the case studies presented, all three wells had a short transitional phase, and the model performed well with balanced accuracy higher than 98.0%. In summary, the proposed system for online monitoring and anomaly detection presented in Chapter 3 has been successfully validated and applied to the analysis of real-time data. It exhibits high accuracy rates in detecting anomalies, making it a valuable tool for supporting the decision-making process in oil well monitoring.

The Transformer model presented in Chapter 4 focuses on detecting spurious events involving ICVs in IWC and DHSVs. Testing results demonstrate that TRANS-D outperformed previous models, achieving a balanced accuracy (ACCb) of 0.9694 and an F1-score of 0.9574 in predicting ICV closure or partial closure events. This represents a 38.5% improvement in accuracy compared to the existing models discussed in Chapters 2 and 3 for the same type of events. These results underscore the model's precision and reliability, showcasing significant advancements over earlier approaches such as DD+LSTM and LOF, while serving as a complementary tool. Additionally, the transformer model exhibited good accuracy in detecting spurious DHSV closure events, reaching approximately 98.6% accuracy using a publicly available database, comparable to other documented models. The model's capacity to handle diverse and complex data patterns establishes it as a robust tool for anomaly detection in critical offshore well operations. A notable advantage of the TRANS algorithm is its resilience to concept and data drift, common in dynamic offshore settings. By maintaining high detection rates as reservoir conditions evolve, TRANS ensures consistent and reliable anomaly detection, crucial for minimizing production interruptions and ensuring well integrity over time. However, comparing the computational performance of the Transformer model, it requires greater installed processing capacity and longer training time when compared to the other two models, DD+LSTM and LOF, which may hinder its implementation in real-time well monitoring.

Table 22 provides a qualitative summary of the three developed models, presenting a consolidated view of aspects such as the complexity of model implementation, the need for large amounts of training samples, computational cost, and model generalization where is the model's ability to operate for any type of well: producer, injector, with or without ICV valves and any casing strings and tubing configuration.

Table 22 - Qualitative analysis of the developed models.

model	Complexity	Training dataset size	Computational Cost	Generalization
LOF	Low	Low	Low	Medium
DD+LSTM	Medium	Low	Medium	High
TRANS-D	High	High	High	Low

Future research could focus on optimizing LSTM and Transformer models by exploring approaches to minimize computational costs and enhance their applicability in analyzing short transients for real-time monitoring of offshore wells.

Other future area is the development of new metrics to better evaluate the models applied to time series in cases of imbalanced data, with few samples of anomalous events, short transient periods, and unclassified data.

Another future research should expand the transformer-based approach from anomaly detection to anomaly prediction, enhancing its utility in proactive operational management through continuous feedback mechanisms. A key development would be designing a general model that can be trained using data from multiple wells, broadening its applicability. Integrating the TRANS model into digital twin frameworks also represents a promising avenue for enhancing well integrity monitoring. Digital twins provide synthetic sensors for real-time simulation and monitoring, allowing the advanced anomaly detection of TRANS to enhance predictive maintenance strategies. This integration would enable continuous adaptation to shifting operational environments, amplifying the model's contribution to sustainable and efficient offshore well operations.

The industrial impact of this study is significant, with prospects for large-scale adoption in intelligent well completion systems and potential adaptation to other complex well control systems or multivariate fault detection scenarios. The Transformers model not only enhances operational efficiency but also serves as a critical tool for ensuring the economic viability and safety of offshore oil and gas operations.

REFERENCES

Agência Nacional do Petróleo, Gás Natural e Biocombustíveis. RESOLUÇÃO ANP Nº 46, DE 1º11.2016, DOU 3.11.2016- RETIFICADO DOU 7 DE NOVEMBRO DE 2016 Available in: https://atosoficiais.com.br/anp/resolucao-n-46-2016?origin=instituicao&q=46/2016 Access in: 28 may 2023.

AGOSTINI, C.E.; SAMPAIO, M.A. **Probabilistic Neural Network with Bayesian-based, spectral torque imaging and Deep Convolutional Autoencoder for PDC bit wear monitoring**, J. Pet. Sci. Eng. 193, Out. 2020.

AL-HAJRI N. M.; AL-GHAMDI A.; TARIQ Z.; MAHMOUD M. **Scale-prediction/inhibition design using machine-learning techniques and probabilistic approach**. *SPE Production & Operations* 35(4):987–1009, 2020. Available in: https://doi.org/10.2118/198646-PA Access in: 28 may 2023.

ALHARBI, B.; LIANG, Z.; ALJINDAN, J. M.; AGNIA, A. K.; AND ZHANG X. **Explainable and Interpretable Anomaly Detection Models for Production Data**. *SPE Journal* 27: 349–363, 2022. Available in: https://doi.org/10.2118/208586-PA Access in: 28 may 2023.

ANIFOWOSE F.; ABDULRAHEEM A.; AL-SHUHAIL A. **A parametric study of machine learning techniques in petroleum reservoir permeability prediction by integrating seismic attributes and wireline data.** *J Pet Sci Eng* **176**:762–774, 2019. Available in: https://doi.org/10.1016/j.petrol.2019.01.110 Access in: 28 may 2023.

ANJOS, J. L; ARANHA, P. E.; MARTINS, A.L.; OLIVEIRA, F.L.; GONCALVES, C. J.; SILVA, D. R.; DUDEK, C.L.; LIMA, C.B. **Digital Twin for Well Integrity with Real Time Surveillance**. Offshore Technology Conference, Houston, Texas, USA, 4-7 May. OTC-30574-MS, 2020, Available in: https://doi.org/10.4043/30574-MS Access in: 28 may 2023.

ARANHA, P.E., SCHNITZLER, E., MOREIRA JR.; DUCCINI, L.E.; MARTINS, A.L.; FALCHETTO, A. B.; ANJOS, J.L. **Field Life Extension: Real Time Well Integrity**

Management Offshore Technology Conference, Houston, Texas, USA, 2-5 May. OTC-31816-MS, 2022, Available in: https://doi.org/10.4043/31816-MS Access in: 28 may 2023.

ARANHA, P.E., POLICARPO, N.A. AND SAMPAIO, M.A. **Unsupervised machine learning model for predicting anomalies in subsurface safety valves and application in offshore wells during oil production**. J Petrol Explor Prod Technol 14, 567–581, 2024a, Available in: https://doi.org/10.1007/s13202-023-01720-4 Access in: 07 jan 2025.

ARANHA, P. E., LOPES, L. G. O., PARANHOS SOBRINHO, E. S. et al. **A System to Detect Oilwell Anomalies Using Deep Learning and Decision Diagram Dual Approach.** SPE J. 29: 1540–1553, 2024b, Available in: doi: https://doi.org/10.2118/218017-PA Access in: 07 jan 2025.

BOURGOYNE JR, A. T.; MILLHEIN, K.K.; CHENEVERT, M.E.; YOUNG JR, F. S. **Applied Drilling Engineering**, Society of Petroleum Engineers, Richardson, 1986.

BRECHAN, B.; SANGESLAND, S.; STEIN D. **Well Integrity – Managing the Risk Using Accurate Design Factors**. *SPE Norway One Day Seminar*, Bergen, Norway. SPE-195604-MS, 2019, Available in: https://doi.org/10.2118/195604-MS: Access in: 28 may 2023.

BREUNING, M. M.; KRIEGEL, H. P.; NG, R. T. **LOF: identifying de nsity-based local outliers.** ACM sigmoid record, 2000, Available in: https://github.com/scikit-learn/scikit-learn/blob/36958fb24/sklearn/neighbors/_lof.py Access in: 08 aug 2025..

CAMPOS, G; PIEDADE, T.S.; RAMOS, A.C.; DOS ANJOS, J.L.; AZEVEDO, A.C.; ABDU, J.P.S.; TERRA, F.S.; SILVA, L.P.; **Special P&A with Resin and Microcement Pumped from Interception Well Due to Multi-String Collapse**, Offshore Technology Conference held in Houston, Texas, USA, 6 – 9 May, 2019.

CAHILL, J. **Measuring Subsea Well Annulus Pressure and Temperature**. 2011. Available in: https://www.emersonautomationexperts.com/2011/industry/oil-

gas/measuring-subseawell-annulus-pressure-and-temperature Access in: 28 may 2023.

CARPENTER, C. **Intelligent Completion Installations Instrumental in Brazilian Presalt Development.** *J Pet Technol* 72 (2020): 59–60. Available in: https://doi.org/10.2118/0520-0059-JPT Access in: 07 jan 2025.

CHENG J., MAO D., SALAMAH M., HORNE R. **Scale buildup detection and characterization in production wells by deep learning methods**. *SPE Production & Operations* **37(4)**:616–631, 2022, Available in: https://doi.org/10.2118/205988-PA Access in: 28 may 2023.

CHOLLET F., 2015. **Keras**. Available in: https://github.com/fchollet/keras Access in: 28 may 2023.

D'ALMEIDA, A. L.; BERGIANTE, N. C. R.; DE SOUZA FERREIRA, G.; LETA, F.R.; LIMA, C.B.C; LIMA, G.B.A. **Digital transformation: a review on artificial intelligence techniques in drilling and production applications**. *Int J Adv Manuf Technol* **119**:5553–5582, 2022, Available in: https://doi.org/10.1007/s00170-021-08631-w Access in: 28 may 2023.

DOSOVITSKIY, A., BEYER, L., KOLESNIKOV, A. et al. **An image is worth 16x16 words: Transformers for image recognition at scale. International Conference on Learning Representations**, 2021, Available in: https://openreview.net/forum?id=YicbFdNTTy. Access in: 07 jan 2025.

ELAVARASAN, D., VINCENT, D. R., SHARMA, V., ZOMAYA, A. Y., SRINIVASAN, K. **Forecasting yield by integrating agrarian factors and machine learning models: A survey. Computers and Electronics in Agriculture**, vol. 155, pp. 257–282, 2018 Available in: https://doi.org/10.1016/j.compag.2018.10.024 Access in: 28 may 2023.

FERNANDES, W., KOMATI, K.S. & ASSIS DE SOUZA GAZOLLI, K. **Anomaly detection in oil-producing wells: a comparative study of one-class classifiers in**

a multivariate time series dataset. J Petrol Explor Prod Technol 14, 343–363, 2024 Available in: https://doi.org/10.1007/s13202-023-01710-6 Access in: 07 jan 2025.

FIGUEIREDO, I.S.; CARVALHO, T.F.; SILVA, W.J.D.; GUARIEIRO, L.L.N.; NASCIMENTO, E.G.S. **Detecting Interesting and Anomalous Patterns In Multivariate Time-Series Data in an Offshore Platform Using Unsupervised Learning**, OTC-31297-MS, Offshore Technology Conference, Houston, Texas, August, 2021. Available in: https://doi.org/10.4043/31297-MS Access in: 28 may 2023.

GEIGER, A., LIU, D., ALNEGHEIMISH, S., CUESTA-INFANTE, A. et al. **TadGAN: Time series anomaly detection using generative adversarial networks**. 2020 IEEE International Conference on Big Data (Big Data), 2020, pp. 33–43. Available in: http://dx.doi.org/10.1109/BigData50022.2020.9378139 Access in: 07 jan 2025.

GIDH, Y. K., PURWANTO, A., IBRAHIM, H.; **Artificial Neural Network Drilling Parameter Optimization System Improves ROP by Predicting/Managing Bit Wear**. SPE Intelligent Energy International, Utrecht, The Netherlands, 2012. Disponível em: https://doi.org/10.2118/149801-MS Acesso em: 28 mai. 2023.

GJELSVIK E. L.; FOSSEN M.; TNDEL K., **Current overview and way forward for the use of machine learning in the field of petroleum gas hydrates**. Fuel 334, Part 2, 2023. Available in: https://doi.org/10.1016/j.fuel.2022.126696 Access in: 28 may 2023.

GURINA E.; KLYUCHNIKOV N.; ZAYTSEV A.; ROMANENKOVA, E.; ANTIPOVA, K.; SIMON, I.; MAKAROV, V.; KOROTEEV. D., **Application of machine learning to accidents detection at directional drilling**. *J Pet Sci Eng*, 184, 2020. Available in: https://doi.org/10.1016/j.petrol.2019.106519 Access in: 28 may 2023.

HUANG, C.-Z.A., VASWANI, A., USZKOREIT, J. et al. **Music transformer**. 2019, Available in: http://dx.doi.org/10.48550/ARXIV.1809.04281. Access in: 07 jan 2025.

HUFFNER L. N., TRIERWEILER J. O., FARENZENA M., **Are complex black-box models for permanent downhole gauge pressure estimation necessary?** J Pet

Sci Eng 173:715–732, 2019, Available in: https://doi.org/10.1016/j.petrol.2018.10.047 Access in: 28 may 2023.

KIM J., KANG H., KANG P. **Time-series anomaly detection with stacked Transformer representations and 1D convolutional network**, Engineering Applications of Artificial Intelligence, Volume 120, 2023 Available in: https://doi.org/10.1016/j.engappai.2023.105964. Access in: 07 jan 2025.

KINGMA D. P.; BA J., **Adam: A method for stochastic optimization.** 2014, CoRR abs/1412.6980

KLUTH, E. L. E., VARNHAM, M. P., CLOWES, J. R., et al, **Advanced Sensor Infrastructure for Real Time Reservoir Monitoring**. SPE European Petroleum Conference, Paris, France, October 2000. Available in: https://doi.org/10.2118/65152-MS Access in: 07 jan 2025.

LARZALERE B., **LSTM autoencoder for anomaly detection**. 2019, Available in: https://towardsdatascience.com/lstm-autoencoder-for-anomaly-detection-e1f4f2ee7ccf,accessed:2019-10-30 Access in: 28 may 2023.

LI D.; CHEN D.; GOH J.; NG S. **Anomaly detection with generative adversarial networks for multivariate time series.** CoRR abs/1809.04758, 2018. Available in: https://doi.org/10.48550/arXiv.1809.04758 Access in: 28 may 2023.

LIU, C.; LI, Y.; XU, M. **An integrated detection and location model for leakages in liquid pipelines.** *J Pet Sci Eng* 175: 852-867, 2019. Available in: https://doi.org/10.1016/j.petrol.2018.12.078 Access in: 28 may 2023.

LIU, Y.; YAO, K. T.; LIU, S. **Semi-supervised failure prediction for oil production wells.** *Proceedings - IEEE International Conference on Data Mining*, 434–441, 2011. Available in: https://doi.org/10.1109/ICDMW.2011.151 Access in: 28 may 2023.

LUIBIMOVA, S.; KHUZINA, L. **On the issue of corrosion in the operation of oil and gas wells**. *E3S Web of Conferences* 225, 03006, II International Conference Corrosion

in the Oil & Gas Industry, 2021. Available in: https://doi.org/10.1051/e3sconf/202122503006 Access in: 28 may 2023.

MA J.; PERKINS S., **Time-series novelty detection using one-class support vector machines.** *Proceedings of the International Joint Conference on Neural Networks*, vol 3, pp. 1741–1745, 2003, Available in: https://doi.org/10.1109/IJCNN.2003.1223670 Access in: 28 may 2023.

MACHADO, A.P.F.; VARGAS, R.E.V.; CIARELLI, P.M.; MUNARO, C. J. **Improving performance of one-class classifiers applied to anomaly detection in oil wells**. *J Pet Sci Eng* 218: 110983. 2022. Available in: https://doi.org/10.1016/j.petrol.2022.110983 Access in: 28 may 2023.

MALHOTRA P.; VIG L.; SHROFF G.; AGARWAL P. **Long short-term memory networks for anomaly detection in time series.** *23rd European Symposium on Artificial Neural Networks*, *ESANN 2015*, Bruges, Belgium, April 22-24, 2015. Available in: https://www.esann.org/sites/default/files/proceedings/legacy/es2015-56.pdf Access in: 28 may 2023.

MARCHI E.; VESPERINI F.; EYBEN F.; SQUARTINI, S.; SCHULLER, B. **A novel approach for automatic acoustic novelty detection using a denoising autoencoder with bidirectional lstm neural networks**. *2015 IEEE International Conference on Acoustics, Speech and Signal Processing (ICASSP)*, pp. 1996–2000, 2015. Available in: https://doi.org/10.1109/ICASSP.2015.7178320 Access in: 28 may 2023.

MARINS, M.A.; BARROS, B.D.; SANTOS, I.H.; BARRIONUEVO, D.C.; VARGAS, R.E.V.; PREGO, T.M.; LIMA, A.A.; CAMPOS, M.L.R.; SILVA, E.A.B.; NETTO, S.L. **Fault detection and classification in oil wells and production/service lines using random forest.** *J Pet Sci Eng* 197: 107879, 2021. Available in: https://doi.org/10.1016/j.petrol.2020.107879 Access in: 28 may 2023.

MARINS, M. A.; NETTO, S. L. **Machine learning tecniques applied to hydrate failure detection on production lines**. UFRJ Institutional Repository, 1 (1), 67, 2018.

MATTIA F. D.; GALEONE P.; SIMONI M. D.; GHELFI E. **A survey on GANs for anomaly detection.** CoRR abs/1906.11632, 2019. Available in: http://arxiv.org/abs/1906.11632 Access in: 28 may 2023.

MITCHELL, R. F.; MISKA S. F. **Fundamentals of Drilling Engineering,** SPE Textbook Series vol. 12, Richardson, 2016.

MONDAY C. U.; ODUTOLA T. O., **Application of machine learning in gas-hydrate formation and trendline prediction.** *SPE Symposium: Artificial Intelligence - Towards a Resilient and Efficient Energy Industry*, 2021. Available in: https://doi.org/10.2118/208653-MS Access in: 28 may 2023.

MOREIRA, N.; LAZARO, A. F.; MINUCCI, F. R. et al. **Well Integrity Management Based on New Operating Limits - A New Method for Extending the Well Lifespan and Changes in Operating Conditions**. Offshore Technology Conference, Houston, Texas, USA, May 2024. Available in: https://doi.org/10.4043/35440-MS Access in: 07 jan 2025.

NAKAO, T.; HANAOKA, S.; NOMURA, Y. et al. **Unsupervised Deep Anomaly Detection in Chest Radiographs**. J Digit Imaging 34, 418–427, 2021. Available in: https://doi.org/10.1007/s10278-020-00413-2 Access in: 07 jan 2025.

NOSHI, C.I.; SCHUBERT, J.J. **The Role of Machine Learning in Drilling Operations; A Review.** SPE/AAPG Eastern Regional Meeting, Pittsburgh, Pennsylvania, USA, 2018. Available in: https://doi.org/10.2118/191823-18ERM-MS Acesso em: 28 mai. 2023.

OLIVEIRA, I. M. N.; LIMA JUNIOR, E. T.; VIEIRA, T. M. A. et al. **Deep Transformer Networks Applied to Anomaly Detection in Oil and Gas Wells**. Offshore Technology Conference, Houston, Texas, USA, 2025. Available in: https://doi.org/10.4043/35939-MS Access in: 29 abr. 2025.

PARI, M. N.; KABIR, A. H.; MOTAHHARI, S. M. et al. **Smart well- Benefits, Types of Sensors, Challenges, Economic Consideration, and Application in Fractured**

Reservoir. SPE Saudi Arabia Section Technical Symposium, Al-Khobar, Saudi Arabia, May 2009. Available in: https://doi.org/10.2118/126093-MS Access in: 07 jan 2025.

SABOKROU M.; KHALOOEI M.; FATHY M.; ADELI, E. **Adversarially learned one-class classifier for novelty detection**. CoRR abs/1802.09088, 2018. Available in: http://arxiv.org/abs/1802.09088 Access in: 28 may 2023.

SATHE, S.; AGGARWAL, C. **LODES: Local Density meets Spectral Outlier Detection**. SIAM Conference on Data Mining, 2016. Available in: https://epubs.siam.org/doi/pdf/10.1137/1.9781611974348.20 Access in: 07 jan 2025.

SCHNITZLER; E., SILVA, D. A. FILHO; MARQUES, et al. **Road to Success and Lessons Learned in Intelligent Completion Installations at the Santos Basin Pre-salt Cluster** SPE Annual Technical Conference and Exhibition, Houston, Texas, USA, 2015. Available in: https://doi.org/10.2118/174725-MS Access in: 07 jan 2025.

SCHNITZLER; E.,GONÇALEZ, L. F; ROMAN, et al. **100th Intelligent Completion Installation: A Milestone in Brazilian Pre-Salt Development**. SPE Annual Technical Conference and Exhibition, Calgary, Alberta, Canada, 2019. Available in: https://doi.org/10.2118/195935-MS. Access in: 07 jan 2025.

SCIKIT-LEARN. **Outlier detection**, 2022 Available in: https://scikit-learn.org/stable/modules/outlier_detection.html Access in: 28 may 2023.

SHAKER, F. M.; JAAFAR, D. **Risk-Based Inspection Due to Corrosion Consequences for Oil and Gas Flowline: A Review**, *Iraqi Journal of Chemical and Petroleum Engineering* 23: 67-73, 2022. Available in: https://doi.org/10.31699/IJCPE.2022.3.9 Access in: 28 may 2023.

SHAKER, F. M.; SADEQB, D. J. **Protecting Oil Flowlines from Corrosion Using 5-ACETYL-2-ANILINO-4-DIMETHYLAMINOTHIAZOLE** *Pakistan Journal of Medical & Health Sciences* 16, 2022. Available in: https://doi.org/10.53350/pjmhs22166571 Access in: 28 may 2023.

SHAWE-TAYLOR J.; ZLICAR B. **Novelty detection with one-class support vector machines**. Advances in Statistical Models for Data Analysis, Springer International Publishing, pp. 231–257, 2015. Available in: https://doi.org/10.1007/978-3-319-17377-124 Access in: 28 may 2023.

SILVA, A. C. A.; OLIVEIRA, I.M.N..; ARANHA, P.E. et al **Detection of unexpected events in oil wells using machine learning with local outlier factor**, *Brazilian Journal of Petroleum and Gas*, vol. 18, 4, 279-287, 2024 Available in: DOI: 10.5419/bjpg2024-0018 Access in: 10 mar 2025.

TANG, H.; ZHANG, S.; ZHANG, F.; VENUGOPAL, S. **Time series data analysis for automatic flow influx detection during drilling.** *J Pet Sci Eng* 172: 1103-1111, 2019. Available in: https://doi.org/10.1016/j.petrol.2018.09.018 Access in: 28 may 2023.

TANG J.; FAN B.; XIAO L.; TIAN S.; ZHANG F.; ZHANG L.; WEITZ D. **A new ensemble machine-learning framework for searching sweet spots in shale reservoirs**. *SPE Journal* 26, pp. 482–497, 2021. Available in: https://doi.org/10.2118/204224-PA Access in: 28 may 2023.

TARIQ, Z.; ALJAWAD, M.S.; HASAN, A.; MURTAZA, M.; MOHAMMED, E.; EL-HUSSEINY, A.; ALARIFI, S.A.; MAHMOUD, M.; ABDULRAHEEM, A. **A systematic review of data science and machine learning applications to the oil and gas industry.** *J Petrol Explor Prod Technol* 11, 4339–4374, 2021 Available in: https://doi.org/10.1007/s13202-021-01302-2 Access in: 10 sep 2023.

TOGNI, R., **Predictive model for drilling phase duration of oil & gas wells**. Master's degree in Computer Science and Engineering, Politecnico di Milano. Milão, Itália, 2018

TURAN, E.M.; JASCHKE, J. **Classification of undesirable events in oil well operation,** 23rd International Conference on Process Control (PC), Štrbské Pleso, Slovakia. 1-4 June. 2021. Available in: https://folk.ntnu.no/jaschke/preprints/2021/TuranClassification_PC/009.pdf Access in: 10 sep 2023.

VARGAS, R.E.V.; MUNARO, C.J.; CIARELLI, P.M.; ARAÚJO, J.C.D. **Proposal for Two Classifiers of Offshore Naturally Flowing Wells Events Using k-Nearest Neighbors, Sliding Windows and Time Multiscale**, 6th International Symposium on Advanced Control of Industrial Processes (AdCONIP), Taipei, Taiwan, Mai. 28-31, 2017.

VARGAS, R.E.V.; MUNARO, C.J.; CIARELLI, P.M.; MEDEIROS, A.G.; AMARAL, B.G.; BARRIONUEVO, D.C.; ARAÚJO, J.C.D.; RIBEIRO, J.L.; MAGALHÃES, L.P. **A realistic and public dataset with rare undesirable real events in oil wells**. J. Pet. Sci. Eng. 180, 62–77. 2019.

VÁVRA J.; HROMADA M. **Optimization of the Novelty Detection Model Based on LSTM Autoencoder for ICS Environment**, Intelligent Systems Applications in Software Engineering , pp. 306–319. 2019. Available in: https://doi.org/10.1007/978-3-030-30329-7_28 Access in: 28 may 2023.

VENKATASUBRAMANIAN V. **A review of process fault detection and diagnosis part i: Quantitative model-based methods**. *Computers & Chemical Engineering* 27(3):293–311, 2003. Available in: https://doi.org/10.1016/S0098-1354(02)00160-6 Access in: 28 may 2023.

WANG S.; CHEN S., **Application of the long short-term memory networks for well-testing data interpretation in tight reservoirs.** *J Pet Sci Eng* **183**, 2019 Available in: https://doi.org/10.1016/j.petrol.2019.106391 Access in: 28 may 2023.

YAKOOT, M.S.; ELGIBALY, A.A.; RAGAB, A.M.S.; MAHMOUD, O. **Well integrity management in mature fields: a state-of-the-art review on the system structure and maturity**. *J Petrol Explor Prod Technol* 11, 1833–1853, 2021. Available in: https://doi.org/10.1007/s13202-021-01154-w Access in: 28 may 2023.

YOUSEFZADEH R.; BEMANI A.; ALIREZA K.; AHMADI M. **An insight into the prediction of scale precipitation in harsh conditions using different machine learning algorithms.** *SPE Production & Operations* pp. 1–19, 2022. Available in: https://doi.org/10.2118/212846-PA Access in: 28 may 2023.

YUAN, Z.; SCHUBERT, J.; ESTEBAN, U. C.; CHANTOSE, P.; TEODORIU, C. **Casing Failure Mechanism and Characterization under HPHT Conditions in South Texas**, *International Petroleum Technology Conference*. International Petroleum Technology Conference, 2013. Available in: https://doi.org/10.2523/iptc-16704-ms Access in: 28 may 2023.

WU, N., GREEN, B., BEN, X., et al. **Deep transformer models for time series forecasting: The influenza prevalence case**. 2020, Available in: arXiv:2001.08317. Access in: 07 jan 2025.

ZHAO, J., SHEN, Y., CHEN, W., ZHANG, Z., JOHNSTON, S. **Machine Learning–Based Trigger Detection of Drilling Events Based on Drilling Data**. SPE Eastern Regional Meeting, Lexington, Kentucky, USA, 2017. Available in: https://doi.org/10.2118/187512-MS Access in:: 28 mai. 2023.

ZHAO X.; JIN F.; LIU X.; ZHANG Z.; CONG Z.; LI Z.; TANG J. **Numerical study of fracture dynamics in different shale fabric facies by integrating machine learning and 3-D lattice method: A case from Cangdong Sag, Bohai Bay basin, China**, *J Pet Sci Eng* **218**, 2022. Available in: https://doi.org/10.1016/j.petrol.2022.110861 Access in: 28 may 2023.

ZHONG Z.; SUN A. Y.; WANG Y.; REN, B. **Predicting field production rates for waterflooding using a machine learning-based proxy model.** *J Pet Sci Eng* **175**, 2020. Available in: https://doi.org/10.1016/j.petrol.2020.107574 Access in: 28 may 2023.

ZHOU, H., ZHANG, S., PENG, J., et. al. **Informer: Beyond efficient transformer for long sequence time-series forecasting**. In: Proceedings of the AAAI Conference on Artificial Intelligence, Vol. 35. pp. 11106–11115. 2021. Access in: 07 jan 2025.